

DESIGN, SYNTHESIS AND CHARACTERIZATION OF ACTIVATABLE  
PHOTOSENSITIZERS FOR PHOTODYNAMIC THERAPY

A THESIS

SUBMITTED TO DEPARTMENT OF CHEMISTRY  
AND THE GRADUATE SCHOOL OF ENGINEERING AND SCIENCE  
OF BİLKENT UNIVERSITY

IN PARTIAL FULFILLMENT OF THE REQUIREMENTS

FOR THE DEGREE OF

MASTER OF SCIENCE

By

FATMA PİR ÇAKMAK

July 2012

I certify that I have read this thesis and that in my opinion it is fully adequate, in scope and in quality, as a thesis of the degree of Master of Science.

.....  
Prof. Dr. Engin U. Akkaya (Principal Advisor)

I certify that I have read this thesis and that in my opinion it is fully adequate, in scope and in quality, as a thesis of the degree of Master of Science.

.....  
Assoc. Prof. Dr. Dönüş Tuncel

I certify that I have read this thesis and that in my opinion it is fully adequate, in scope and in quality, as a thesis of the degree of Master of Science.

.....  
Assoc. Prof. Dr. Mustafa Özgür Güler

Approved for the Graduate School of Engineering and Science:

.....  
Prof. Dr. Levent Onural  
Director of the Graduate School of Engineering and Science

## ABSTRACT

### DESIGN, SYNTHESIS AND CHARACTERIZATION OF ACTIVATABLE PHOTOSENSITIZERS FOR PHOTODYNAMIC THERAPY

Fatma Pir Çakmak

M.S. in Department of Chemistry  
Supervisor: Prof. Dr. Engin U. Akkaya  
July, 2012

Search for new noninvasive methods for diseases has been significant question for years. Therapeutic properties of light are combined with proper chromophore in order to create fundamentals of photodynamic therapy which is a new treatment modality for cancer and other various non-oncological diseases. The method relies on the activation of photosensitizer by using light of certain wavelength and generation of cytotoxic singlet oxygen species in response. Reactive oxygen species kill the targeted tissue within smaller effective diameter through apoptosis/ necrosis mechanism. Through this method, new PDT agents can be proposed and their properties can be tuned by manipulation of other photophysical processes. In this thesis, synthesis, characterization novel water soluble, near IR absorbing Bodipy photosensitizer will be discussed. As opposed to other photosensitizers in literature, this photosensitizer is rationally designed to have singlet oxygen generation capability only in cancer tissue as a result of glutathione triggered activation.

*Keywords:* Bodipy, photodynamic therapy, Glutathione, water soluble

## ÖZET

### FOTODİNAMİK TERAPİ İÇİN IŞIK DUYARLAŞTIRICILARIN SENTEZİ VE KARAKTERİZASYONU

Fatma Pir Çakmak

Yüksek Lisans, Kimya Bölümü  
Tez Yöneticisi: Prof. Dr. Engin U. Akkaya  
Temmuz, 2012

Hastalıklar için non-invaziv yöntemler geliştirmek araştırmaların önemli bir sorusu olarak yıllardır ele alınmaktadır. Işığın terapatik etkileri ve uygun kromofor kullanımı harmanlanarak kanser ve diğer hastalıklar için kullanılan fotodinamik terapinin temelleri oluşturulmaktadır. Method uygun dalga boyunda ışık kullanımı ile ışık duyarlaştırıcılarının aktivasyonu sonucu sitotoksik singlet oksijen üretimine dayanmaktadır. Reaktif oksijen molekülleri etkili küçük bir yarıçapta apoptozis ve nekroz mekanizmaları ile hedeflenen dokuyu öldürmektedir. Diğer fotofiziksel yöntemlerin kullanımı ile yeni fotodinamik terapi ajanları tasarlanıp özellikleri tasarlanabilir. Bu tezde, orijinal suda çözünebilen, yakın kızıl ötesi soğuran Bodipy fotoduyarlaştırıcının sentezi ve karakterizasyonu tartışılacaktır. Bu fotoduyarlaştırıcı literatürdeki diğer fotoduyarlaştırıcıların aksine sadece kanserli bölgede glutatyon ile aktive olup reaktif oksijen üretme yeteneğine sahiptir.

*Anahtar Kelimeler:* Bodipy, Fotodinamik terapi, Glutatyon, suda çözünür

*Dedicated to Humanity...*

## ACKNOWLEDGEMENT

There is not any word that can fully describe my gratitude to my supervisor Prof. Dr. Engin U. Akkaya. I have learnt from him a lot, one of them is how to be a good scientist. I can assure that I am going to challenge other adventures paths in my life with his support.

I would like to thank İlke Şimşek Turan for her partnership in this research. She has been great partner in our work. Also I want to thank Ayşegül Gümüő, Fazlı Sözmey, Ziya Köstereli, Elif Ertem, Ahmet Bekdemir, Tuba Yaşar, Tuğçe Durgut, Onur Buyukcakir, Nisa Yeşilgül, Gizem Çeltek, Bilal Uyar, Ahmet Atılgan, Hatice Turgut and other SCL members for sharing the same ambiance with me.

I would like to thank Fatma Kayacı, Aslı Çelebioğlu, Yelda Ertaş, Zeynep Aytaç, Oya Ustahüseyin, Ruslan Garifullin, Selman Erkal, Gözde Uzunnallı, Can Uran and rest of UNAM members for their valuable friendship.

Finally, I want to express my gratitude to my family and my husband, Özgür Çakmak for their love, support, and understanding.

## LIST OF ABBREVIATIONS

<b>BODIPY</b>	: Boradiazaindacene
<b>DMF</b>	: Dimethylformamide
<b>GSH</b>	: Glutathione
<b>HOMO</b>	: Highest Occupied Molecular Orbital
<b>LED</b>	: Light Emitting Diode
<b>LUMO</b>	: Lowest Unoccupied Molecular Orbital
<b>NMR</b>	: Nuclear Magnetic Resonance
<b>PDT</b>	: Photodynamic Therapy
<b>PeT</b>	: Photoinduced Electron Transfer
<b>TEG</b>	: Triethylene Glycol
<b>TFA</b>	: Trifluoroacetic Acid
<b>THF</b>	: Tetrahydrofuran
<b>TLC</b>	: Thin Layer Chromatography

## TABLE OF CONTENTS

<b>CHAPTER 1: INTRODUCTION</b> .....	1
1.1. Photodynamic Therapy .....	1
1.1.1 Photosensitizers .....	2
1.1.1.1 Porphyrin Related Photosensitizers .....	3
1.1.1.2 Non- Porphyrin Related Photosensitizers .....	5
1.1.2 Photochemistry of Photodynamic Therapy .....	9
1.1.3 Biological Response .....	12
1.2 Activatable PDT Agent .....	15
1.3 Glutathione Sensing and Signaling .....	20
1.3.1 Photoinduced Electron Transfer and Examples .....	21
1.3.2 Photoinduced Charge Transfer .....	24
1.3.3 FRET Based Sensing .....	27
1.3.4 Other Process and Examples .....	29
<b>CHAPTER 2: EXPERIMENTAL</b> .....	32
<b>EXPERIMENTAL</b> .....	32
2.1. General .....	32
2.2. Synthesis of Target Molecules .....	33
2.2.1. Synthesis of Compound 30 .....	33
2.2.2. Synthesis of Compound 31 .....	34
2.2.3. Synthesis of Compound 32 .....	35
2.2.4. Synthesis of Compound 33 .....	36
2.2.5. Synthesis of Compound 34 .....	37
2.2.6. Synthesis of Compound 35 .....	38
2.2.7. Synthesis of Compound 36 .....	39
2.2.8. Synthesis of Compound 37 .....	40

2.2.9.	Synthesis of Compound 38.....	41
2.2.10.	Synthesis of Compound 39.....	42
2.2.11.	Synthesis of Compound 40.....	43
<b>CHAPTER 3: RESULTS and DISCUSSION.....</b>		<b>45</b>
3.1.	General Perspective.....	45
3.2.	Design Strategies For Activatable Photosensitizers.....	46
3.3.	Spectral Proof For Activation Process .....	49
3.4.	Singlet Oxygen Genration Measurements .....	53
<b>CHAPTER 4: CONCLUSION.....</b>		<b>55</b>
<b>REFERENCES .....</b>		<b>56</b>
<b>APPENDIX A – NMR SPECTRA .....</b>		<b>68</b>
<b>APPENDIX B – MASS SPECTRA .....</b>		<b>91</b>

## LIST OF FIGURES

<b>Figure 1.</b> PDT agents as second generation.....	4
<b>Figure 2.</b> Non-porphyrin related PDT agents .....	7
<b>Figure 3.</b> Perrin–Jablonski energy diagram for a PS molecule .....	9
<b>Figure 4.</b> Photochemical Reactions during PDT action .....	11
<b>Figure 5.</b> Biological Response toward PDT action .....	13
<b>Figure 6.</b> FRET deactivated Photosensitizer design.....	17
<b>Figure 7.</b> Mechanism target-specific activatable probes .....	18
<b>Figure 8.</b> pH-activatable Bodipy derivatives .....	19
<b>Figure 9.</b> Logic gate integrated PDT agent .....	20
<b>Figure 10.</b> Principle of cation recognition by fluorescent PET sensors .....	21
<b>Figure 11.</b> Crown containing, podand and calixarene based PET sensors.....	22
<b>Figure 12.</b> Oxidative PET sensor.....	23
<b>Figure 13.</b> Spectral displacements of PCT sensors. ....	25
<b>Figure 14.</b> Crown containing PCTsensors.....	26
<b>Figure 15.</b> ICT dependent thiol Probe .....	27
<b>Figure 16.</b> Schematic representation Förster-type energy transfer.....	27
<b>Figure 17.</b> FRET based thiol sensing probe . ....	29
<b>Figure 18.</b> GSH structure.....	29
<b>Figure 19.</b> Structures of Thiol Probes.....	30
<b>Figure 20.</b> Synthesis of Compound 30 .....	33
<b>Figure 21.</b> Synthesis of Compound 31 .....	34
<b>Figure 22.</b> Synthesis of Compound 32 .....	35
<b>Figure 23.</b> Synthesis of Compound 33 .....	36
<b>Figure 24.</b> Synthesis of Compound 34 .....	37
<b>Figure 25.</b> Synthesis of Compound 35 .....	38
<b>Figure 26.</b> Synthesis of Compound 36 .....	39
<b>Figure 27.</b> Synthesis of Compound 37 .....	40
<b>Figure 28.</b> Synthesis of Compound 38 .....	41
<b>Figure 29.</b> Synthesis of Compound 39 .....	42
<b>Figure 30.</b> Synthesis of Compound 40 .....	43
<b>Figure 31.</b> Targeted Probe Design.....	46
<b>Figure 32.</b> Target Photosensitizers .....	47

<b>Figure 33.</b> Activation of the Photosensitizers.....	48
<b>Figure 34.</b> Absorbance spectrum of Compound 32 and Compound 33 as Bodipy 1 and Probe 1 respectively before and after addition of GSH.....	49
<b>Figure 35.</b> Fluorescence spectrum of Compound 33 as Probe 1 with time, 1 nM GSH and 4 $\mu$ M Probe concentration in DMSO/ 1X PBS buffer solution (1/1, v/v), excitation wavelength was 655 nm.....	49
<b>Figure 36.</b> Absorbance spectrum of Compound 36 and Compound 37 as Bodipy 2 and Probe 2 respectively before and after addition of GSH.....	50
<b>Figure 37.</b> Fluorescence spectrum of Compound 37 as Probe 2 with time, 1 nM GSH and 4 $\mu$ M Probe concentration in DMSO/ 1X PBS buffer solution (1/1, v/v), excitation wavelength was 655 nm.....	51
<b>Figure 38.</b> Absorbance spectrum of Compound 39 and Compound 40 as Bodipy 2 and Probe 2 respectively before and after addition of GSH.....	52
<b>Figure 39.</b> Fluorescence spectrum of Compound 40 as Probe 2 with time, 1 nM GSH and 4 $\mu$ M Probe concentration in DMSO/ 1X PBS buffer solution (1/1, v/v), excitation wavelength was 655 nm.....	52
<b>Figure 40.</b> Absorbance spectrum of trap molecule (2,2'-(Anthracene-9,10-diyl)bis(methylene)dimalonic acid) with Bodipy 1, 4 $\mu$ M in DMSO/ 1X PBS buffer solution (1/1, v/v), LED applied at 660 nm.....	53
<b>Figure 41.</b> Absorbance spectrum of trap molecule (2,2'-(Anthracene-9,10-diyl)bis(methylene)dimalonic acid) with Bodipy 2, 4 $\mu$ M in DMSO/ 1X PBS buffer solution (1/1, v/v), LED applied at 660 nm.....	54
<b>Figure 42.</b> Absorbance spectrum of trap molecule (2,2'-(Anthracene-9,10-diyl)bis(methylene)dimalonic acid) with Bodipy 3, 4 $\mu$ M in DMSO/ 1X PBS buffer solution (1/1, v/v), LED applied at 660 nm.....	54
<b>Figure 43.</b> $^1\text{H}$ NMR spectra of compound 30.....	69
<b>Figure 44.</b> $^{13}\text{C}$ NMR spectra of compound 30.....	70
<b>Figure 45.</b> $^1\text{H}$ NMR spectra of compound 31.....	71
<b>Figure 46.</b> $^{13}\text{C}$ NMR spectra of compound 31.....	72
<b>Figure 47.</b> $^1\text{H}$ NMR spectra of compound 32.....	73
<b>Figure 48.</b> $^{13}\text{C}$ NMR spectra of compound 32.....	74
<b>Figure 49.</b> $^1\text{H}$ NMR spectra of compound 33.....	75
<b>Figure 50.</b> $^{13}\text{C}$ NMR spectra of compound 33.....	76

<b>Figure 51.</b> $^1\text{H}$ NMR spectra of compound 34 .....	77
<b>Figure 52.</b> $^{13}\text{C}$ NMR spectra of compound 34 .....	78
<b>Figure 53.</b> $^1\text{H}$ NMR spectra of compound 35 .....	79
<b>Figure 54.</b> $^{13}\text{C}$ NMR spectra of compound 35 .....	80
<b>Figure 55.</b> $^1\text{H}$ NMR spectra of compound 36 .....	81
<b>Figure 56.</b> $^{13}\text{C}$ NMR spectra of compound 36 .....	82
<b>Figure 57.</b> $^1\text{H}$ NMR spectra of compound 37 .....	83
<b>Figure 58.</b> $^1\text{H}$ NMR spectra of compound 37 .....	84
<b>Figure 59.</b> $^1\text{H}$ NMR spectra of compound 38 .....	85
<b>Figure 60.</b> $^{13}\text{C}$ NMR spectra of compound 38 .....	86
<b>Figure 61.</b> $^1\text{H}$ NMR spectra of compound 39 .....	87
<b>Figure 62.</b> $^{13}\text{C}$ NMR spectra of compound 39 .....	88
<b>Figure 63.</b> $^1\text{H}$ NMR spectra of compound 40 .....	89
<b>Figure 64.</b> $^{13}\text{C}$ NMR spectra of compound 40 .....	90
<b>Figure 65.</b> ESI-HRMS of compound 30 .....	91
<b>Figure 66.</b> ESI-HRMS of compound 31 .....	91
<b>Figure 67.</b> ESI-HRMS of compound 32 .....	92
<b>Figure 68.</b> ESI-HRMS of compound 34 .....	92
<b>Figure 69.</b> ESI-HRMS of compound 35 .....	92
<b>Figure 70.</b> ESI-HRMS of compound 36 .....	93
<b>Figure 71.</b> ESI-HRMS of compound 38 .....	93
<b>Figure 72.</b> ESI-HRMS of compound 39 .....	93

# CHAPTER 1

## INTRODUCTION

### 1.1. Photodynamic Therapy

Therapeutic effects of light<sup>1,2</sup> have been known for thousands of years. Photodynamic therapy (PDT) is a new promising treatment method<sup>3</sup> which was developed just in the last century. Unlike to other traditional cancer therapies, PDT gives damage to targeted tissue<sup>4,5</sup> not surrounding normal cells. PDT depend on systemic localization of photosensitizers in targeted tissue and activation of the sensitizer<sup>6</sup> by using red or near infrared (NIR) light which allow generation of singlet oxygen ( $^1\text{O}_2$ ). Hence this strategy gives damages to cancer cells which exposed to light within therapeutic window (650-800 nm).

Pronounced properties of PDT over conventional strategies help widely use of the method in clinical trials<sup>7</sup>. All current clinical PDT agents have ability to target specific tissue with different range of sensitivity. The method harnesses harmless components as light and photosensitizer turn into destructive elements toward tumor. The other crucial parameter is molecular oxygen for the method. Energy transfer from photosensitizer to molecular oxygen allows transformation of oxygen molecules to reactive singlet oxygen species. These reactive oxygen species has short life time and give its additional energy to surrounding tissue which causes cell death either with apoptosis or necrosis<sup>8</sup>. So far there are various photosensitizers<sup>9</sup> reported for clinical treatments.

Scientists are seeking for new improved version<sup>6</sup> of the method in order to have more sensitive approach for diseases. Since clinical trials have begun, searching for answers also has progressed in the laboratory. Every step and enhancement has been highlighted in the area in view of the fact that cancer has

become the second cause of the death after heart related disorder in the world according to statistics.

### **1.1.1 Photosensitizers**

Several compounds can be considered as appropriate PDT agents<sup>10</sup> due to their ability to produce singlet oxygen nonetheless only a few of them could be used in clinical trial<sup>7,11</sup> even less could be commercially available<sup>12,13,14</sup>. Most common photosensitizers<sup>15</sup> have porphyrinoid structure. One of them is the first used hematoporphyrin derivative, Photofrin<sup>16,17</sup> which has been approved in Europe, Canada, Japan and United States<sup>4</sup> although it doesn't carry optimal properties<sup>18,19</sup> of a photosensitizer for PDT. The reasons<sup>20</sup> for wide use of hematoporphyrin derivatives<sup>21,22</sup> in first generation photosensitizer are wide knowledge of these compounds and their resemblance with natural porphyrins which can be found in living organism.

For aiming ideal photosensitizers for PDT, there are many requirements should be kept in mind. Suitable photosensitizer agents for PDT should have ease of purification / synthesis<sup>23</sup> for beginning. Another important factor is related with the wavelength of the light. The photosensitizers need to have maximum absorption in the region 600-800 nm which is optimum range<sup>15,24</sup> for energy necessity and deep tissue penetration in addition to this; minimum absorption<sup>25</sup> should be in the region 400-600 nm in order to reduce skin photosensitivity. Dark toxicity and phototoxicity<sup>20,11</sup> is one of the important drawbacks of the sensitizers which have been used in clinical trials. Also compounds which are going to be used as PDT agents need to be photostable towards photodegradation and other reactive oxygen species. Upon administration of the photosensitizer, it should be highly selective for malignant tissue<sup>26</sup> instead of healthy tissues. Well characterized single compound<sup>15</sup> is needed in order to have dependable examination of sensitizer in PDT mechanism. High quantum yields<sup>20</sup> for phosphorescence and singlet oxygen generation can be added to our lists for designing new sensitizers.

Biocompatibility of the compounds determines its direct application. In order to increase biocompatibility, solubility<sup>27,23</sup> carries important role for administration and distribution of the sensitizers *in vivo* applications. Although solubility is significant character of photosensitizers, there are many studies enable of hydrophobic PDT agents administration through improving of water soluble carriers<sup>28,29,30</sup>. Also these carriers can be characterized for additional selectivity by manipulating specific interactions.

### 1.1.1.1 Porphyrin Related Photosensitizers

Second generation PDT agents<sup>24</sup> are designed after photofrin<sup>31</sup> and they still depend on the diverse types of polypyrrole macrocycles. A range of them have begun to be used in phase I/ II and II/III clinical trials<sup>15,32</sup> (Fig. 1). m-Tetrahydroxyphenyl chlorin<sup>33,34</sup> (compound 1) also known as Temoporfin and Foscan has been used for treatment for the head and neck cancers in Europe. Although scientist obtained promising results for this compound, extended skin photosensitivity is reported as a negative aspect<sup>35</sup>. Compound 2 resembles more like the photofrin as hematoporphyrin derivatives<sup>9</sup>. Compound 3 belongs to porphyrin family and called protoporphyrin IX<sup>36,37,38</sup> which is also precursor of 5-aminolevulinic acid (ALA). Mono-L-aspartyl chlorine e6 (Npe6) is another second generation photosensitizer illustrated as compound 4 which has been used for lung cancer in phase I/ II trials<sup>4, 39</sup>. Palladium bacteriochlorin (Tookad)<sup>40</sup> is an example of co-coordinated metal atoms within tetrapyrrole which is showed as compound 5 in Fig.1. Compound 6 has been used for clinical trials for breast cancer and other cutaneous tumors under the name of Verteporfin<sup>41,42</sup>. It is benzoporphyrin derivative monoacid ring A (BDP-MA) which is also used for age related molecular degeneration (AMD)<sup>43</sup>. All of the examples are at different phase of clinical trials. Although some of them show a few promising results<sup>44,45</sup>, there is many improvements needed for ideal photosensitizer. There are also many drawback related with these compound. One of them is toxicity

which has been observed during clinical trials. Studies also has important role in the improvement of new generation photosensitizers. With the help of the results obtaining from clinical trials, scientist could interpret them and

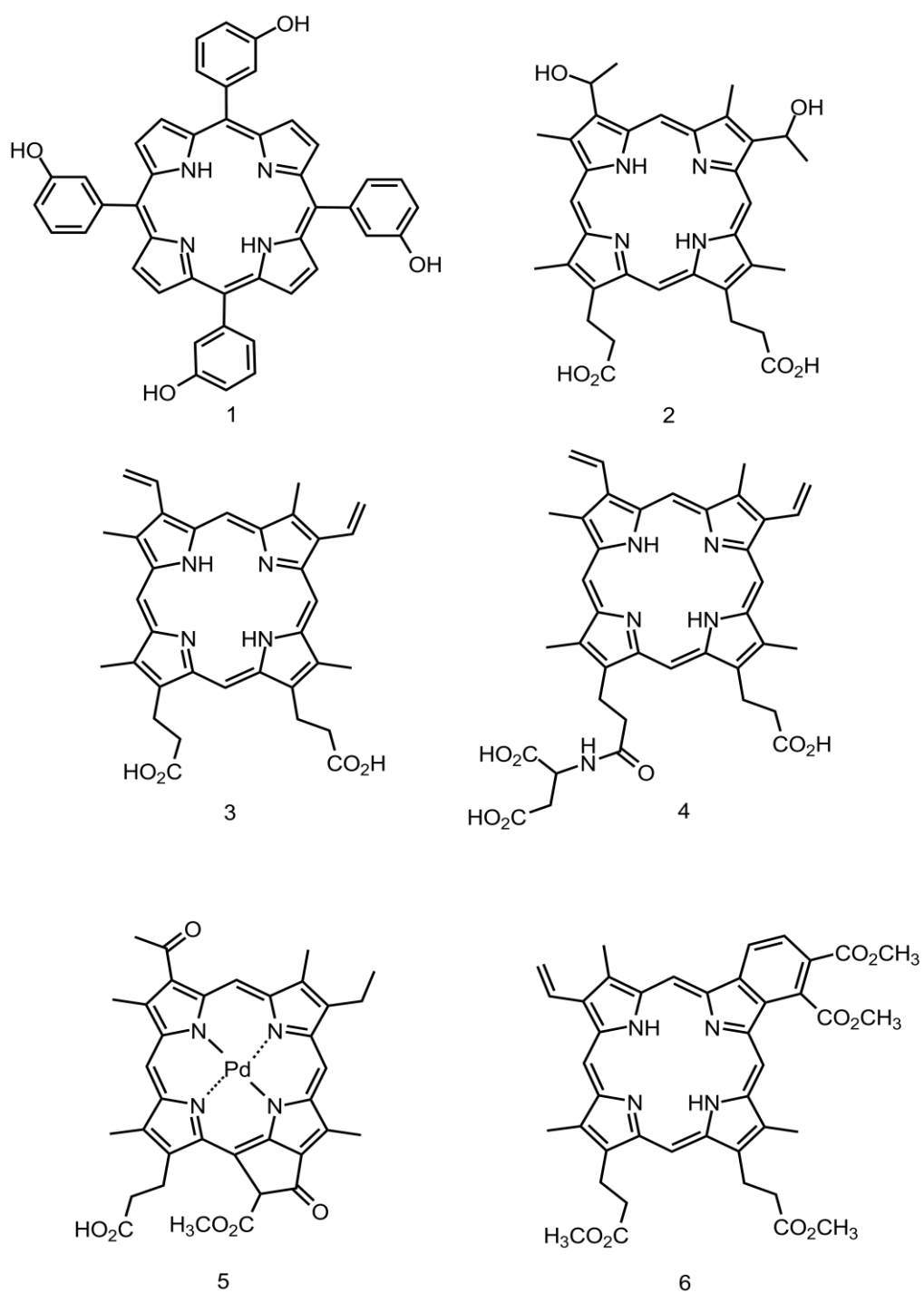


**Figure 1.** PDT agents as second generation

demonstrate the significant characteristic of ideal photosensitizer. Understanding of the concept has gained new aspects with the help of the experience during the period of clinical trials.

In Fig.1, we could find examples of the photosensitizer which is called second generation. There are also other photosensitizers which are also porphyrin related. Core modified porphyrin can be example of this class. These sensitizers have been tried to be improved during clinical trials. Some of them are far from being ideal PDT agents in order to have better treatment of cancer and other diseases. Since this thesis is more related to cancer, examples will be more associated to it. Various types of cancer types were used in these clinical trials as it can be seen through the examples<sup>11</sup>.

#### **1.1.1.2 Non- Porphyrin Related Photosensitizers**

Due to the several drawbacks of porphyrin related compounds, scientists have found alternatives. The major negative aspects are poor light absorption in near infra-red and long timed skin photosensitivity<sup>15</sup>. Although one of the important reasons is to choose porphyrin related compounds as photosensitizers is they are naturally occurring substance, there are many instances of natural non-porphyrin related compounds<sup>46</sup>. Considering the factors needed for ideal photosensitizers, there are many researches aiming to design optimum PDT agents.

Compound 7 (in Fig.2) is an example of Psoralen derivatives<sup>47</sup> which has been applied for thousands of years in Middle East and East for mostly skin disorders. Studies enlighten the structure-activity relation and synthetic pathways for different kinds of them. It is claimed that these compounds selective for cancer cells. Other important results propose these compounds result cross linking in DNA<sup>48</sup>. This characteristic can be deadly for especially in

the case of non-tumor tissues. Various types of Psoralen show different properties in PDT action. Clinical trials are continuing with these compounds.

Compound 8 is an example of anthracyclines and called Doxorubicin<sup>49</sup> which has suitable light absorption properties and tumor selectivity. Even though this favorable properties of this compound, it has harmful effects on healthy tissues. Pharmacology of the substance has been cracked through the clinical trials. Lower dose of this compound could show better cytotoxic effect towards tumors when compared to other photosensitizers. Negative aspects of this compound for PDT need to be improved with the help of the knowledge which is gained during various researches.

Merocyanine<sup>50</sup> (Compound 9) is illustrated in Fig.2 as a model for cyanine dyes which is an early subject of PDT. They are known for their antibacterial property and straightforward synthesis. Their absorption is not in the optimum range but it can be modified through manipulating length of polymethine chains. However this arouses other problems as decrease in stability and solubility. Since PDT agents are designed for *in vivo* applications, all the properties of photosensitizer should be carefully considered. Also these dyes have been used in clinical trials in order to understand its characteristic better. Structure of this compound enables extensive design of different series<sup>51</sup>. On the other hand, low quantum yields of singlet oxygen generation are observed during trials as disadvantage. Heavy atom effect could be used to increase the quantum yield for singlet oxygen but other negative aspects of this compound need to be improved.

With a more common name methylene blue<sup>52</sup> as a derivative of phenothiazinium dyes is shown in Fig.2. as compound 10. It has been used extensively for clinical diagnosis and tumor marker although its use as photosensitizer is new when compared to others. Its performance has been diminished by malignant cells even though it gives damage to DNA during PDT action<sup>53</sup>. Other reason not to use of methylene blue for PDT action can be its dark toxicity. Different synthetic pathways are also available.

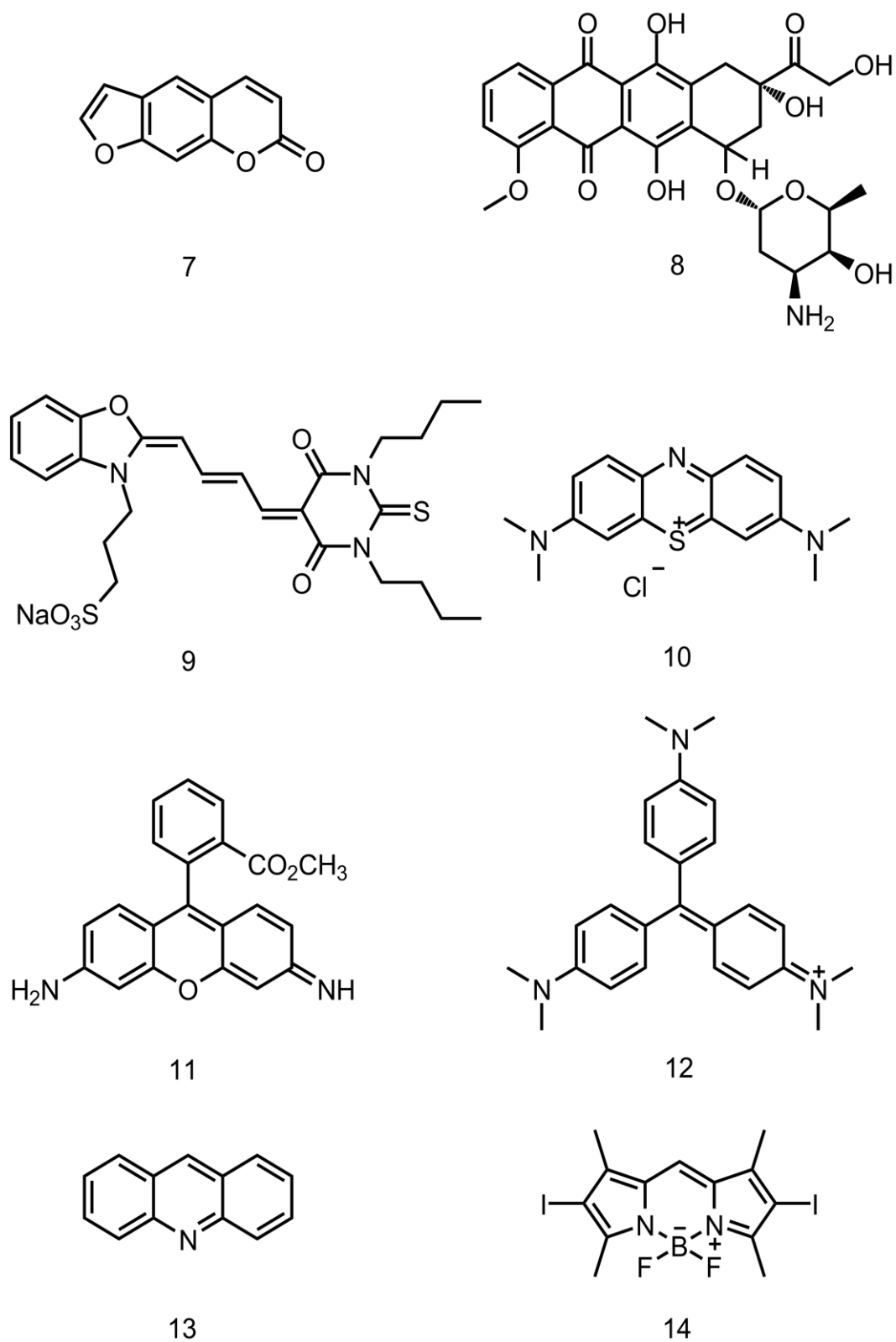


**Figure 2.** Non-porphyrin related PDT agents

Another popular dye is Rhodamine derivatives<sup>54</sup> which are demonstrated as compound 11 in Fig.2. It has been known for its use for fluorescent probe. This dye shows high fluorescence quantum yields which enable to have increased singlet oxygen generation efficiency compared to others. However, dark toxicity of this compound and short wavelength absorption made Rhodamine far away from being ideal photosensitizer<sup>55</sup>.

Triarylmethane derivative crystal violet is illustrated as compound 12 which is recognized for its antimicrobial and antitumor properties<sup>56</sup>. It is also used for PDT action though it is hard to explore its singlet oxygen generation efficiency because of its structure. Low dark toxicity and absorption at proper wavelength can be listed as advantages of these compounds. Also clinical trials suggest that dye has high photoactivity against tumors. In addition its charge allow cell uptake<sup>57</sup>.

Compound 13 is an example of acridines family<sup>46</sup> as a simple compound called acridine. This group is widely studied heterocyclic compound. Its PDT effect has known for a century by now. Another characteristic of this compound is use of fluorescent probe. Although this knowledge, acridines compounds have been used in clinical trials less than expected. Upon the photoirradiation<sup>58</sup>, compound gives enhanced damage to DNA strands and there are many commercially available acridines in market. Phototoxicity and short wavelength absorption of these compounds can be listed its drawbacks.

The last but not the least non-porphyrin related photosensitizer is called Bodipy<sup>59</sup> and illustrated as compound 14. Although these compounds have been known for years, it has been studied for PDT just for last years. Ease of synthesis, ease of purification, good photostability, absorption in therapeutic window, high extinction coefficients and good quantum yields for singlet oxygen generation are the reasons for these compounds to use in PDT methods. Also many researchers have proposed its excellent photophysical characteristic<sup>23</sup> which allow manipulation to meet the criteria of ideal PDT agents.

## 1.1.2 Photochemistry of Photodynamic Therapy

Localization of the photosensitizer in targeted tumor tissue is administrated. Upon irradiation, photosensitizer absorbs energy at determined proper wavelength, and get excited to upper energy level. Its energy is transferred to oxygen molecules which cause cell death in the end.

Absorption of a photon by ground state photosensitizer ( $S_0$ ), allow excitation of molecules to its short lived excited singlet state ( $S_1$ ) by using conventional light sources. Singlet and triplet state lifetimes are differ from each other. Singlet lifetimes generally determined in nanoseconds whereas triplet lifetimes are defined in the range of microsecond to millisecond<sup>60</sup>.

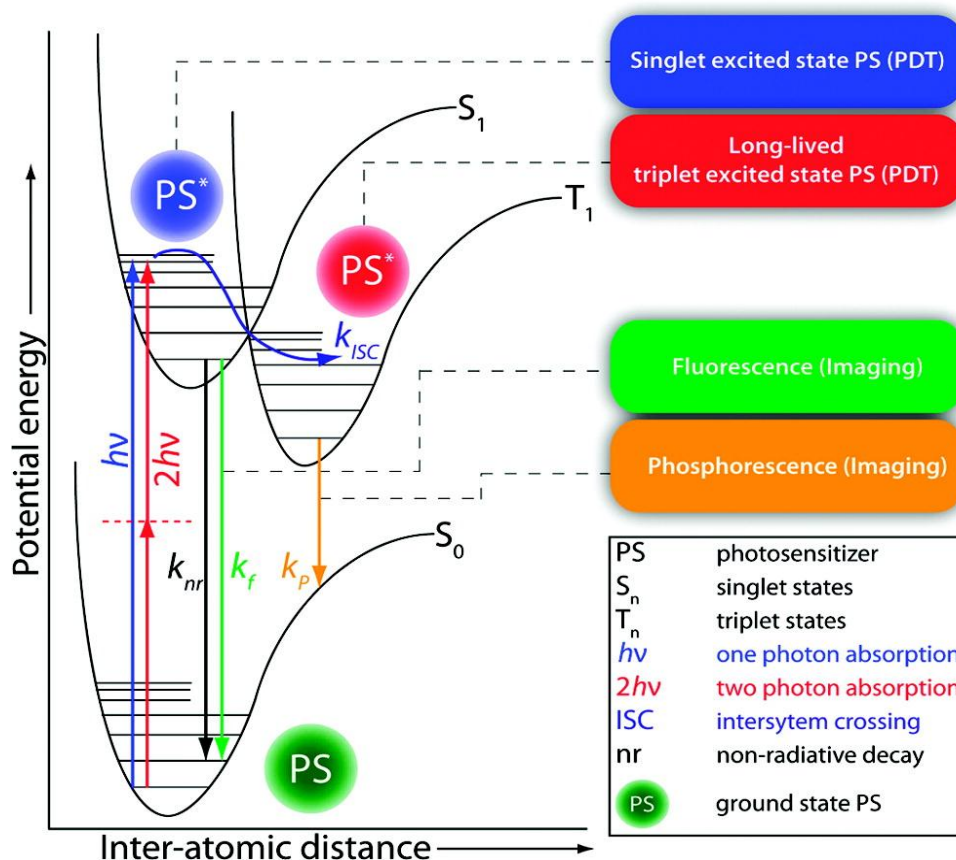


**Figure 3.** Perrin–Jablonski energy diagram for a PS molecule<sup>60</sup> Copyright © 2010, American Chemical Society. Adapted with permission

Other excited states may be possible<sup>61</sup> for the substance depending of the nature of the photosensitizer and the wavelength of the light used in the experiment. Singlet excited state lifetime is very short to enable interaction between photosensitizer and oxygen molecules hence the damage caused by the molecules at this singlet excited state is insignificant. Due to its longer lifetime, triplet excited states ( $T_1$ ) are preferred for biological applications of photochemistry. At this point there are two options occur for photosensitizer: radiative or non-radiative paths.

It can re-emit its energy via fluorescence route or it can go through intersystem crossing process. Also non-radiative decay can be possible for molecules in other cases in which molecule produce heat during the process. Rate constant demonstrated for fluorescence  $k_f$ , for non-radiative decay  $k_{nr}$  and for intersystem crossing  $k_{isc}$  in the Fig.3. Although there are studies showing that internal conversion in non radiative decay path can be manipulated for photosensitized tissue damage, the most important path for dispersing energy to surroundings more specifically to molecular oxygen is internal conversion since it favors to excited triplet state ( $T_1$ ). As it is mentioned, excited triplet state ( $T_1$ ) has longer lifetime allowing energy transfer probable. On the other hand transition from singlet state to triplet state is spin forbidden and vice versa which also is the reason longer lifetime of triplet state. Heavy atoms such as chlorine, iodine modifications to photosensitizer increase intersystem crossing rate leading enhanced photodynamic activity. In order to generate singlet oxygen species ( $^1O_2$ ) from molecular oxygen ( $^3O_2$ ), certain amount energy is needed in which determine the upper limit of wavelength of therapeutic window for photodynamic therapy. This energy which is  $22 \text{ kcal mol}^{-1}$  is very low. Furthermore there is other possibility as phosphorescence rate illustrated  $k_p$  for excited triplet state other than transferring its energy to surroundings. Other more complex photophysical incidents can take place for molecules<sup>3,60</sup>.

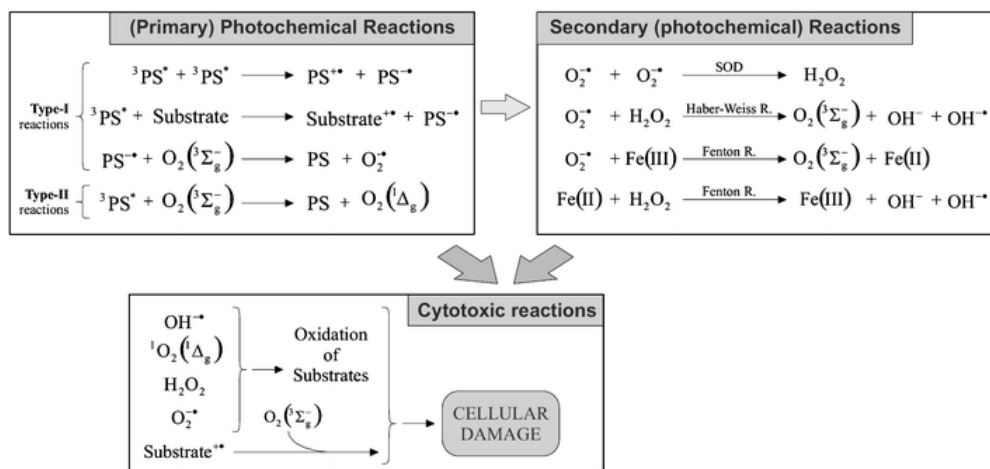


**Figure 4.** Photochemical Reactions during PDT action<sup>62</sup> Copyright © 2008, Springer-Verlag London Limited Adapted with permission

Another question arises about possible pathways for generation of reactive singlet oxygen. It can be divided into two groups as Type I and Type II<sup>62</sup> (Fig. 4). Type I procedure includes hydrogen-atom abstraction or electron transfer between excited photosensitizer and substance which produce free radicals. These radicals can interact with oxygen molecule in order to generate reactive oxygen species as superoxide radical which is not sufficient reactive to give damage. These superoxide radicals instead generate hydrogen peroxide ( $\text{H}_2\text{O}_2$ ) which can give damage to tissues through various pathways<sup>63,64</sup>. In Type II mechanism, energy transfer occurs from triplet excited state of photosensitizer to molecular oxygen directly. This energy transfer leads to reactive singlet oxygen generation which is known for a variety of interaction with biological substances in response causing cell death through oxidative stress. Oxygen and photosensitizer concentration are just examples of the parameters which define the mechanism of generation of reactive oxygen species<sup>64,65</sup>.

Oxygen has a destructive role independent of the reaction types. Oxygen level in tissue is needed to meet the required amount for tissue damage. Also, there are studies confirming this hypothesis. In its ground state, oxygen has two unpaired electrons which is the reason for its triplet state. Through energy transfer, these electrons pair up and become a singlet state which leads to the destruction of

tumors. Singlet oxygen is extremely polarized zwitterion hence lifetime is very short around microseconds in organic solvent and shorter in aqueous environment. This relatively short lifetime let its activity in restricted area about maximum 30 nm in diameter<sup>66</sup>. These small diameters ensure the localized damage to cells. Since research results shows that Type II mechanism is more often the case for PDT action, leading role for cell damage belongs to singlet oxygen. It worth to note that for variety of photosensitizer, energy transfer between photosensitizer and molecular oxygen can occur even photosensitizer is in singlet state. The reason for energy transfer can be the large energy gap between singlet state and triplet state while singlet state of photosensitizer has long enough lifetimes for the process. Although it is hard to measure singlet oxygen's ability to damage tissue because of its reactivity and short lifetime, there are many studies propose direct and indirect evidence for the method. Singlet oxygen exposure to tissues can be determined by using trap molecules experimentally<sup>62,67</sup>.

There are also different types of light sources available for PDT action but the most convenient ones are the lasers. Light source is important since proper wavelength needed for application and dosimetry of light shouldn't be analyzed uncomplicatedly. Also it can be helpful to determine tissue depth for the action<sup>68</sup>.

### **1.1.3 Biological Response**

In the Fig.5, PDT mechanism is illustrated through various scenario possibilities<sup>69</sup>. Tumor damage which is caused by reactive oxygen species could

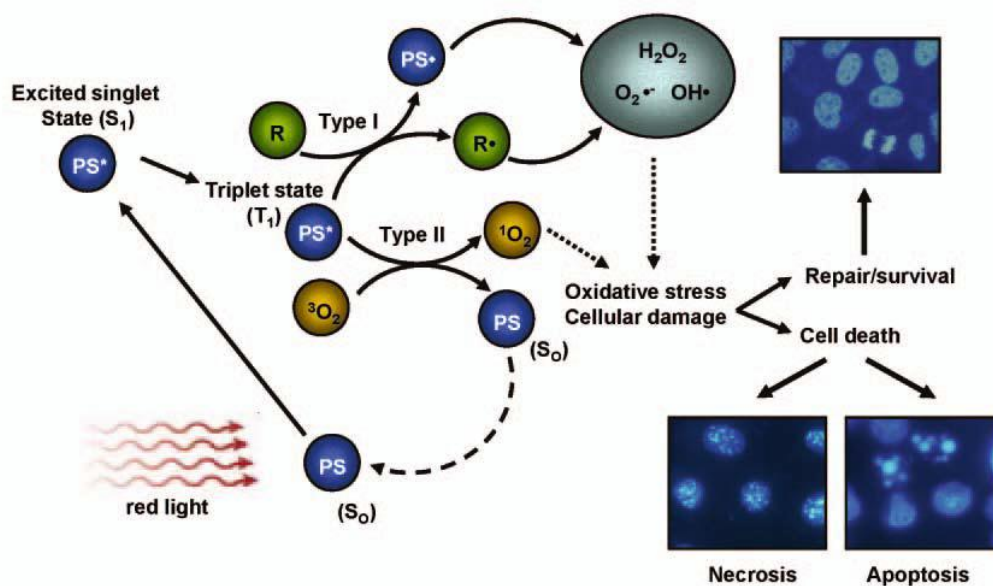


**Figure 5.** Biological Response toward PDT action<sup>69</sup> Copyright © 2008,  
Springer-Milan Adapted with permission

kill cells through necrosis/apoptosis or cells can survive. Three different mechanisms are mostly recognized for antitumor outcome of PDT action<sup>8</sup>. Direct tumor damage can be said as first situation in which singlet oxygen species killed malignant cells directly. In other case damage is given to vasculature causing infraction in malignant tissues. In the last case, immune response to tumor cells can be evoked and the damage will be given by immune system<sup>70</sup>. Contributions of the each case to tumor destruction have been hard to clarify but it is sure that all of them are needed for control of the process<sup>8</sup>. Different studies claimed that necrosis will be dominant at optimum conditions in which adequate light exposure and photosensitizers amount are available. In other possibilities, it could be said that cells will undergo apoptosis mechanism of death. Apoptosis and necrosis mechanism are very different process. Necrosis has known longer than apoptosis in literature. Apoptosis is cell suicide mechanism or programmed cell death toward various effects based on genetic in sum. Necrosis is early death of cells as a response toward generally external effects and accepted as not beneficial process compared to apoptosis<sup>71</sup>.

There are many examples reveal the damage to tumor cells are succeed through vascular destruction. Tumor cells as healthy cells need nutrition supplied from blood vessels to survive even more than healthy cells. Growth factors determine through signals which are produced in tissue the blood vessels progression. Destruction of vasculature system in targeted tissue is promising method for malignant diseases. Hypoxia and anoxia resulting from microvascular collapse are reported in tumor destruction process during PDT action<sup>72,73,74</sup>. There are various studies confirming different photosensitizer's vascular limitation, thrombus generation and decrease in malignant growth. VEGF and other angionic factors are affected during PDT action<sup>75</sup>. Further studies are needed in order to comprehend the vasculator damage mechanism as a result of PDT.

Many important scientists have been showed the direct effect of cell killing through PDT in which optimum conditions are supplied and sufficient reactive oxygen species are generated<sup>76</sup>. Large part of the cell death is performed by the vascular shutdown which leads deficiency of nutrition and oxygen in tumor cells. Photofrin is significant for this concept although it destruct widely tissues around the tumor in unselective manner<sup>75</sup>. Different parameters are effective tumor damage and precluding the direct malignant cell killing. Proximity of the blood vessels is one of the factors that affect the direct cell killing. Depending on the administration methods, distribution of the photosensitizers will vary. Heterogeneous distributions also limit the direct cell killing process in tumor tissue. Another limitation occurs from oxygen deficiency in tumor tissue<sup>26,77,78</sup>. Many reasons can be listed but most important one can be said PDT effects which decrease the amount oxygen concentration<sup>79</sup> depending on the light fluence rate. Direct tumor is not completely negligible part of PDT action. It is a part of the all process, enable us understand its features and close us to solve its full mechanism<sup>80</sup>.

Last tumor damage mechanism is the evoking immune response. However these processes have not been recognized fully, scientists are claiming

that PDT action effects immune system<sup>81</sup>. Both activation and suppression is observed in different type of the photosensitizers present. Activation of specific immune response towards tumor tissue is highlighted research subject in literature<sup>82</sup>. It can be very useful factor in order to fight tumor tissue more effectively. On the contrary, depending on the complex parameters, scientists have also reported suppression of immune response during PDT action<sup>83</sup>. Further investigations are needed to examine potential of PDT as systemic immune therapy<sup>84</sup>.

## **1.2 Activatable PDT Agent**

Depending on the different conditions of tumor tissues than healthy tissues, new methodologies are improved in order to enhance sensitivity of PDT method. Administration of photosensitizer in targeted region could decrease the side effects of PDT action. With the purpose of targeting, several methods can be applied as antibody targeted, protein conjugated, targeting ligand modification and vascular objected. Third generations of photosensitizers are employed by modification of second generation of photosensitizer for targeted purposes. The need for third generation of photosensitizer arouse from the limitations of previous generation. Healthy tissue damage and restricted feasibility of method because of the delivery challenge are significant driving force for researches to improve new more sensitive techniques<sup>6</sup>.

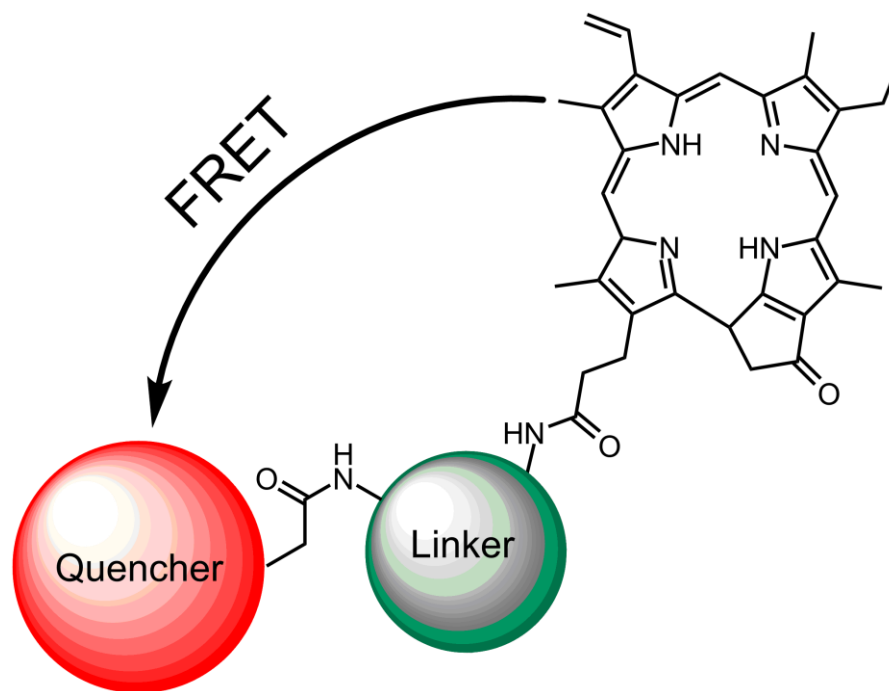
Antibody targeting delivery has been progressed for decades<sup>85,86,87</sup>. However, there is not any example of clinical trials for this established technique yet. Through the recognition of overexpressed antigen over cells, this method let photosensitizer to locate targeted tissue. Although promising results obtained from various studies<sup>88</sup>, this method has some drawbacks which affect the efficiency of PDT action. Because of the high molecular weights of the antibodies compared to photosensitizers, function and the amount of the photosensitizer could be confined to some extent. Antibodies are not the only

option for targeted PDT action. Also other kind of proteins could be used in order to increase therapeutic effects of PDT<sup>89</sup>.

Another promising method is small ligand conjugation<sup>90</sup>. In this technique, small ligands recognize overexpressed molecules over the cell. Folate molecules which are overexpressed in malignant cells can be example of this method. Coupling of the folate molecule with photosensitizer will increase the uptake rate of photosensitizer into cancer cells<sup>91</sup>. Peptides and molecular sugar are also used for targeting function in PDT<sup>92</sup>. VEGF and RGD could be listed for peptide targeting<sup>93</sup>. Nucleic acid based aptamers<sup>94</sup> are also subject to targeting. Various type of cancer is interest of the targeted PDT mechanism. These methods can be manipulated for the purposes. For example, vasculature of the tumor cells can be targeted instead of targeting tumor cells. Due to deficiency of the nutrition and oxygen, tumor cell will be killed through indirect targeting. Prohibition of the activation of photosensitizer in healthy tissue will be the significant advantage of the targeted PDT<sup>95</sup>. Reducing the damage toward the healthy tissue is important for patient's life standards.

Manipulating different mechanism as photophysical properties of photosensitizer, deactivation can be achieved. Through designing activation process within malignant cells, photosensitizer could be used to destruct tumor tissue only. For this purposes, many different type of molecules are proposed and called quencher which change the excitation characteristic of photosensitizer. Quenching methods can use of Förster resonance energy transfer (FRET), photoinduced electron transfer (PeT) and self quenching<sup>96</sup>.

FRET deactivation<sup>97</sup> process is applied through conjugation of chromophore to photosensitizer by linker molecules. FRET is energy transfer process which occur nanometer range. Chromophore as quencher absorbs the energy photosensitizer emits as illustrated in Fig. 6. For this energy transfer,



15

**Figure 6.** FRET deactivated Photosensitizer design

chromophore need to absorb in the range which photosensitizer emits. Also linker length is important parameter in order to determine efficiency of quencher. Longer linker could decrease energy transfer yield due to the FRET distance limitations based on spectral overlap between quencher and photosensitizer. After effective FRET process, fluorescence of the photosensitizer will be quenched thus; singlet oxygen generation will decrease dramatically. In Fig.6, compound 15<sup>97</sup> (pyropheophorbide-a) is used as photosensitizer. Fluorescence rate is used instead of singlet oxygen rate, which is relatively easier to measure. In addition to this design, self-quenching could be employed as other methodology for FRET process. Although using more photosensitizer will increase singlet oxygen rate, solubility problems could arouse through these designs with unpredicted challenges which can affect the reactive oxygen species proportion. FRET deactivation method has shown promising results<sup>97</sup>.

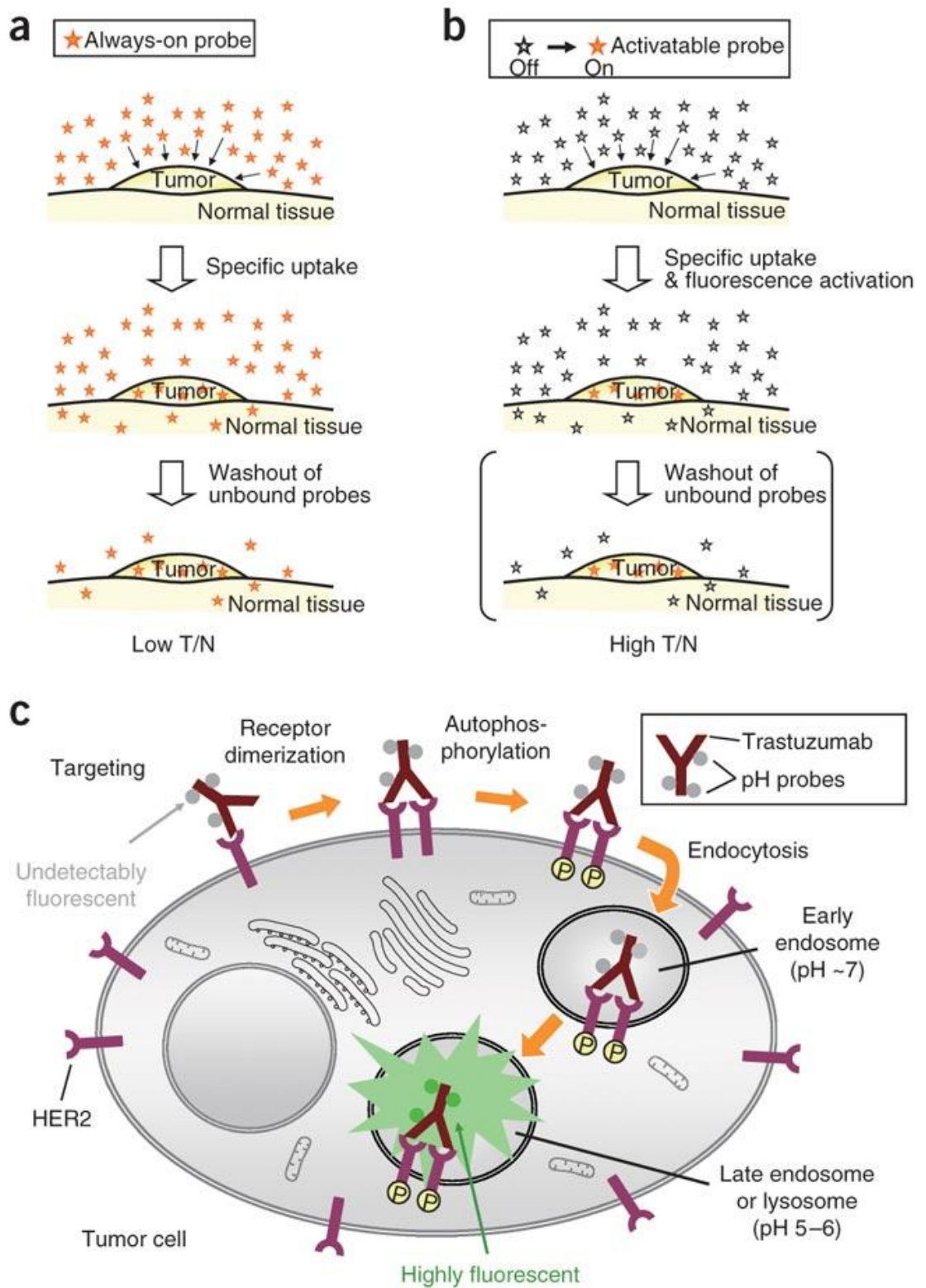


**Figure 7.** Mechanism target-specific activatable probes<sup>98</sup> Copyright © 2008, Rights Managed by Nature Publishing Group, Adapted with permission

The method in which direct use of probe is applied has disadvantages like low tumor to normal cell ratio and background signal. Through activatable photosensitizer design, all of the drawback previously mentioned can be minimized. Illustration of these concepts<sup>98</sup> and also probe-antibody conjugate in cells is available in Fig. 7 which is reported by Urano *et al.*. This representation is an example for breast cancer targeted methodology. HER2 receptor is overexpressed over the tumor cell. Through using monoclonal antibody trastuzumab, targeting is accomplished.

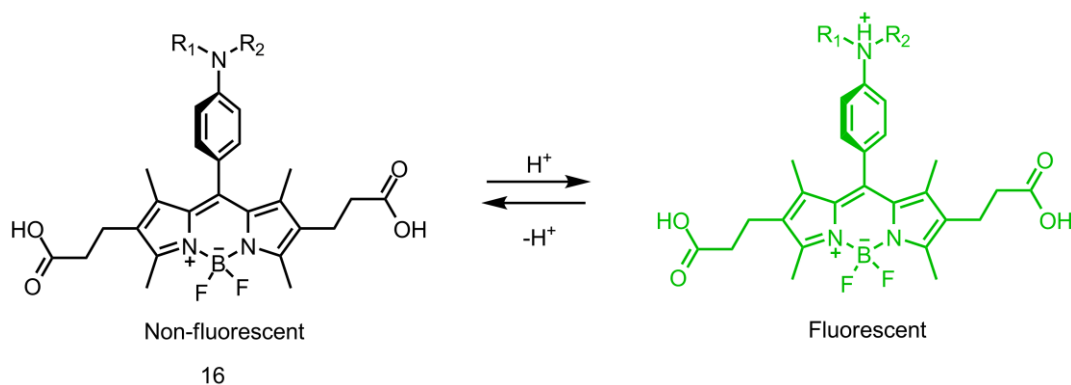


**Figure 8.** pH-activatable Bodipy derivatives

In Fig. 8, an example of off-on switching (compound 16) is reported. Manipulating PeT process, chromophore moiety gets activated in acidic medium. Although this design is used for imaging, it can be modified for PDT action. Activation is achieved based on the pH difference between lysosome (pH 5-6) and cytoplasm (pH 7.4). While PeT process is occurring, energy transfer will not be possible from photosensitizer to molecular oxygen. Hence reactive oxygen species could not be produced. Deactivation of the PeT route through acidic environment in this case will enable singlet oxygen generation<sup>98</sup>.

Also other photosensitizer<sup>99</sup> which is activated through two different parameters is planned as proof of principle by Akkaya *et al.* Crown ether moiety is conjugated to iodinated Bodipy core. PeT process is manipulated in

the crown part of the design. Pyridine moieties are united through third and fifth position through Knoevenagel reaction in order to sense the pH difference between normal tissue and tumor tissues. Design is illustrated in Fig. 9 as compound 17.

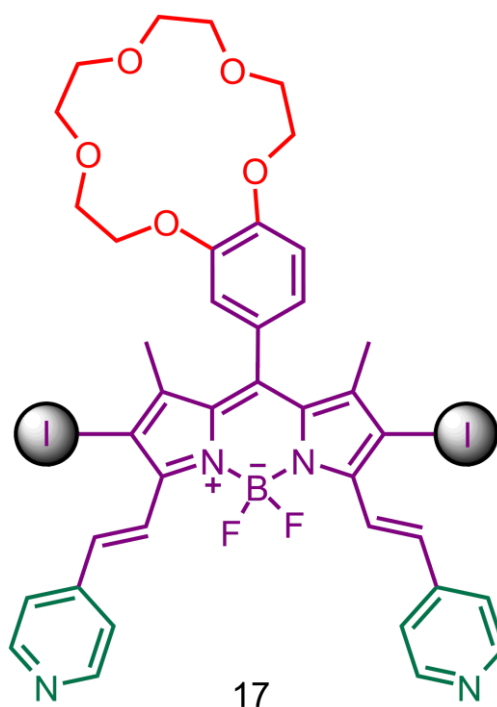


**Figure 9.** Logic gate integrated PDT agent

Based on pH and  $\text{Na}^+$  concentration, AND logic gate is employed as an example of activatable PDT agent. This photosensitizer gets activated in high  $\text{Na}^+$  concentration and acidic environment. If either of them is not case, singlet oxygen level in medium is negligible<sup>99</sup>.

### 1.3 Glutathione Sensing and Signaling

Thiol derivatives such as cysteine (Cys), homocysteine (Hcy) and glutathione (GSH) have important roles in biological activity thus researches have been carried out in order to develop sensitive thiol probes for years. Many

different methods have been improved for these purposes. Different type of reaction mechanism as cleavage and addition has been used for progress. Each of the thiol derivatives mentioned before have different and significant properties<sup>100</sup>. GSH sensing and its mechanism will be our primary subject since its concentration is higher in tumor cells up to 50 folds<sup>101,102</sup> than healthy cells and could be used for PDT action. In order to understand sensing mechanism which used our study, we need to understand firstly PeT mechanism.

### 1.3.1 Photoinduced Electron Transfer and Examples

Photoinduced electron transfer (PET) is a signaling phenomenon which relies on emission intensity. In certain cases, excited molecule can transfer an electron from other potential donor to its low lying orbital before relaxation occurs. The process which is called photoinduced electron transfer has a major role in photosynthesis and is well studied. PET process can be divided into two categories depending on the electron transfer direction between fluorophore and receptor. If donor is fluorophore, process is called oxidative (reverse) PET. In generally seen examples in literature, acceptor is fluorophore as in the case in Fig. 10 and it is called reductive PET<sup>103</sup>.

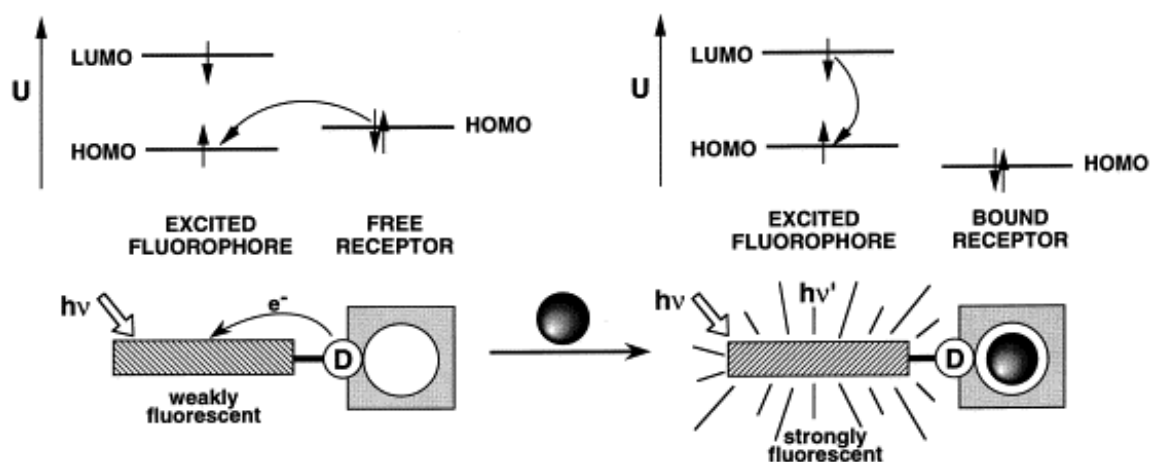


**Figure 10.** Principle of cation recognition by fluorescent PET sensors<sup>103</sup>

Copyright © 2000, Elsevier, Adapted with permission

Fig. 10 demonstrates working principal for PET mechanism in fluoroionophores. In this design, receptor part includes electron donating groups. Due to excitation of fluorophore, an electron from the highest occupied molecular orbital (HOMO) transferred to the lowest unoccupied molecular orbital (LUMO). Electron transfer blocks usual relaxation pathway of excited fluorophore. This route causes quenching of fluorescence until energy level of HOMO of the receptor is lowered through binding of analyte. PET process is disturbed and this let increase in fluorescence<sup>103</sup>.

Beside major role in photochemical reactions in photosynthesis<sup>104</sup>, PET is widely admitted in fluorescent sensor for diverse of analyte as cations, anion and neutral molecules<sup>105,106</sup>. Both of excitation and emission accomplished through fluorophore module. Receptor module is used to control for complexation/ decomplexation with analyte molecule. Spacer parts of the design help to separate fluorophore and receptor but also hold them close enough for electron transfer. These mechanisms can be utilized to develop designs for on- off and off-on systems. In Fig.10 shows control over PET mechanism by using analyte molecules. This design is an example of off-on type signaling system. Upon addition of analyte, fluorescence increases which sense existence of our analyte molecule<sup>107</sup>.

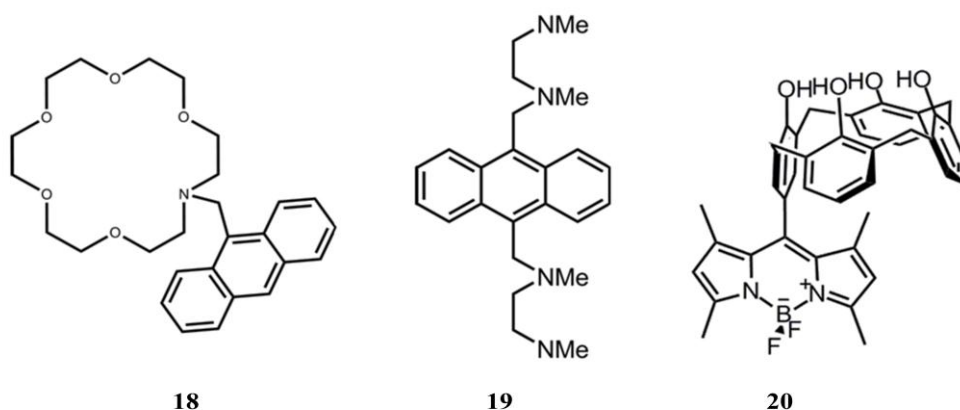


**Figure 11.** Crown containing, podand based and calixarene based PET sensors.

There are many fluorescent chemosensors designed according to this principle. Selectivity for specific ions achieved through appropriate selection of recognition moiety. A typical example is crown ether compounds as a recognition moiety as in Fig. 11, compound 18<sup>108</sup> other example compound 19<sup>109</sup> is podand based PET sensor which is selective for Zn<sup>2+</sup> because of the strong affinity towards to nitrogen atom. Unfortunately, this sensor is working in very limited pH and also sensitive to Cu (II). In the last design<sup>110</sup> by Akkaya group et al., a Bodipy fluorophore is attached to calix[4]arene which is donor part of the design because of the oxygen lone pairs. Protonation of this oxygen made PET route less favorable. With changing pH, up to 10 –fold increase will be observed in fluorescence.

There are also different examples<sup>111</sup> leading us to discover oxidative PET process in which fluorophore act as an electron donor towards electron deficient receptor. One of the examples is reported as a thiol sensor by Nagano<sup>112</sup> illustrated in Figure 4. compound 21.

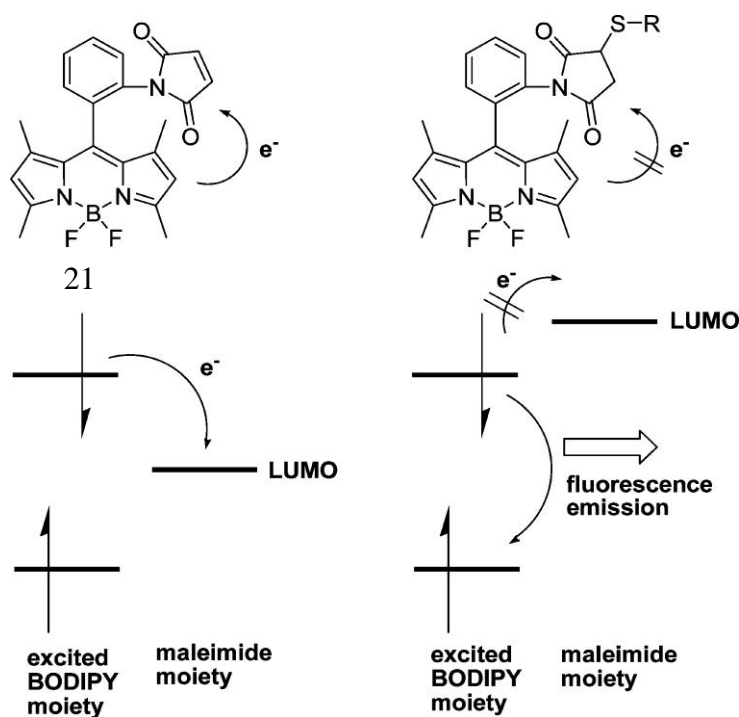


**Figure 12.** Oxidative PET sensor<sup>112</sup> Copyright © 2007, American Chemical Society. Adapted with permission

In this particular example molecule 21, maleimide moiety is utilized as a PET acceptor whereas Bodipy is as fluorophore. Thiol reacts with maleimide and 350-fold increase in fluorescence signal is observed. Also Nagano group study effect of distance between donor and acceptor through using both meta and para- maleimide bound structures. Research shows that Omaleimide is the most efficient PET acceptor than metamaleimide and para-maleimide. Results lead us to conclude that while groups are getting closer, PET is getting more effective<sup>112</sup>.

### 1.3.2 Photoinduced Charge Transfer

One of the other mechanisms which are used to manipulate fluorescence characteristic of molecules is Photoinduced Charge Transfer. Principles of PCT were first introduced in explanation for increase acidity of phenol molecule<sup>113</sup>. On the other hand, generalization of these ideas and utilization in metal sensing could not be understood until Valeur<sup>114,115,116</sup>. In PCT, spacer unit is removed between receptor and signaling modules. Fluorophore is directly integrated with receptor that is part of  $\pi$ -electron system of the fluorophore. Either fluorophore or receptor should be electron rich and other one electron poor. Excitation of this integrated system leads to redistribution of electron density then to substantial dipole which causes Intramolecular charge transfer from donor to acceptor. Interaction between receptor and target molecule results either stabilization of HOMO or LUMO level or destabilization. These energy levels can act independently each other since one of them can be stabilized and other one destabilized, it depends on the molecular structure. These stabilization / destabilization arrange energy difference between HOMO and LUMO levels that can be followed over the reflection over emission or absorption spectra of molecules. Not only electron donor/ acceptor characteristic of receptor but also target molecules ionic features are important for determining red/ blue spectral shifts<sup>117</sup>.

Excited state of fluorophore has similar appearance with resonance structure of molecules. Photophysical properties of the fluorophore will be

changed upon interaction with cation/ anion due to the ion effects on efficiency of Intramolecular charge transfer. For instance electron donating group (amino group) can be part of the fluorophore system and interaction with cation will reduce electron donor nature of it. This change will prepare a basis for reduction of conjugation that can be proved through blue shift. Dipole interactions can be used to illustrate the photophysical changes upon cation binding. Interaction between electron donating groups and cation will destabilize the excited state which results an increase energy gap between  $S_1$  and  $S_0$  energy levels. Due to reciprocal relation between energy and wavelength, this increase in energy will decrease wavelength. Existence of analyte (targeting moiety) can be turn to a signal through blue shift as illustrated in Fig. 13<sup>103</sup>.

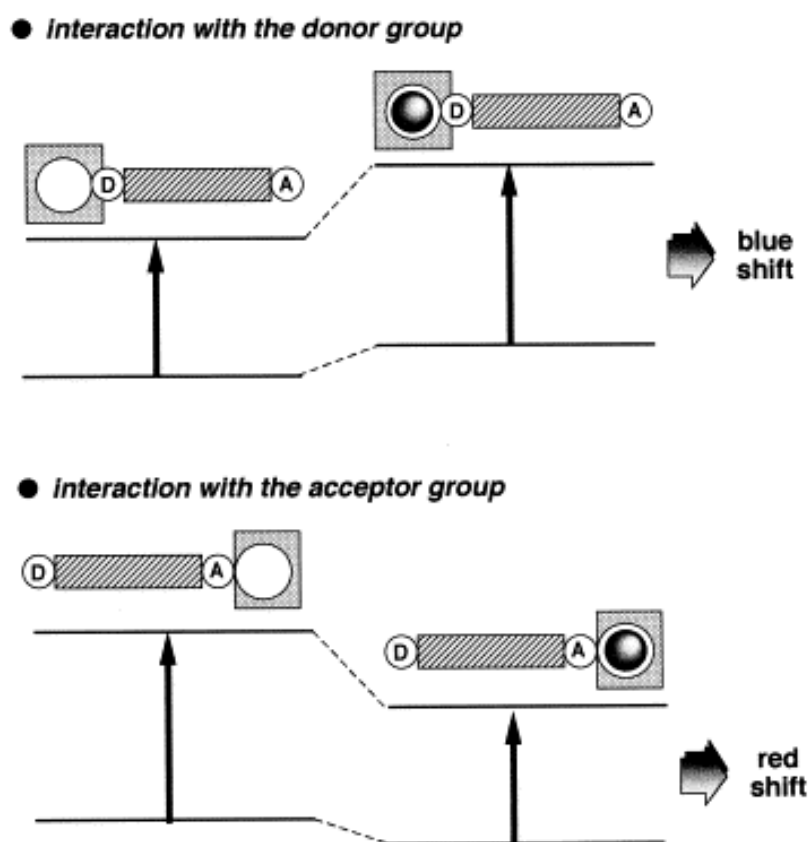


**Figure 13.** Spectral displacements of PCT sensors<sup>103</sup>. Copyright © 2000, Elsevier, Adapted with permission

On the contrary, interaction between cation and acceptor group (carbonyl) will be different. This will increase the electron withdrawing nature of this group and excited state will be stabilized more due to charge-dipole interaction. If the excited state is analyzed, we need to consider the resonance structure of the acceptor group; the carbonyl group will be negatively charged, which leads to the stabilization of the excited state with the help of interaction between the cation and the acceptor group. Stabilization will decrease the energy gap between  $S_1$  and  $S_0$ . In this example, the signal of the analyte will be obtained through a red shift in both absorption and emission spectra as a result of the decrease in energy gap as in Fig. 13.<sup>103</sup> In PCT, both of the fluorescence and absorption spectra will shift towards the same direction, either of blue or red shift. Effects of charge and size of the cation cannot be ignored in this process<sup>117</sup>.

Many fluoroionophores have been designed according to these principles, including azacrown groups as a cation receptor conjugated to an electron withdrawing group to sense a cation<sup>116,118</sup>.

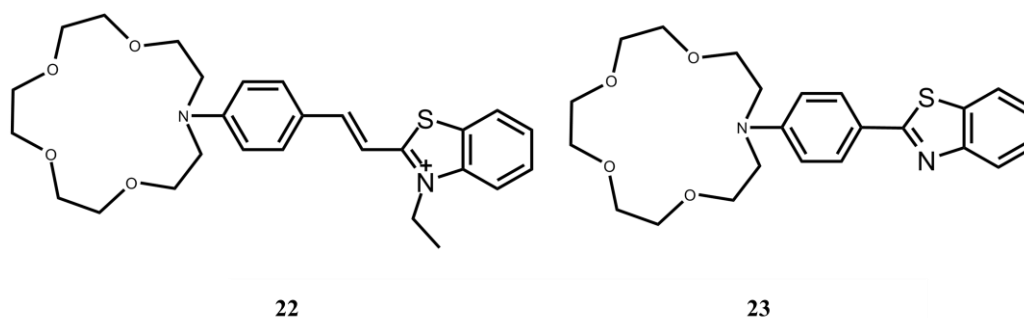


**Figure 14.** Crown containing PCT sensors.

Upon cation binding, compounds 22<sup>119</sup> and 23<sup>120</sup> show a blue shift in both absorption and emission spectra according to the PCT mechanism in Fig. 14. There are also many other examples.

Other fluorescent thiol (compound 24<sup>121</sup>) probe is introduced by Lin *et al.*. Diethylaminocoumarin is used as the fluorophore moiety in Fig. 15. The fluorophore is also conjugated to an  $\alpha,\beta$ -unsaturated ketone in order to sense thiol

groups. Through pyridine moiety ICT can draw out from diethyl amino group to pyridine group. After interaction with the thiol groups, conjugation of the pyridine group to the chromophore will be blocked also ICT process too.

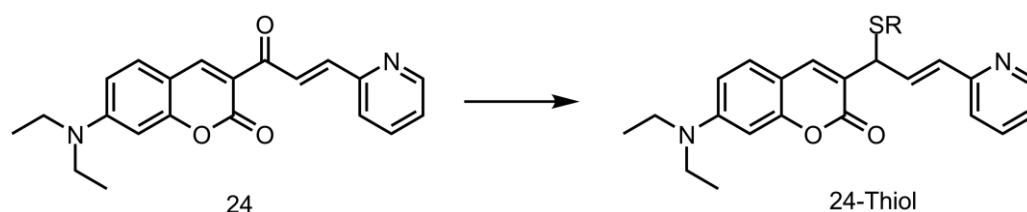


**Figure 15.** ICT dependent thiol Probe

Compound 24 shows low fluorescence intensity compared to 24-thiol compound. The reason can be non-fluorescent ICT mode. This difference let the use of this compound as off-on probe for thiol groups<sup>121</sup>.

### 1.3.3 FRET Based Sensing

Förster resonance energy transfer (FRET) or through space energy transfer is a nonradiative process which does not depend on the orbital interaction. An excited state donor transfers energy to a proximal ground state acceptor through long range dipole-dipole interactions. In this mechanism, it is more likely to observe larger separation between donor and acceptor molecules.

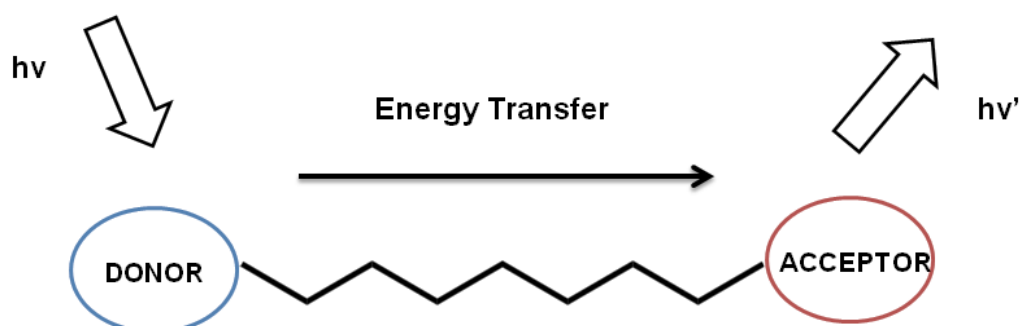


**Figure 16.** Schematic representation Förster-type (through-space) energy transfer.

The spectral overlap<sup>122,123</sup> between donor emission and acceptor absorbance is significantly important while there is no conjugation between donor and acceptor units as in Fig. 16.

Other deactivation process<sup>124</sup> will compete with energy transfer process since it is through bond. Internal conversion through vibrational relaxation, quantum yield of donor are a few examples of photophysical properties of chromophore that can cause deactivation process.

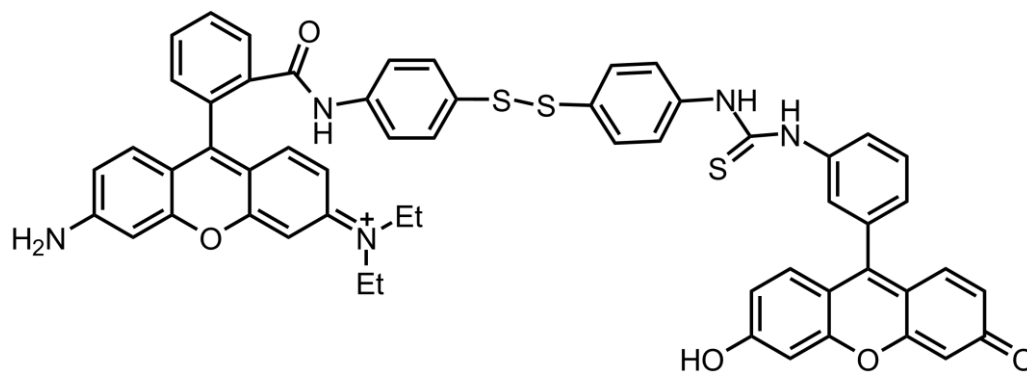
Donor (D) and acceptor (A) units separated by a distance of R, energy transfer rate ( $k_{\text{FRET}}$ ) can be defined by using Förster distance ( $R_0$ ) which is the distance between donor and acceptor units at which half of excited molecules transfer energy to acceptor molecules as in the equation below.

$$R_0 = 9.78 \times 10^3 [\kappa^2 n^{-4} Q_D J(\lambda)] \quad (\text{equation 2})$$

$$k_{\text{FRET}} = [900 (\ln 10) \kappa^2 \Phi_D J(\lambda)] / [128 \pi^5 n^4 N \tau_D R_{DA}^6] \quad (\text{equation 3})$$

In these equations,  $\kappa$  represents the orientation factor between excited state donor and ground state acceptor where it is related with dipole-dipole interaction of donor and acceptor units.  $n$  stands for refractive index of the solvent where  $Q_D$  stands for the quantum yield of donor in the absence of acceptor unit.  $J$  is Förster overlap integral of donor emission and acceptor absorbance,  $\tau_D$  is lifetime of excited donor without of acceptor unit. Last of all  $R_{DA}$  is the distance between donor and acceptor. As it is in 6<sup>th</sup> power, importance of distance is obvious<sup>41</sup>. Generally it should be between 10-100 Å to be effective<sup>125</sup>.

In Fig. 6, compound 15 is an example for manipulation of FRET process. Another example is compound 25<sup>126</sup> which is proposed by Karuso *et al.* in Fig. 17. Disulfide linker is used here for thiol sensitivity. Fluorescein and Rhodamine



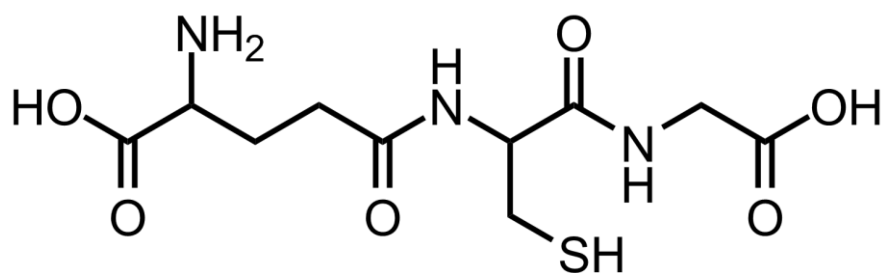
25

**Figure 17.** FRET based thiol sensing probe based chromophores used for energy transfer.

Upon addition of GSH, cleavage of the disulfide bond occurs which lead diminish in FRET yield and enhance fluorescence intensity at 520nm<sup>126</sup>.

### 1.3.4 Other Process and Examples

GSH structure<sup>100</sup> is demonstrated in Fig.18. Different types of methodologies for sensing mechanism have been developed. One of them is using maleimide moiety conjugated to different molecules. One of the examples for this method has been shown in Fig.12. Michael addition is taking place through manipulating PeT process<sup>112</sup>.



**Glutathione (GSH)**

**Figure 18.** GSH structure

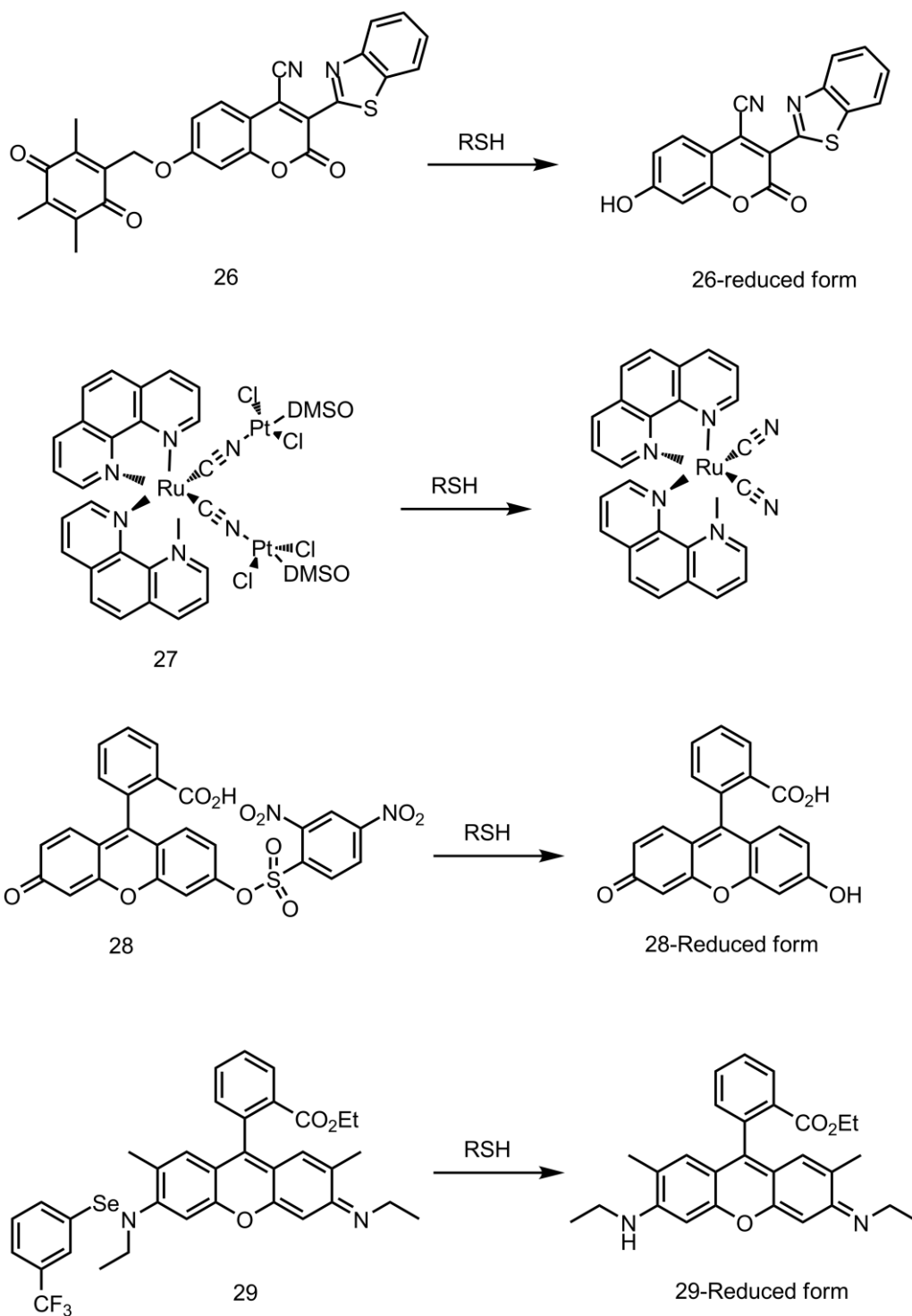


**Figure 19.** Structures of Thiol Probes

One of the examples is available in Fig. 19 as compound 26<sup>127</sup> for quinone-methide type rearrangement due to results obtained from experiments. Huang *et al.* proposed new fluorimetric probe for detection of biological

probes. Spontaneous and irreversible reaction takes place with the thiol derivatives. These probe could be used various purpose for sensing glutathione over amino acids.

Another method is based on displacement approach with the example compound 27. Lam *et al.* presented a neutral trinuclear heterobimetallic cyano-bridged Ru (II)/Pt (II) complex, cis-Ru(phen)<sub>2</sub>-[CN-Pt(DMSO)Cl<sub>2</sub>]<sub>2</sub> an example<sup>128</sup> for thiol sensing. Emission of the complex is diminished through the re-organization due to cyano groups. After addition of thiol group, Pt and thiol are coordinated which lead the increase of the emission again. GSH could be determined using this mechanism depending on the emission intensity change.

GSH could be sensed through cleavage of sulfonamide and sulfonate ester as in the case for compound 28. Maeda *et al.* propose combination of the Rhodamine dye and the 2, 4-dinitrobenzenesulfonyl (DNBS) moiety<sup>129</sup>. Fluorescence intensity enhance after the cleavage of the DNBS group. The probe is very sensitive towards the GSH and gives quick response.

The last example stands for Se-N cleavage based sensing mechanism. Tang *et al.* reported compound 29, fluorescence probe for glutathione sensing which is based on combination of Rhodamine dye and Se-N bonds<sup>130</sup>. Fluorescence intensity increases through the cleavage of the Se-N bonds. Sensing could be achieved by manipulating fluorescence intensity.

## CHAPTER 2

### EXPERIMENTAL

#### 2.1. General

All chemicals and solvents obtained from Sigma-Aldrich were used without further purification. Reactions were monitored by thin layer chromatography using Merck TLC Silica gel 60 F<sub>254</sub>. Chromatography on silica gel was performed over Merck Silica gel 60 (particle size: 0.040-0.063 mm, 230-400 mesh ASTM).

<sup>1</sup>H NMR and <sup>13</sup>C NMR spectra were recorded at room temperature on Bruker DPX-400 (operating at 400 MHz for <sup>1</sup>H NMR and 100 MHz for <sup>13</sup>C NMR) in CDCl<sub>3</sub> with tetramethylsilane (TMS) as internal standard. Coupling constants (*J values*) are given in Hz and chemical shifts are given in parts per million (ppm). Splitting patterns are designated as s (singlet), d (doublet), t (triplet), q (quartet), m (multiplet), and p (pentet). Mass spectra were recorded with Agilent Technologies 6224 TOF LC/MS

Absorption spectra in solution were obtained using a Varian Cary-100 and Varian Cary 5000 UV-VIS-NIR absorption spectrophotometer. Fluorescence measurements were done on a Varian Eclipse spectrofluorometer. Spectrophotometric grade solvents were used for spectroscopy experiments. Bodipy dyes are synthesized as activatable photosensitizer for photodynamic therapy. For water solubility 3,4,5-tris(2-(2-(2-methoxyethoxy)ethoxy)ethoxy) benzaldehyde<sup>23</sup> were synthesized according to literature.

## 2.2. Synthesis of Target Molecules

### 2.2.1. Synthesis of Compound 30

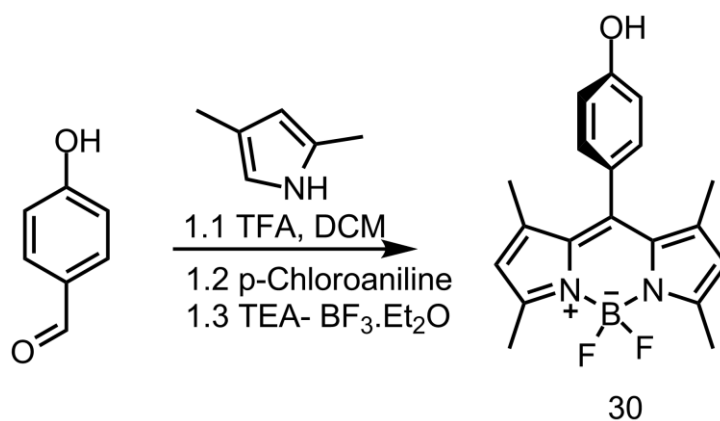


**Figure 20.** Synthesis of Compound 30

To a stirred argon degassed solution of  $\text{CH}_2\text{Cl}_2$  (300 mL) for 30 min, 2,4-dimethyl pyrrole (12.3 mmol, 1.17 g) and 4-hydroxybenzaldehyde (6.0 mmol, 0.75 g) were added in it under argon atmosphere. 1-2 drops of TFA was added, mixture stirred for overnight at room temperature. Then p-Chloranil (6.0 mmol, 0.77 g) in 30 ml  $\text{CH}_2\text{Cl}_2$  was added to the reaction mixture, stirring was continued for 2-3 h. After 2-3 h,  $\text{Et}_3\text{N}$  (5 mL) and  $\text{BF}_3\cdot\text{OEt}_2$  (5 mL) were introduced. 100 mL of water was added into the reaction mixture and then extracted into the  $\text{CHCl}_3$  (3 x 100 mL).  $\text{Na}_2\text{SO}_4$  was used as a drying agent. The organic layer was concentrated *in vacuo* and the crude product was purified by column chromatography packed with silica gel using  $\text{CHCl}_3$  as the eluant. Orange-Red solid was obtained (0.65 g, 32 %).  $^1\text{H}$  NMR (400 MHz,  $\text{CDCl}_3$ ):  $\delta_{\text{H}}$  7.14 (d,  $J = 8.2$  Hz, 2H, ArH), 6.97 (d,  $J = 8.5$  Hz, 2H, ArH), 6.00 (s, 2H, ArH), 2.57 (s, 6H,  $\text{CH}_3$ ), 1.46 (s, 6H,  $\text{CH}_3$ ).  $^{13}\text{C}$  NMR (100 MHz,  $\text{CDCl}_3$ ):  $\delta_{\text{C}}$  156.36, 155.32, 143.19, 141.80, 132.02, 129.39, 127.15, 121.16, 116.12, 14.57 ppm. MS (TOF- ESI):  $m/z$ : Calcd for  $\text{C}_{19}\text{H}_{19}\text{BF}_2\text{N}_2\text{O}$ : 338.1558  $[\text{M}-\text{H}]^-$ , Found: 338.1493  $[\text{M}-\text{H}]^-$ ,  $\Delta=8.71$  ppm.

### 2.2.2. Synthesis of Compound 31

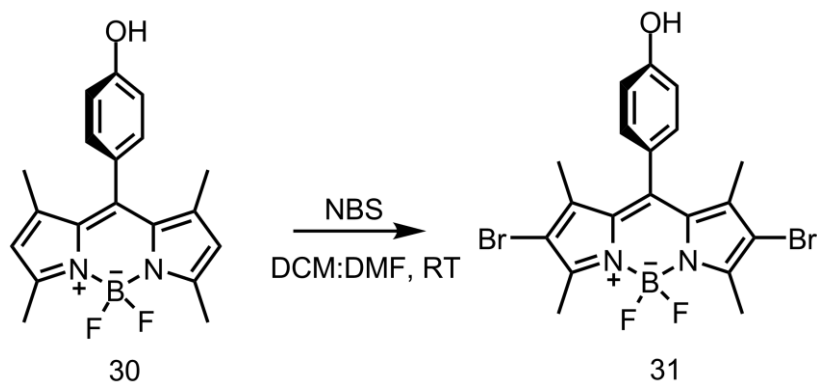


**Figure 21.** Synthesis of Compound 31

Compound **30** (0.176 mmol, 60 mg) is dissolved in 20 mL mixture (DMF/DCM, 1:1, v/v). Then, *N*-Bromosuccinimide (0.37 mmol, 66mg) is dissolved in DCM (10 mL) and added dropwise to reaction mixture. The mixture is stirred at room temperature. The reaction is monitored by TLC. After finishing starting material, reaction is stopped by adding 100 mL of water. The mixture is extracted into DCM (3x 100 mL). The organic phase was dried over  $\text{Na}_2\text{SO}_4$  and concentrated *in vacuo*. Then crude product was purified by silica gel column chromatography (Acetone/ Hexane, 1:4, v/v). Red solid was obtained (0.084 g, 95%).  $^1\text{H}$  NMR (400 MHz,  $\text{CDCl}_3$ ):  $\delta_{\text{H}}$  7.13 (d,  $J = 8.97$  Hz, 2H, ArH), 7.01 (d,  $J = 8.5$  Hz, 2H, ArH), 5.18 (s, H, OH), 2.62 (s, 6H,  $\text{CH}_3$ ), 1.47 (s, 6H,  $\text{CH}_3$ ).  $^{13}\text{C}$  NMR (100 MHz,  $\text{CDCl}_3$ ):  $\delta_{\text{C}}$  161.2, 157.33, 146.87, 144.69, 134.71, 132.89, 128.95, 120.16, 114.52, 17.49 ppm. MS (TOF-ESI):  $m/z$ : Calcd for  $\text{C}_{19}\text{H}_{17}\text{BBr}_2\text{F}_2\text{N}_2\text{O}$ : 493.9769  $[\text{M}-\text{H}]^-$ , Found: 493.9713  $[\text{M}-\text{H}]^-$ ,  $\Delta=3.87$  ppm.

### 2.2.3. Synthesis of Compound 32

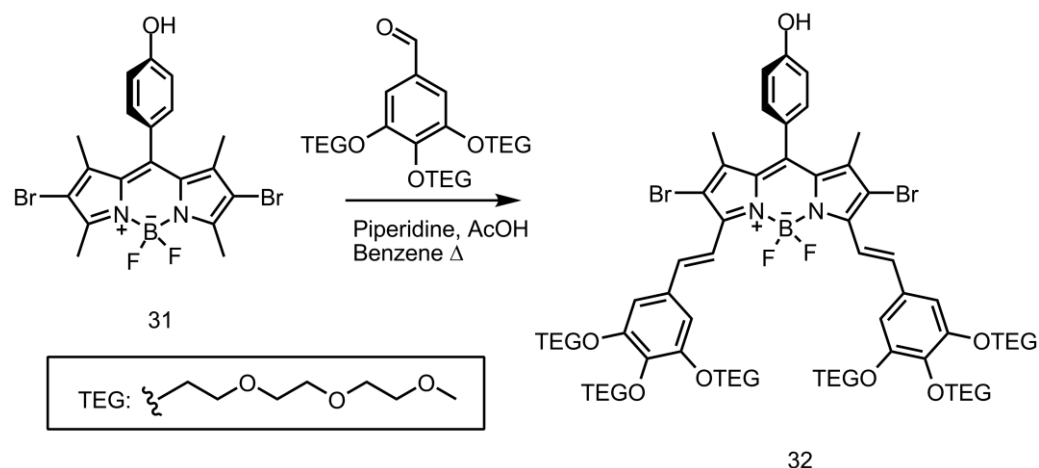


**Figure 22.** Synthesis of Compound 32

Compound **31** (0.187 mmol, 93 mg) and 3,4,5-tris(2-(2-(2-methoxyethoxy)ethoxy)ethoxy) benzaldehyde (0.393 mmol, 233 mg) were added into a 100 mL round-bottomed flask equipped with a Dean-Stark apparatus. 40 mL of benzene, acetic acid (0.2 mL) and piperidine (0.2 mL) were added and mixture were stirred at reflux temperature. The reaction was monitored by TLC and continued until starting material was finished. Water (100 mL) was added to reaction mixture which was cooled to room temperature. Mixture was extracted into DCM (3x 100 mL). The organic phase was dried over  $\text{Na}_2\text{SO}_4$  and concentrated *in vacuo*. The crude product was purified by silica gel column chromatography (DCM/ MeOH, 95:5, v/v). The product was collected as green solid (130 mg, 42 %).  $^1\text{H}$  NMR (400 MHz,  $\text{CDCl}_3$ ):  $\delta_{\text{H}}$  7.90 (d,  $J = 16.5$  Hz, 2H, CH), 7.44 (d,  $J = 16.6$  Hz, 2H, CH), 7.09 (d,  $J = 8.3$  Hz, 2H, ArH), 6.94 (d,  $J = 8.3$  Hz, 2H, ArH), 6.84 (s, 4H, ArH), 4.22 (t,  $J = 4.9$  Hz, 14H,  $\text{OCH}_2$ ), 3.88 (t,  $J = 4.9$  Hz, 8H,  $\text{OCH}_2$ ), 3.83 (t,  $J = 4.9$  Hz, 4H,  $\text{OCH}_2$ ), 3.78 – 3.73 (m, 14H,  $\text{OCH}_2$ ), 3.71 – 3.62 (m, 28H,  $\text{OCH}_2$ ), 3.58 (dd,  $J = 6.0, 3.4$  Hz, 4H,  $\text{OCH}_2$ ), 3.55 – 3.51 (m, 8H,  $\text{OCH}_2$ ), 3.40 (s, 6H,  $\text{OCH}_3$ ), 3.36 (s, 10H,  $\text{OCH}_3$ ), 1.41 (s, 6H,  $\text{CH}_3$ ).  $^{13}\text{C}$  NMR (100 MHz,  $\text{CDCl}_3$ ):  $\delta_{\text{C}}$  157.75, 152.82, 147.78, 141.16, 140.02, 138.64, 133.07, 132.43, 129.63,

126.15, 117.36, 116.45, 110.09, 107.54, 72.50, 71.92, 70.63, 69.74, 69.02, 58.98, 14.08 ppm. MS (TOF- ESI):  $m/z$ : Calcd for  $C_{75}H_{109}BBr_2F_2N_2O_{25}$ : 1642.5747  $[M-H]^-$ , Found: 1642.5585  $[M-H]^-$ ,  $\Delta=9.86$  ppm.

## 2.2.4. Synthesis of Compound 33

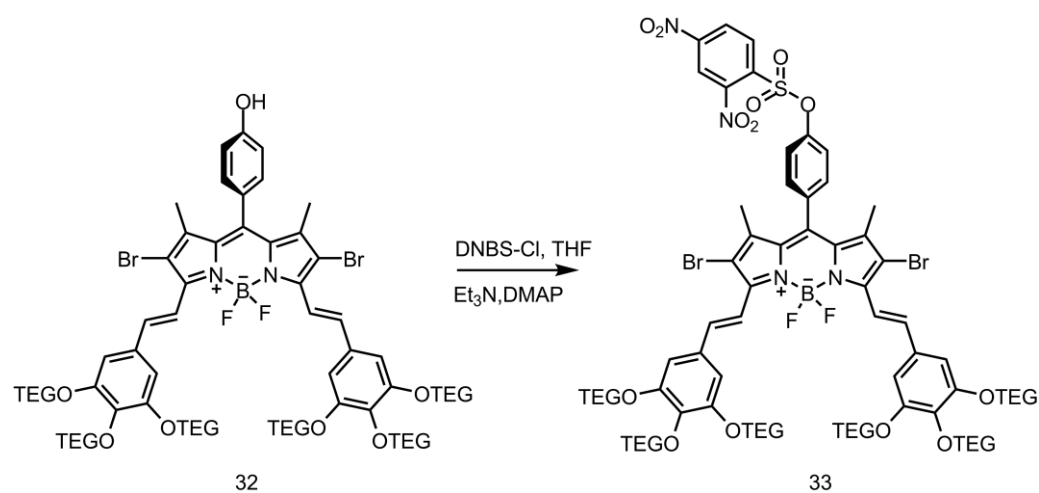


**Figure 23.** Synthesis of Compound 33

Compound **32** (0.24 mmol, 400 mg) was dissolved in dry THF (30 mL). Then triethylamine (0.12 mL) was added and stirred for 30 min at room temperature. A solution of 2, 4-dinitrobenzenesulfonyl chloride (0.77 mmol, 200 mg) in dry THF (20 mL) was added dropwise at 0 °C. The mixture was heated to 40 °C and stirred for overnight. Then reaction was cooled to room temperature and solvent was evaporated. Crude product was purified by silica gel column chromatography (DCM/ MeOH, 95:5, v/v). The product was collected as pale green solid (274 mg, 60 %).  $^1H$  NMR (400 MHz,  $CDCl_3$ ):  $\delta_H$  8.71 (s, 1H), 8.57 (dd,  $J = 8.6, 2.2$  Hz, 1H, ArH), 8.26 (d,  $J = 8.6$  Hz, 1H, ArH), 7.98 (d,  $J = 16.5$  Hz, 2H, CH), 7.50 (s, 1H), 7.47 – 7.42 (m, 2H, CH), 7.41 – 7.31 (m, 3H, ArH), 6.86 (s, 4H, ArH), 4.22 (dt,  $J = 7.5, 5.4$  Hz, 15H,  $OCH_2$ ), 3.90 – 3.84 (m, 9H,  $OCH_2$ ), 3.84 – 3.79 (m, 6H,  $OCH_2$ ), 3.77 – 3.70 (m, 15H,  $OCH_2$ ), 3.68 – 3.60 (m, 30H,  $OCH_2$ ), 3.59 – 3.54 (m, 5H,  $OCH_2$ ), 3.53 (dt,  $J =$

4.5, 3.9 Hz, 12H, OCH<sub>2</sub>), 3.39 (s, 5H, OCH<sub>3</sub>), 3.36 (s, 12H, OCH<sub>3</sub>), 1.38 (s, 6H, CH<sub>3</sub>). <sup>13</sup>C NMR (100 MHz, CDCl<sub>3</sub>): δ<sub>C</sub> 152.90, 151.16, 149.54, 148.97, 140.46, 140.09, 136.67, 135.01, 133.77, 133.28, 132.09, 130.69, 126.44, 123.34, 120.52, 116.85, 111.10, 107.79, 72.51, 71.93, 70.63, 69.71, 69.09, 58.99, 14.02 ppm.

### 2.2.5. Synthesis of Compound 34

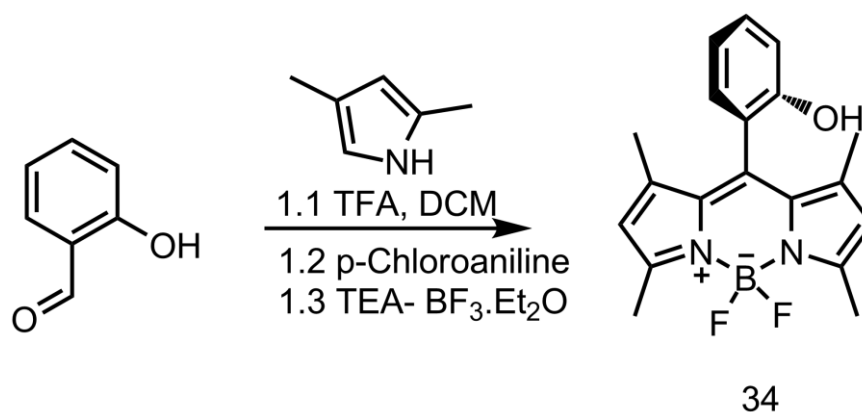


**Figure 24.** Synthesis of Compound 34

To a stirred argon degassed solution of 300 mL CH<sub>2</sub>Cl<sub>2</sub> for 30 min, 2,4-dimethyl pyrrole (12.3 mmol, 1.17 g) and 2-hydroxybenzaldehyde (6.0 mmol, 0.75 g) were added in it under argon atmosphere. 1-2 drops of TFA is added, mixture stirred for overnight at room temperature. Then p-Chloroaniline (6.0 mmol, 0.77 g) in 30 ml CH<sub>2</sub>Cl<sub>2</sub> is added to the reaction mixture, stirring was continued for 2-3 h. After 2-3 h, Et<sub>3</sub>N (5 mL) and BF<sub>3</sub>.OEt<sub>2</sub> (5 mL) were introduced. 100 mL of water was added into the reaction mixture and then extracted into the CHCl<sub>3</sub> (3 x 100 mL). Na<sub>2</sub>SO<sub>4</sub> was used as a drying agent. The organic layer was concentrated *in vacuo* and the crude product was purified by column chromatography packed with silica gel using (CHCl<sub>3</sub>) as the eluant. Orange solid (0.51 g, 25%). <sup>1</sup>H NMR (400 MHz, CDCl<sub>3</sub>): δ<sub>H</sub> 7.40 (t, *J* = 7.2 Hz, 1H, ArH), 7.14 (d, *J* = 6.3 Hz, 1H, ArH), 7.08 (t, *J* = 7.4 Hz, 1H, ArH), 7.03 (d,

$J = 8.2$  Hz, 1H, ArH), 6.02 (s, 2H, ArH), 2.58 (s, 6H, CH<sub>3</sub>), 1.53 (s, 6H, CH<sub>3</sub>).  
<sup>13</sup>C NMR (100 MHz, CDCl<sub>3</sub>):  $\delta_C$  156.26, 152.29, 142.79, 135.09, 131.11, 129.16, 121.68, 121.55, 120.95, 116.54, 14.64, 13.72 ppm. MS (TOF- ESI):  
m/z: Calcd for C<sub>19</sub>H<sub>19</sub>BF<sub>2</sub>N<sub>2</sub>O: 338.1558 [M-H]<sup>-</sup>, Found: 338.1523 [M-H]<sup>-</sup>,  
 $\Delta=0.1$  ppm.

### 2.2.6. Synthesis of Compound 35

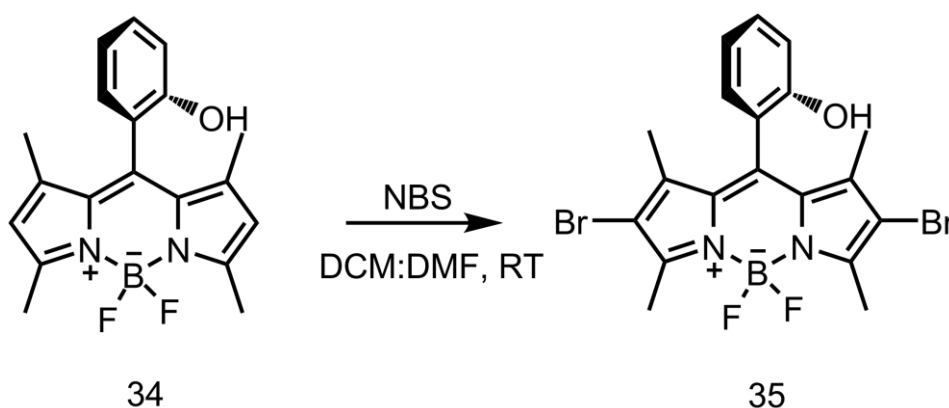


**Figure 25.** Synthesis of Compound 35

Compound **34** (0.176 mmol, 60 mg) is dissolved in 20 mL mixture (DMF/DCM, 1:1, v/v). Then, *N*-Bromosuccinimide (0.37 mmol, 66mg) is dissolved in DCM (10 mL) and added dropwise to reaction mixture. The mixture is stirred at room temperature. The reaction is monitored by TLC. After finishing starting material, reaction is stopped by adding 100 mL of water. The mixture is extracted into DCM (3x 100 mL). The organic phase was dried over Na<sub>2</sub>SO<sub>4</sub> and concentrated *in vacuo*. Then crude product was purified by silica gel column chromatography (EtOAc/ Hexane, 1:6, v/v). Red solid was obtained (0.031 g, 35%). <sup>1</sup>H NMR (400 MHz, CDCl<sub>3</sub>):  $\delta_H$  7.45 (dt,  $J = 8.7, 4.4$  Hz, 1H, ArH), 7.11 (d,  $J = 4.3$  Hz, 2H, ArH), 7.04 (d,  $J = 8.3$  Hz, 1H, ArH), 4.96 (s, 1H, OH), 2.63 (s, 6H, CH<sub>3</sub>), 1.53 (s, 6H, CH<sub>3</sub>). <sup>13</sup>C NMR (100 MHz, CDCl<sub>3</sub>):  $\delta_C$  131.63, 129.09, 122.06, 120.57, 116.78, 31.60, 29.21, 22.51, 14.18, 13.75,

13.02, 1.01 ppm. MS (TOF- ESI):  $m/z$ : Calcd for  $C_{19}H_{17}BBr_2F_2N_2O$ : 493.9769  
[ $M-H$ ]<sup>-</sup>, Found: 493.9772 [ $M-H$ ]<sup>-</sup>,  $\Delta=5.47$  ppm.

### 2.2.7. Synthesis of Compound 36

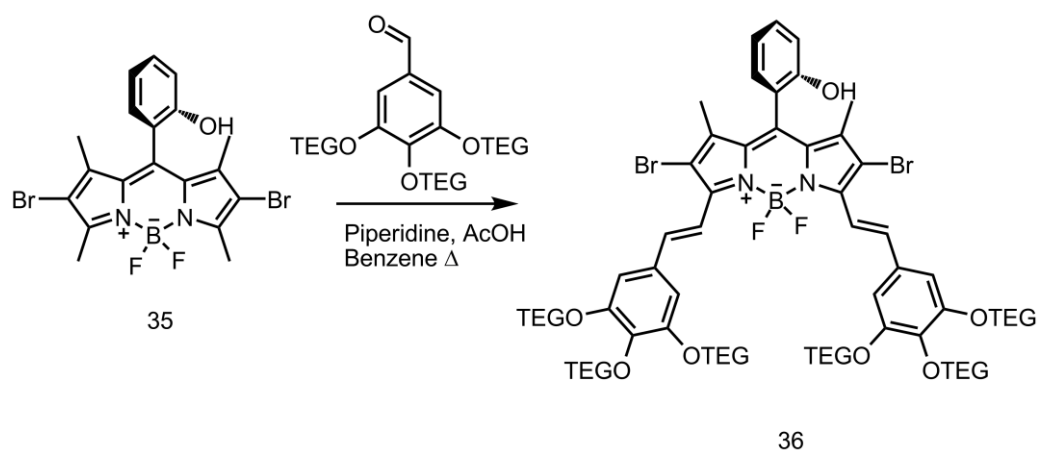


**Figure 26.** Synthesis of Compound 36

Compound **35** (0.193 mmol, 96 mg) and 3,4,5-tris(2-(2-(2-methoxyethoxy)ethoxy)ethoxy)benzaldehyde (0.405 mmol, 240 mg) were added into a 100 mL round-bottomed flask equipped with a Dean-Stark apparatus. 40 mL of benzene, acetic acid (0.2 mL) and piperidine (0.2 mL) were added and mixture was stirred at reflux temperature. The reaction was monitored by TLC and continued until starting material was finished. Water (100 mL) was added to reaction mixture which was cooled to room temperature. Mixture was extracted into DCM (3x 100 mL). The organic phase was dried over  $Na_2SO_4$  and concentrated in vacuo. The crude product was purified by silica gel column chromatography (DCM/ MeOH, 95:5, v/v). The product was collected as green solid (134 mg, 41 %).  $^1H$  NMR (400 MHz,  $CDCl_3$ ):  $\delta_H$  7.96 (d,  $J = 16.5$  Hz, 2H, CH), 7.33 (dd,  $J = 9.7, 5.3$  Hz, 2H, ArH), 7.00 (s, 2H, ArH), 6.97 (d,  $J = 4.5$  Hz, 2H, ArH), 6.88 (s, 2H, ArH), 4.26 (t,  $J = 4.7$  Hz, 8H,  $OCH_2$ ), 4.18 (dd,  $J = 10.3, 5.1$  Hz, 4H,  $OCH_2$ ), 3.88 (t,  $J = 4.8$  Hz, 10H,  $OCH_2$ ), 3.81 (t,  $J = 5.0$  Hz, 4H,  $OCH_2$ ), 3.74 (dd,  $J = 8.8, 3.8$  Hz, 14H,

OCH<sub>2</sub>), 3.70 – 3.61 (m, 28H, OCH<sub>2</sub>), 3.55 (dd, *J* = 7.6, 3.5 Hz, 6H, OCH<sub>2</sub>), 3.54 – 3.50 (m, 10H, OCH<sub>2</sub>), 3.38 (s, 6H, OCH<sub>3</sub>), 3.35 (s, 10H, OCH<sub>3</sub>), 1.26 (s, 6H, CH<sub>3</sub>). <sup>13</sup>C NMR (100 MHz, CDCl<sub>3</sub>): δ<sub>C</sub> 213.74, 153.15, 152.74, 148.04, 141.26, 140.20, 139.25, 132.64, 132.09, 131.50, 129.12, 121.25, 120.82, 116.90, 116.59, 110.53, 107.78, 72.45, 71.90, 70.81, 70.66, 70.52, 69.70, 69.03, 58.99, 12.88 ppm. MS (TOF- ESI): *m/z*: Calcd for C<sub>75</sub>H<sub>109</sub>BBr<sub>2</sub>F<sub>2</sub>N<sub>2</sub>O<sub>25</sub>: 1642.5747 [M-H]<sup>-</sup>, Found: 1642.5604 [M-H]<sup>-</sup>, Δ=8.72 ppm.

### 2.2.8. Synthesis of Compound 37

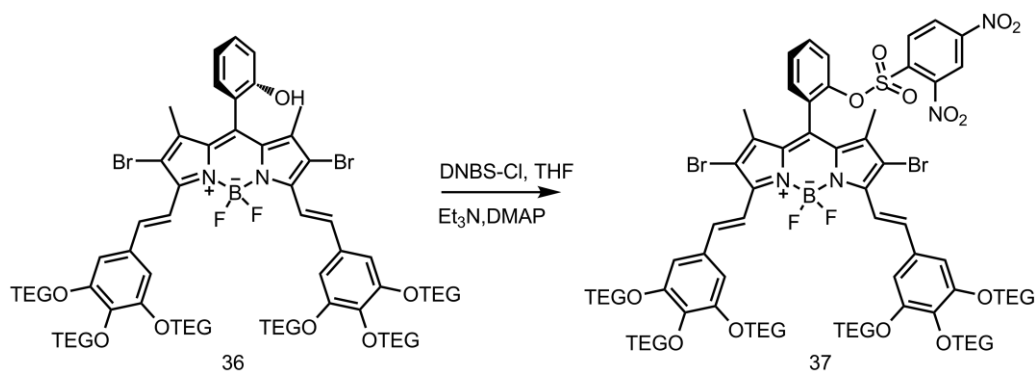


**Figure 27.** Synthesis of Compound 37

Compound **36** (0.14 mmol, 230 mg) was dissolved in dry THF (30 mL). Then triethylamine (0.12 mL) was added and stirred for 30 min at room temperature. A solution of 2, 4-dinitrobenzenesulfonyl chloride (0.77 mmol, 200 mg) in dry THF (20 mL) was added dropwise at 0 °C. The mixture was heated to 40 °C and stirred for overnight. Then reaction was cooled to room temperature and solvent was evaporated. Crude product was purified by silica gel column chromatography (DCM/ MeOH, 95:5, v/v). The product was collected as pale green solid (130 mg, 35 %). <sup>1</sup>H NMR (400 MHz, CDCl<sub>3</sub>): δ<sub>H</sub> 8.82 (d, *J* = 2.6 Hz, 1H, ArH), 8.59 (s, 1H, ArH), 8.32 (dd, *J* = 9.1, 2.6 Hz, 1H, ArH), 8.25 (dd, *J* = 8.6, 2.1 Hz, 1H, ArH), 7.94 (d, *J* = 16 Hz, 2H, CH), 7.77 (d, *J* = 8.6 Hz, 1H, ArH), 7.72 (t, *J* = 7.8 Hz, 1H, ArH), 7.67 – 7.60 (m, 1H, ArH), 7.55 (t, *J* = 7.5 Hz, 1H, ArH), 7.46 (d, *J* = 5.4 Hz, 1H, ArH), 7.41 (s, 1H, ArH),

7.35 (d,  $J = 7.6$  Hz, 1H, ArH), 7.27 (d,  $J = 6.6$  Hz, 1H, ArH), 7.22 (s, 1H, ArH), 7.17 (t,  $J = 7.3$  Hz, 1H, ArH), 6.84 (s, 4H, ArH), 4.23 (ddd,  $J = 16.5, 10.7, 5.5$  Hz, 13H, OCH<sub>2</sub>), 3.88 (dd,  $J = 9.6, 4.3$  Hz, 7H, OCH<sub>2</sub>), 3.86 – 3.79 (m, 6H, OCH<sub>2</sub>), 3.73 (dd,  $J = 7.7, 4.9$  Hz, 13H, OCH<sub>2</sub>), 3.69 – 3.60 (m, 27H, OCH<sub>2</sub>), 3.54 (ddd,  $J = 13.3, 6.8, 3.7$  Hz, 13H, OCH<sub>2</sub>), 3.37 (dd,  $J = 10.4, 2.6$  Hz, 18H, OCH<sub>3</sub>), 1.62 (s, 2H, CH<sub>3</sub>), 1.48 (s, 4H, CH<sub>3</sub>). <sup>13</sup>C NMR (100 MHz, CDCl<sub>3</sub>):  $\delta_C$  153.58, 152.88, 152.56, 150.25, 149.02, 147.69, 147.52, 140.96, 140.63, 134.30, 131.96, 130.91, 128.69, 127.25, 126.07, 125.32, 122.48, 121.50, 121.09, 119.29, 116.36, 111.22, 107.84, 72.51, 71.93, 70.62, 69.70, 69.07, 58.97, 13.73, 13.57 ppm.

### 2.2.9. Synthesis of Compound 38

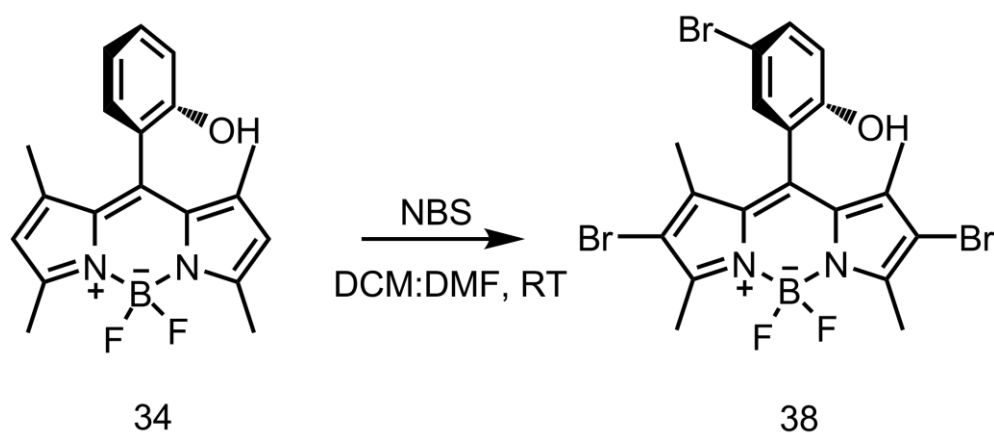


**Figure 28.** Synthesis of Compound 38

Compound **34** (0.176 mmol, 60 mg) is dissolved in 20 mL mixture (DMF/DCM, 1:1, v/v). Then, N-Bromosuccinimide (0.37 mmol, 66mg) is dissolved in DCM (10 mL) and added dropwise to reaction mixture. The mixture is stirred at room temperature. The reaction is monitored by TLC. After finishing starting material 5-10 minutes were waited, reaction is stopped by adding 100 mL of water. The mixture is extracted into DCM (3x 100 mL). The organic phase was dried over Na<sub>2</sub>SO<sub>4</sub> and concentrated in vacuo. Then crude

product was purified by silica gel column chromatography (Acetone/ Hexane, 1:4, v/v). Red solid was obtained (0.031 g, 35%).  $^1\text{H}$  NMR (400 MHz,  $\text{CDCl}_3$ ):  $\delta_{\text{H}}$  7.54 (dt,  $J = 8.7, 2.3$  Hz, 1H, ArH), 7.27 (d,  $J = 2.8$  Hz, 1H, ArH), 6.96 (d,  $J = 8.7$  Hz, 1H, ArH), 5.68 (d,  $J = 5.5$  Hz, 1H, OH), 2.54 (s, 6H,  $\text{CH}_3$ ), 1.59 (s, 6H,  $\text{CH}_3$ ).  $^{13}\text{C}$  NMR (100 MHz,  $\text{CDCl}_3$ ):  $\delta_{\text{C}}$  155.07, 151.75, 140.46, 134.43, 131.51, 122.50, 118.75, 113.58, 112.29, 29.69, 13.65, 13.29 ppm. MS (TOF-ESI):  $m/z$ : Calcd for  $\text{C}_{19}\text{H}_{16}\text{BBr}_3\text{F}_2\text{N}_2\text{O}$ : 572.8874  $[\text{M}-\text{H}]^-$ , Found: 572.8837  $[\text{M}-\text{H}]^-$ ,  $\Delta=6.45$  ppm.

### 2.2.10. Synthesis of Compound 39

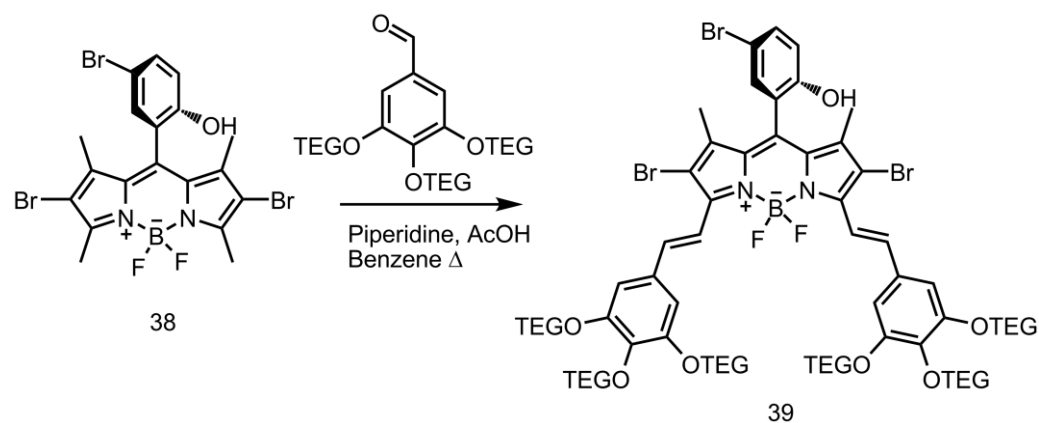


**Figure 29.** Synthesis of Compound 39

Compound **38** (0.348 mmol, 200 mg) and 3,4,5-tris(2-(2-(2-methoxyethoxy)ethoxy)ethoxy) benzaldehyde (0.731 mmol, 433 mg) were added into a 100 mL round-bottomed flask equipped with a Dean-Stark apparatus. 40 mL of benzene, acetic acid (0.2 mL) and piperidine (0.2 mL) were added and mixture was stirred at reflux temperature. The reaction was monitored by TLC and continued until starting material was finished. Water (100 mL) was added to reaction mixture which was cooled to room temperature. Mixture was extracted into DCM (3x 100 mL). The organic phase was dried over  $\text{Na}_2\text{SO}_4$  and concentrated in vacuo. The crude product was

purified by silica gel column chromatography (DCM/ MeOH, 95:5, v/v). The product was collected as green solid (240 mg, 40 %).  $^1\text{H}$  NMR (400 MHz,  $\text{CDCl}_3$ ):  $\delta_{\text{H}}$  7.97 (d,  $J = 16.5$  Hz, 2H, CH), 7.44 (dd,  $J = 9.1, 2.3$  Hz, 1H, ArH), 7.30 (d,  $J = 14.4$  Hz, 2H), 7.13 (d,  $J = 2.6$  Hz, 1H, ArH), 6.96 (d,  $J = 8.8$  Hz, 1H, ArH), 6.88 (s, 4H, ArH), 4.26 (d,  $J = 2.7$  Hz, 8H,  $\text{OCH}_2$ ), 4.21 – 4.17 (m, 4H,  $\text{OCH}_2$ ), 3.89 (t,  $J = 4.8$  Hz, 9H,  $\text{OCH}_2$ ), 3.81 (dd,  $J = 5.8, 4.2$  Hz, 4H,  $\text{OCH}_2$ ), 3.76 – 3.70 (m, 14H,  $\text{OCH}_2$ ), 3.68 – 3.60 (m, 27H,  $\text{OCH}_2$ ), 3.58 – 3.54 (m, 6H,  $\text{OCH}_2$ ), 3.54 – 3.50 (m, 7H,  $\text{OCH}_2$ ), 3.38 (s, 8H,  $\text{OCH}_3$ ), 3.35 (s, 10H,  $\text{OCH}_2$ ), 1.28 (s, 6H,  $\text{CH}_3$ ).  $^{13}\text{C}$  NMR (100 MHz,  $\text{CDCl}_3$ ):  $\delta_{\text{C}}$  152.74 , 152.59 , 148.25 , 141.02 , 140.37 , 139.50 , 134.35 , 132.45 , 131.98 , 131.54 , 122.80 , 118.93 , 116.42 , 112.75 , 110.72 , 107.92 , 77.39 , 77.07 , 76.75 , 72.47 , 71.92 , 70.82 , 70.67 , 70.52 , 69.70 , 69.07 , 58.97 , 13.12 ppm. MS (TOF- ESI):  $m/z$ : Calcd for  $\text{C}_{75}\text{H}_{108}\text{BBr}_3\text{F}_2\text{N}_2\text{O}_{25}$ : 1720.4852  $[\text{M}-\text{H}]^-$ , Found: 1720.4714  $[\text{M}-\text{H}]^-$  ,  $\Delta=8.02$  ppm.

### 2.2.11. Synthesis of Compound 40

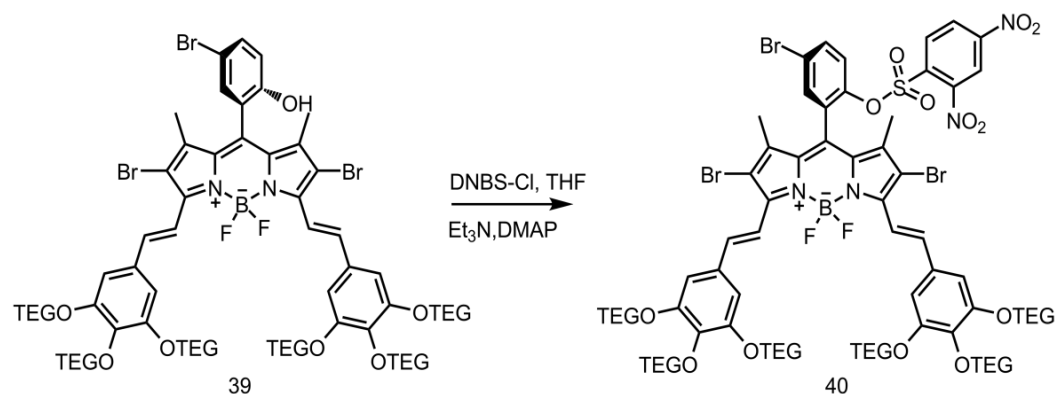


**Figure 30.** Synthesis of Compound 40

Compound **39** (0.24 mmol, 400 mg) was dissolved in dry THF (30 mL). Then triethylamine (0.12 mL) was added and stirred for 30 min at room temperature. A solution of 2, 4-dinitrobenzenesulfonyl chloride (0.77 mmol, 200 mg) in dry THF (20 mL) was added dropwise at 0 °C. The mixture was

heated to 40 °C and stirred for overnight. Then reaction was cooled to room temperature and solvent was evaporated. Crude product was purified by silica gel column chromatography (DCM/ MeOH, 95:5, v/v). The product was collected as pale green solid (274 mg, 60 %). <sup>1</sup>H NMR (400 MHz, CDCl<sub>3</sub>): δ<sub>H</sub> 8.61 (s, 1H, ArH), 8.26 (dd, *J* = 8.6, 2.5 Hz, 1H, ArH), 7.96 (d, *J* = 16.4 Hz, 2H, CH), 7.83 (dd, *J* = 8.9, 2.6 Hz, 1H, ArH), 7.78 (d, *J* = 8.9 Hz, 1H, ArH), 7.57 – 7.49 (m, 2H, ArH), 7.24 (d, *J* = 16.5 Hz, 2H, CH), 6.85 (s, 4H, ArH), 4.30 – 4.17 (m, 13H, OCH<sub>2</sub>), 3.90 (t, *J* = 6.3 Hz, 9H, OCH<sub>2</sub>), 3.84 (t, *J* = 10 Hz, 5H, OCH<sub>2</sub>), 3.76 – 3.73 (m, 13H, OCH<sub>2</sub>), 3.70 – 3.63 (m, 28H, OCH<sub>2</sub>), 3.57 (dd, *J* = 4.0, 2.1 Hz, 4H, OCH<sub>2</sub>), 3.54 (dd, *J* = 5.8, 3.8 Hz, 8H, OCH<sub>2</sub>), 3.39 (s, 6H, OCH<sub>3</sub>), 3.37 (s, 12H, OCH<sub>3</sub>), 1.57 (s, 6H, CH<sub>3</sub>). <sup>13</sup>C NMR (100 MHz, CDCl<sub>3</sub>): δ<sub>C</sub> 213.36, 152.94, 150.37, 149.35, 147.71, 146.64, 141.34, 140.80, 140.32, 134.91, 134.03, 133.70, 131.87, 131.75, 130.97, 129.24, 126.82, 126.11, 121.97, 121.63, 116.27, 107.96, 72.55, 71.95, 70.68, 70.60, 70.55, 69.72, 69.10, 59.00, 58.98, 13.86.

## CHAPTER 3

### RESULTS & DISCUSSION

#### 3.1. General Perspective

Several difficulties have been got over in order to improve the ideal photosensitizers for PDT. Scientist aimed high phototoxicity and selectivity for tumor tissues, at the same time decreased side effects caused by the method. High absorption coefficients and quantum yields for singlet oxygen generation are the a few features for good photosensitizers. Another important characteristic for photosensitizers is biocompatibility since the method for biological applications. Due to the results obtained from clinical trials, it is a fact that side effects need to diminish. Although second generation photosensitizers have been designed for this need, they couldn't present sufficient selectivity hence the results<sup>131,11</sup>. Through designing activatable water soluble photosensitizers, sensitivity and selectivity of the method are enhancing.

In this study, we have reported three different Bodipy based photosensitizers in order to compare the importance of proximity of 2,4 – dinitrobenzenesulfonyl group. All of them are water soluble through conjugating triethylene glycol derivatives. The main purpose for the design is to increase selectivity of the PDT through activation of the photosensitizers by glutathione which is overexpressed in cancer tissues up to 50 folds<sup>101,102</sup>.

### 3.2. Design Strategies for Activatable Photosensitizers

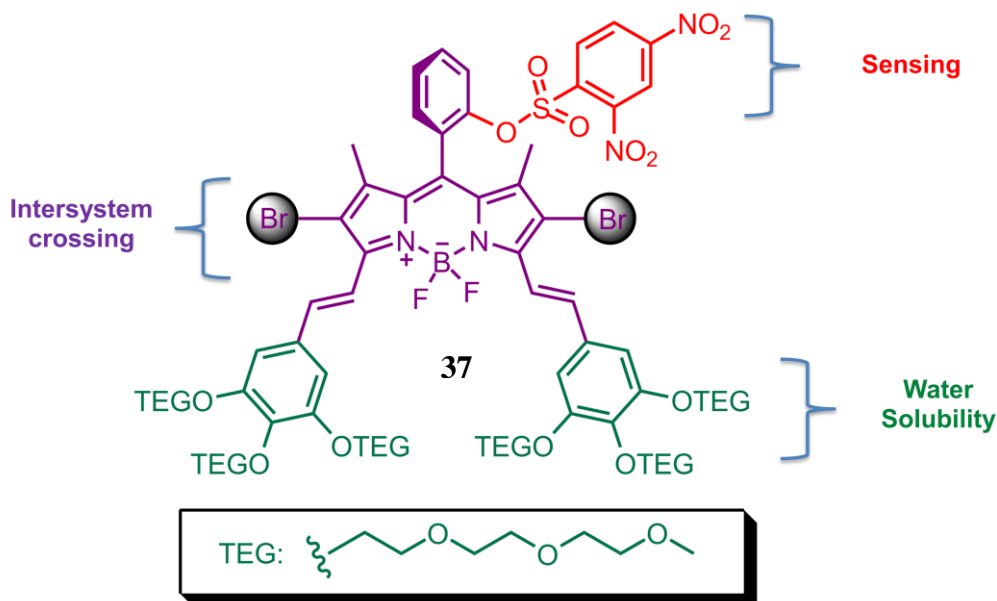


**Figure 31.** Targeted Probe Design

The reason for use Bodipy dyes for PDT action is their exceptional chemical and photophysical properties. This class of dye has high extinction coefficient in visible and near-IR region around  $70\,000 - 100\,000\text{ M}^{-1}\text{ cm}^{-1}$ . Ease of purification and straight forward synthesis are important parameters that enable us modify the dye according to needs for methods. Through adjustments, absorption maxima of Bodipy could shift to longer wavelengths which are in therapeutic window range. Increasing intersystem crossing via heavy atom effect let energy transfer rate also enhances due to longer excited state lifetimes. Due to this rise, singlet oxygen generation efficiency has been improved which enable phototoxicity of the method has been accomplished<sup>59</sup>. Other functional groups could be located over Bodipy core with different type of reactions. In Fig. 31, compound 37 is an example for different variation that leads target photosensitizers. Triethylene glycol groups are used for water solubility for biological applications. 2, 4 dinitrobenzenesulfonyl group is purposed for GSH sensing.

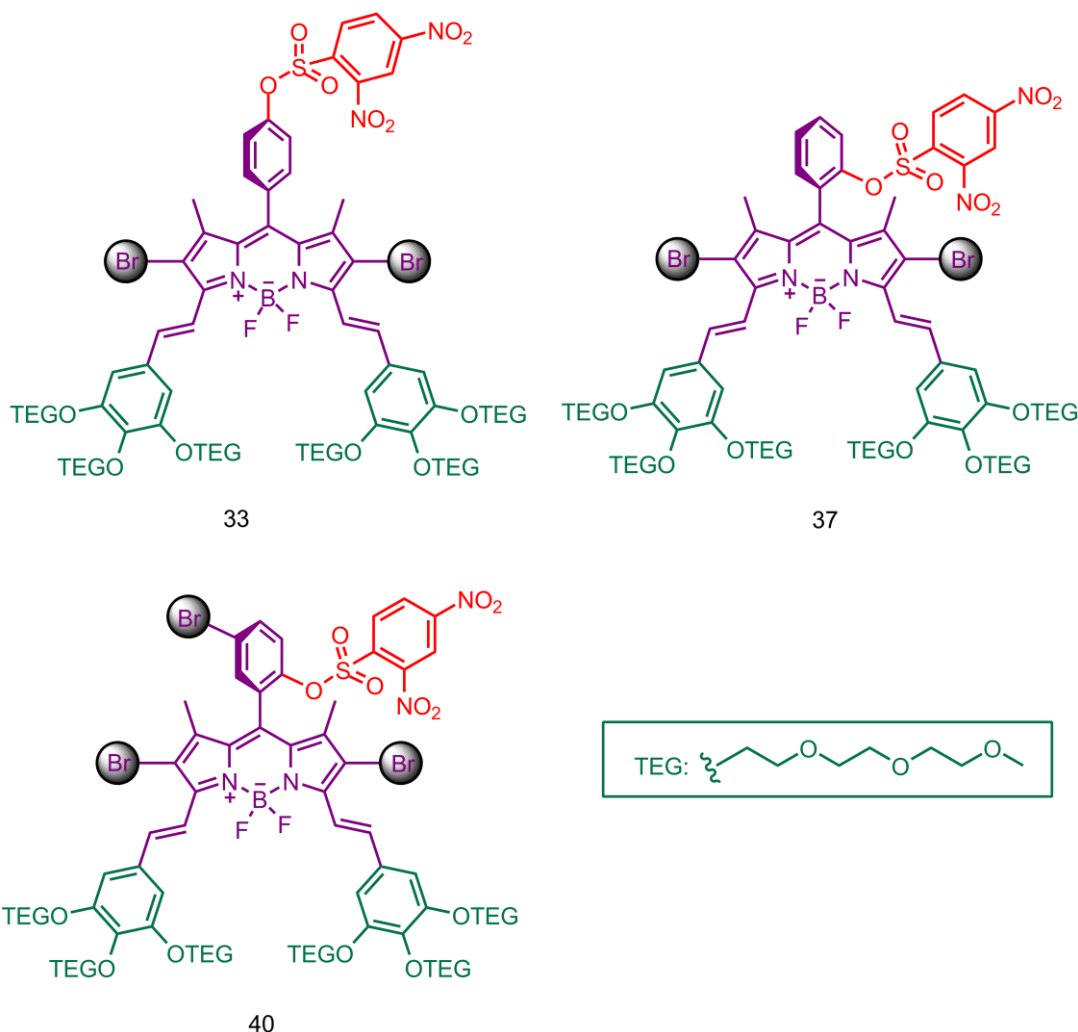


**Figure 32.** Target Photosensitizers

Meso position of the Bodipy which is also called position 8 could be designed with suitable aldehydes for the purpose. Other positions like 1,3,5 and 7 could be modified via Knoevenagel condensation reaction. In these designs, only 3 and 5 positions are used for water solubility design through manipulating triethylene glycol derivatives. Condensation reactions could occur due to the acidic nature of the methyl groups in the positions previously mentioned. Electrophilic bromination is favorable via 2 and 6 positions. In the last step,  $\text{S}_{\text{N}}2$  take place in order to modification of the 2,4 dinitrobenzenesulfonyl chloride to Bodipy core. By means of these reactions, effective photosensitizers are designed for PDT action as in designs in Fig.32<sup>59</sup>.

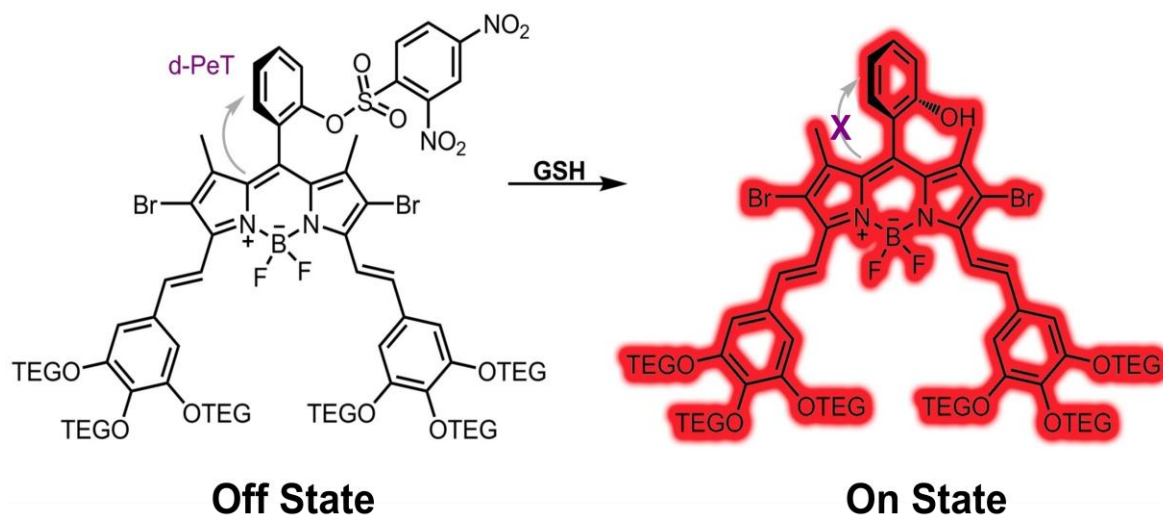


**Figure 33.** Activation of the Photosensitizers

Fluorescence of the probe is quenched through donor-excited photoinduced electron transfer (d-PeT) from Bodipy to 2, 4 dinitrobenzenesulfonyl group. After addition of the glutathione (GSH), fluorescence returns. In this design, almost no fluorescence is observed until addition of the GSH. Visible light is used in order to excite the probe. 2, 4 dinitrobenzenesulfonyl groups act as electron acceptor in the PeT process. In order to tackle certain limitations, our design is highly selective towards glutathione via d-PeT process. In order to understand para and ortho position's importance, different designs are used in the research to compare the results. One of the reasons of these designs is to prove that distance between electron acceptor and electron donor is very significant factor which affect the quenching process. In Fig. 33, illustration of the quenching of the fluorescence and restoring it is available through using compound 37 as an example. Depending on quenching and restore of the PeT mechanism, this process called off-on procedure. Off state is called probe and on state is called Bodipy through the measurements.

### 3.3 Spectral Proof for Activation Process

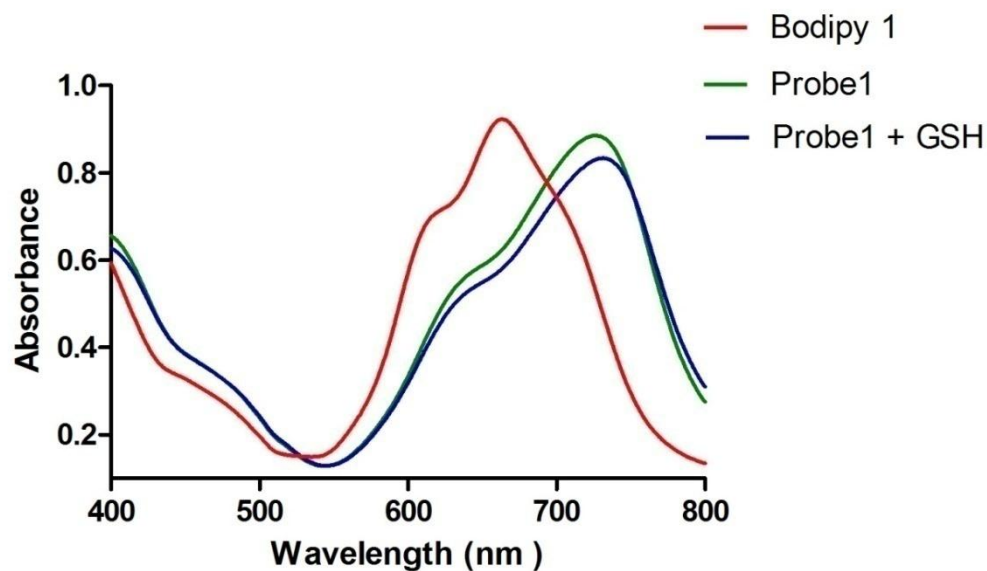


**Figure 34.** Absorbance spectrum of Compound 32 and Compound 33 as Bodipy 1 and Probe 1 respectively before and after addition of GSH.

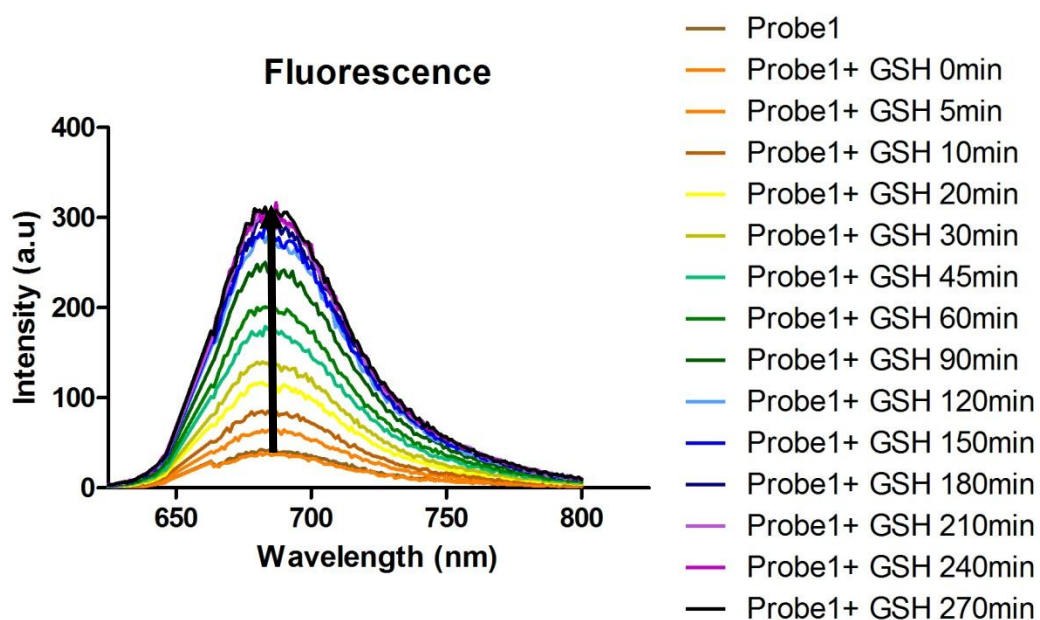


**Figure 35.** Fluorescence spectrum of Compound 33 as Probe 1 with time, 1 nM GSH and 4  $\mu$ M Probe concentration in DMSO/ 1X PBS buffer solution (1/1, v/v), excitation wavelength was 655 nm

Least reactive targeted photosensitizers is compound 33 in which para position is substituted with electron acceptor 2,4 dinitrobenzenesulfonyl group. In Fig.34 and Fig. 35 , absorbance and fluorescence spectra are presented. Through absorbance spectrum, there is 98 nm difference between compound 32 (Bodipy 1) and compound 33 (Probe 1). Fluorescence spectrum is the proof for the off- on state thiol sensitive photosensitizer. Upon the addition of the GSH , 7.3 folds increase observed in spectrum. Measurements were taken until no change was observed in the fluorescence. It took 270 minutes to complete the measurement for this case.

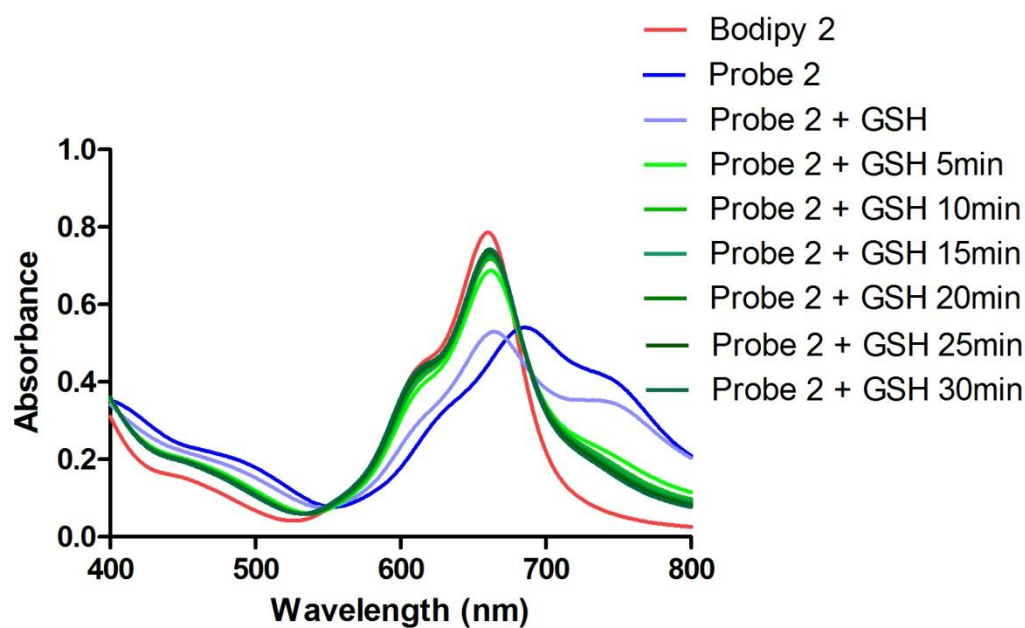


**Figure 36.** Absorbance spectrum of Compound 36 and Compound 37 as Bodipy 2 and Probe 2 respectively before and after addition of GSH.

In Fig. 36 , UV-Vis absorbance spectrum is presented for compound 36 and 37 before and after GSH addition. Reactions toward GSH are so fast that it took only half an hour to measure the changes. Upon addition of GSH, Probe 2's spectrum transforms to Bodipy 2's spectrum showing the transformation

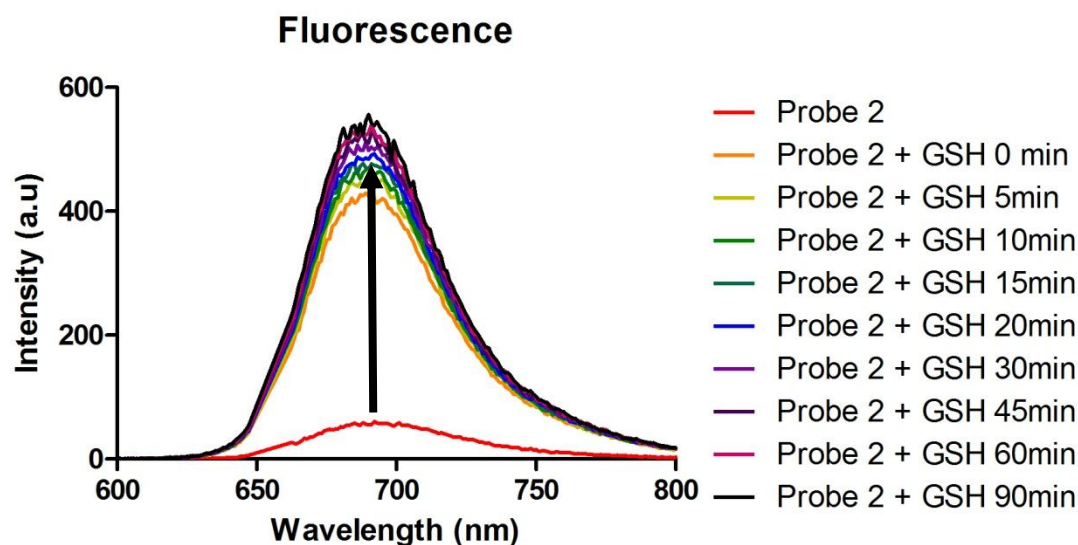


**Figure 37.** Fluorescence spectrum of Compound 37 as Probe 2 with time, 1 nM GSH and 4  $\mu$ M Probe concentration in DMSO/ 1X PBS buffer solution (1/1, v/v), excitation wavelength was 655 nm

since it could be seen through spectrum. Another proof for the transformation is fluorescence spectrum for compound 37 as Probe 2. Upon addition of the GSH, restoration of the fluorescence is took place. No change has been observed after 90 minutes for fluorescence measurements in this case.

Last but not least Probe 3 is the most reactive towards to GSH. In Fig. 38 and 39 absorbance and fluorescence spectra are presented respectively. Half an hour is sufficient for the measurements process in order to observe change for this compound, Probe 2. Upon addition of the GSH, fluorescence restored in 30 minutes which is the fastest response when compared to other Probes for GSH response in this study. Since activation process could be achieved without difficulties, only singlet oxygen generation factor is needed for understand the PDT power of these study.

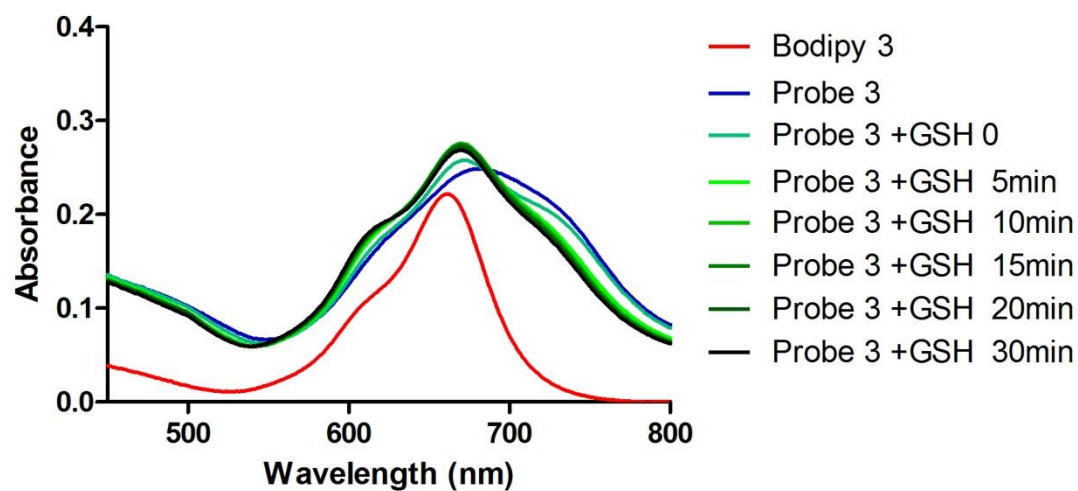


**Figure 38.** Absorbance spectrum of Compound 39 and Compound 40 as Bodipy 2 and Probe 2 respectively before and after addition of GSH.

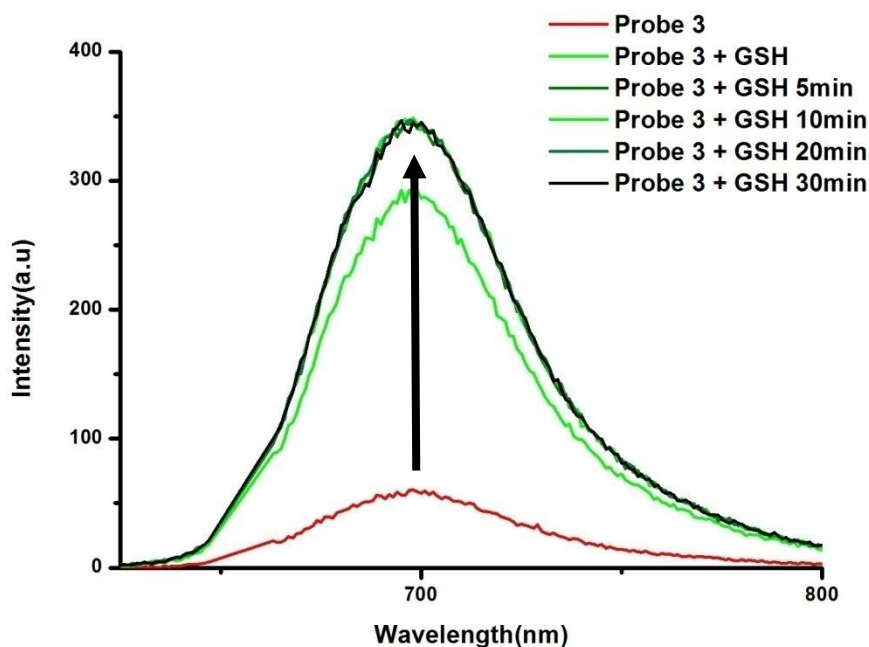


**Figure 39.** Fluorescence spectrum of Compound 40 as Probe 2 with time, 1 nM GSH and 4  $\mu$ M Probe concentration in DMSO/ 1X PBS buffer solution (1/1, v/v), excitation wavelength was 655 nm

### 3.4 Singlet Oxygen Generation

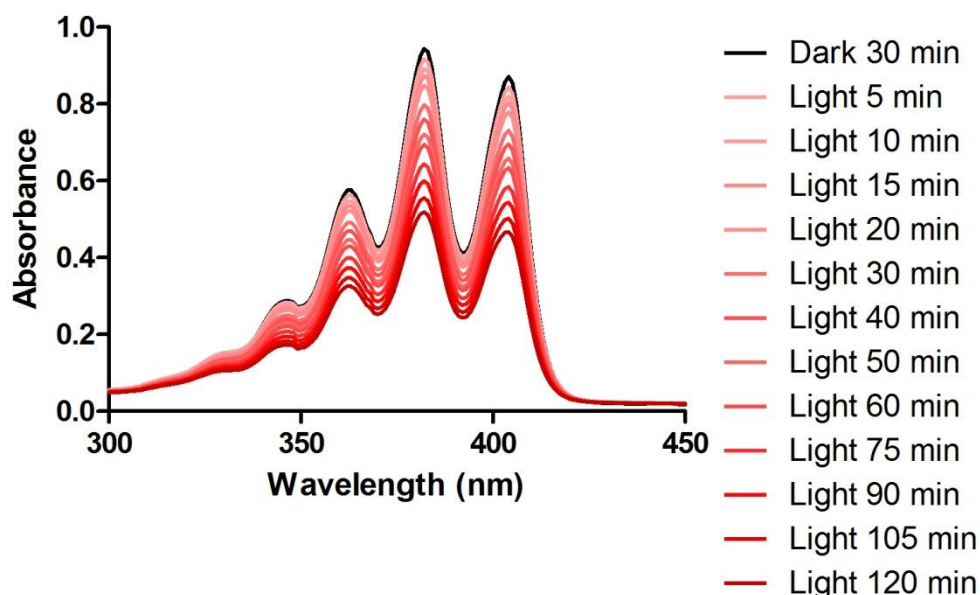


**Figure 40.** Absorbance spectrum of trap molecule (2,2'-(Anthracene-9,10-diyl)bis(methylene)dimalonic acid) with Bodipy 1, 4  $\mu\text{M}$  in DMSO/ 1X PBS buffer solution (1/1, v/v), LED applied at 660 nm.

Trough using trap molecules, singlet oxygen measurements are done. Difficulties of direct measurements of singlet oxygen molecules arouse because of the short life time of these molecules. Trap molecules is reacting with singlet oxygen molecules hence the absorption of trap molecules is decreasing depend on the singlet oxygen amount directly. Measurements are taken in the dark in order to show that there is not any singlet oxygen generation in the dark. Then light is applied at 660 nm to produce reactive oxygen species. As you can see all of the tree spectra show excellent singlet oxygen efficiency.

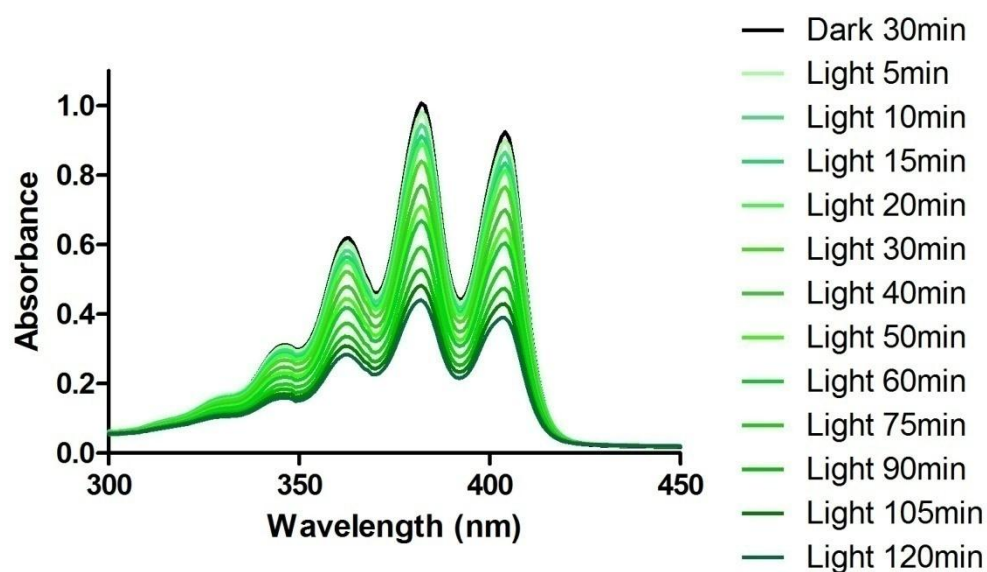


**Figure 41.** Absorbance spectrum of trap molecule (2,2'-(Anthracene-9,10-diyl)bis(methylene)dimalonic acid) with Bodipy 2, 4  $\mu\text{M}$  in DMSO/ 1X PBS buffer solution (1/1, v/v), LED applied at 660 nm

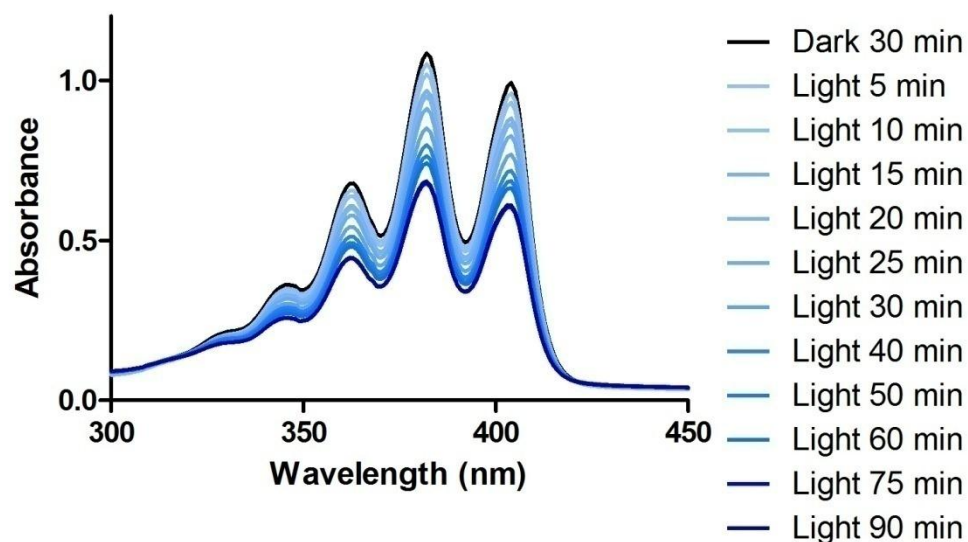


**Figure 42.** Absorbance spectrum of trap molecule (2,2'-(Anthracene-9,10-diyl)bis(methylene)dimalonic acid) with Bodipy 3, 4  $\mu\text{M}$  in DMSO/ 1X PBS buffer solution (1/1, v/v), LED applied at 660 nm

## **CHAPTER 4**

### **CONCLUSION**

In this study, we have synthesized three different photosensitizers for activatable PDT action. This study has been demonstrated the importance of the ortho and para positions for activation process of the photosensitizers for PDT action. Process properties are emphasized through the photophysical changes in spectrum which confirm the logic behind the design.

This is especially important for cancerous diseases. Energy transfer systems are also used for various purposes as imaging of live cell protein localizations, monitoring of drug release. Demand for cure, new treatment modalities for cancer has increasing trends in materials science, biology and chemistry. Significant importance of these systems and contributions to the science cannot be underestimated. Since photodynamic therapy is one of the most informative and sensitive method, applications in research will continue to increase. Through the different remarkable processes, it will be more lucid to see the important assistance of these systems.

We will continue with in vitro experiments for our activatable photosensitizers in order to observe the PDT effect in tumor cells. Upon the our results, new photosensitizers could be designed for literature or clinical trials could be planned.

## REFERENCES

1. Ackroyd, R.; Kelty, C.; Brown, N.; Reed, M., The history of photodetection and photodynamic therapy. *Photochem Photobiol* **2001**, *74* (5), 656-69.
2. Daniell, M. D.; Hill, J. S., A history of photodynamic therapy. *Aust N Z J Surg* **1991**, *61* (5), 340-8.
3. Dolmans, D. E. J. G. J.; Fukumura, D.; Jain, R. K., Photodynamic therapy for cancer. *Nat Rev Cancer* **2003**, *3* (5), 380-387.
4. Dougherty, T. J.; Gomer, C. J.; Henderson, B. W.; Jori, G.; Kessel, D.; Korbely, M.; Moan, J.; Peng, Q., Photodynamic therapy. *J Natl Cancer Inst* **1998**, *90* (12), 889-905.
5. Wilson, B. C.; Patterson, M. S., The physics, biophysics and technology of photodynamic therapy. *Phys Med Biol* **2008**, *53* (9), R61-109.
6. Lovell, J. F.; Liu, T. W. B.; Chen, J.; Zheng, G., Activatable Photosensitizers for Imaging and Therapy. *Chem Rev* **2010**, *110* (5), 2839-2857.
7. Huang, Z., A review of progress in clinical photodynamic therapy. *Technol Cancer Res T* **2005**, *4* (3), 283-293.
8. MacDonald, I. J.; Dougherty, T. J., Basic principles of photodynamic therapy. *J Porphyr Phthalocya* **2001**, *5* (2), 105-129.
9. Allison, R. R.; Downie, G. H.; Cuenca, R.; Hu, X.-H.; Childs, C. J. H.; Sibata, C. H., Photosensitizers in clinical PDT. *Photodiagnosis and Photodynamic Therapy* **2004**, *1* (1), 27-42.
10. Diamond, I.; Granelli, S. G.; McDonagh, A. F.; Nielsen, S.; Wilson, C. B.; Jaenicke, R., Photodynamic therapy of malignant tumours. *Lancet* **1972**, *2* (7788), 1175-7.
11. Detty, M. R.; Gibson, S. L.; Wagner, S. J., Current clinical and preclinical photosensitizers for use in photodynamic therapy. *J Med Chem* **2004**, *47* (16), 3897-3915.

12. Kelly, J. F.; Snell, M. E., Hematoporphyrin derivative: a possible aid in the diagnosis and therapy of carcinoma of the bladder. *J Urol* **1976**, *115* (2), 150-1.
13. Dougherty, T. J.; Kaufman, J. E.; Goldfarb, A.; Weishaupt, K. R.; Boyle, D.; Mittleman, A., Photoradiation therapy for the treatment of malignant tumors. *Cancer Res* **1978**, *38* (8), 2628-35.
14. Gomer, C. J.; Doiron, D. R.; Jester, J. V.; Szirth, B. C.; Murphree, A. L., Hematoporphyrin derivative photoradiation therapy for the treatment of intraocular tumors: examination of acute normal ocular tissue toxicity. *Cancer Res* **1983**, *43* (2), 721-7.
15. Bonnett, R.; Berenbaum, M. C., HPD - a study of its components and their properties. *Adv Exp Med Biol* **1983**, *160*, 241-50.
16. Dougherty, T. J., Studies on the structure of porphyrins contained in Photofrin II. *Photochem Photobiol* **1987**, *46* (5), 569-73.
17. Dougherty, T. J., Photodynamic therapy. *Photochem Photobiol* **1993**, *58* (6), 895-900.
18. Phillips, D., Chemical mechanisms in photodynamic therapy with phthalocyanines. *Prog React Kinet* **1997**, *22* (3-4), 175-300.
19. Moore, J. V.; West, C. M.; Whitehurst, C., The biology of photodynamic therapy. *Phys Med Biol* **1997**, *42* (5), 913-35.
20. Lang, K.; Mosinger, J.; Wagnerova, D. M., Photophysical properties of porphyrinoid sensitizers non-covalently bound to host molecules; models for photodynamic therapy. *Coordin Chem Rev* **2004**, *248* (3-4), 321-350.
21. Boyle, R. W.; Dolphin, D., Structure and biodistribution relationships of photodynamic sensitizers. *Photochemistry and Photobiology* **1996**, *64* (3), 469-485.
22. Ali, H.; van Lier, J. E., Metal complexes as photo- and radiosensitizers. *Chem Rev* **1999**, *99* (9), 2379-2450.

23. Atilgan, S.; Ekmekci, Z.; Dogan, A. L.; Guc, D.; Akkaya, E. U., Water soluble distyryl-boradiazaindacenes as efficient photosensitizers for photodynamic therapy. *Chem Commun* **2006**, (42), 4398-4400.
24. Sharman, W. M.; Allen, C. M.; van Lier, J. E., Role of activated oxygen species in photodynamic therapy. *Method Enzymol* **2000**, 319, 376-400.
25. Jori, G., Far-Red-Absorbing Photosensitizers - Their Use in the Photodynamic Therapy of Tumors. *J Photoch Photobio A* **1992**, 62 (3), 371-378.
26. Henderson, B. W.; Dougherty, T. J., How Does Photodynamic Therapy Work. *Photochemistry and Photobiology* **1992**, 55 (1), 145-157.
27. Clennan, E. L., New mechanistic and synthetic aspects of singlet oxygen chemistry. *Tetrahedron* **2000**, 56 (47), 9151-9179.
28. Smith, L. K., Z; Ostrikov, K; Kumar, S, Nanoparticles in Cancer Imaging and Therapy. *Journal of Nanomaterials* **2012**, 2012, 7.
29. Brigger, I.; Dubernet, C.; Couvreur, P., Nanoparticles in cancer therapy and diagnosis. *Adv Drug Deliver Rev* **2002**, 54 (5), 631-651.
30. Gary-Bobo, M.; Mir, Y.; Rouxel, C.; Brevet, D.; Hocine, O.; Maynadier, M.; Gallud, A.; Da Silva, A.; Mongin, O.; Blanchard-Desce, M.; Richeter, S.; Loock, B.; Maillard, P.; Morère, A.; Garcia, M.; Raehm, L.; Durand, J.-O., Multifunctionalized mesoporous silica nanoparticles for the in vitro treatment of retinoblastoma: Drug delivery, one and two-photon photodynamic therapy. *International Journal of Pharmaceutics* **2012**, 432 (1-2), 99-104.
31. Hunt, D. W.; Sorrenti, R. A.; Renke, M. E.; Waterfield, E.; Levy, J. G., Accelerated myelopoietic recovery in irradiated mice treated with Photofrin. *Int J Immunopharmacol* **1995**, 17 (1), 33-9.
32. Berenbaum, M. C.; Bonnett, R.; Chevretton, E. B.; Akande-Adebakin, S. L.; Ruston, M., Selectivity of meso-tetra(hydroxyphenyl)porphyrins and chlorins and of photofrin II in causing photodamage in tumour, skin, muscle and bladder. The concept of cost-benefit in analysing the results. *Lasers in Medical Science* **1993**, 8 (4), 235-243.

33. Morgan, A. R., Reduced porphyrins as photosensitizers: Synthesis and biological effects. In *Photodynamic Therapy, Basic Principles and clinical applications*, Henderson, B. W. D. T. J., Ed. Marcell D.: New York, 1992; pp 157-172.
34. Ma, L.; Moan, J.; Berg, K., Evaluation of a new photosensitizer, meso-tetra-hydroxyphenyl-chlorin, for use in photodynamic therapy: a comparison of its photobiological properties with those of two other photosensitizers. *Int J Cancer* **1994**, *57* (6), 883-8.
35. Castano, A. P.; Demidova, T. N.; Hamblin, M. R., Mechanisms in photodynamic therapy: part one—photosensitizers, photochemistry and cellular localization. *Photodiagnosis and Photodynamic Therapy* **2004**, *1* (4), 279-293.
36. Kennedy, J. C.; Pottier, R. H.; Pross, D. C., Photodynamic therapy with endogenous protoporphyrin IX: basic principles and present clinical experience. *J Photochem Photobiol B* **1990**, *6* (1-2), 143-8.
37. Roberts, D. J. H.; Stables, G. I.; Ash, D. V.; Brown, S. B., Distribution of Protoporphyrin-Ix in Bowens Disease and Basal Cell Carcinomas Treated with Topical 5-Aminolaevulinic Acid. *5th International Photodynamic Association Biennial Meeting* **1995**, *2371*, 490-494.
38. Stables, G. I.; Ash, D. V., Photodynamic Therapy. *Cancer Treat Rev* **1995**, *21* (4), 311-323.
39. Levy, J. G., Photodynamic therapy. *Trends Biotechnol* **1995**, *13* (1), 14-8.
40. Rosenthal, I.; Krishna, C. M.; Riesz, P.; Benhur, E., The Role of Molecular-Oxygen in the Photodynamic Effect of Phthalocyanines. *Radiat Res* **1986**, *107* (1), 136-142.
41. Richter, A. M.; Kelly, B.; Chow, J.; Liu, D. J.; Towers, G. H. N.; Dolphin, D.; Levy, J. G., Preliminary Studies on a More Effective Phototoxic Agent Than Hematoporphyrin. *J Natl Cancer I* **1987**, *79* (6), 1327-1332.

42. Sternberg, E. D.; Dolphin, D.; Levy, J.; Waterfield, E., Development of Bpdma as a Photodynamic Therapeutic Agent. *J Cell Biochem* **1993**, 178-178.
43. Sharman, W. M.; Allen, C. M.; van Lier, J. E., Photodynamic therapeutics: basic principles and clinical applications. *Drug Discov Today* **1999**, 4 (11), 507-517.
44. Schieweck, K.; Capraro, H. G.; Isele, U.; Vanhoogevest, P.; Ochsner, M.; Maurer, T.; Batt, E., Cgp-55847, Liposome-Delivered Zinc(II)-Phthalocyanine as a Phototherapeutic Agent for Tumors. *Proceedings of Photodynamic Therapy of Cancer* **1994**, 2078, 107-118.
45. Isele, U.; Vanhoogevest, P.; Leuenberger, H.; Capraro, H. G.; Schieweck, K., Pharmaceutical Development of Cgp-55847 a Liposomal Zn-Phthalocyanine Formulation Using a Controlled Organic-Solvent Dilution Method. *Proceedings of Photodynamic Therapy of Cancer* **1994**, 2078, 397-403.
46. Wainwright, M., Non-porphyrin photosensitizers in biomedicine. *Chemical Society Reviews* **1996**, 25 (5), 351-+.
47. Schmitt, I. M.; Chimenti, S.; Gasparro, F. P., Psoralen Protein Photochemistry - a Forgotten Field. *J Photoch Photobio B* **1995**, 27 (2), 101-107.
48. Guiotto, A.; Chilin, A.; Manzini, P.; Dallacqua, F.; Bordin, F.; Rodighiero, P., Synthesis and Antiproliferative Activity of Furocoumarin Isosters. *Farmaco* **1995**, 50 (6), 479-488.
49. Saxton, R. E.; Paiva, M. B.; Lufkin, R. B.; Castro, D. J., Laser Photochemotherapy - a Less Invasive Approach for Treatment of Cancer. *Semin Surg Oncol* **1995**, 11 (4), 283-289.
50. Redmond, R. W.; Srichai, M. B.; Bilitz, J. M.; Schlomer, D. D.; Krieg, M., Merocyanine dyes: effect of structural modifications on photophysical properties and biological activity. *Photochem Photobiol* **1994**, 60 (4), 348-55.

51. Krieg, M.; Bilitz, J. M.; Srichai, M. B.; Redmond, R. W., Effects of structural modifications on the photosensitizing properties of dialkylcarbocyanine dyes in homogeneous and heterogeneous solutions. *Biochim Biophys Acta* **1994**, *1199* (2), 149-56.
52. Orth, K.; Ruck, A.; Beck, G.; Stanescu, A.; Beger, H. G., [Photodynamic therapy of small adenocarcinomas with methylene blue]. *Chirurg* **1995**, *66* (12), 1254-7.
53. Orth, K.; Ruck, A.; Stanescu, A.; Beger, H. G., Intraluminal treatment of inoperable oesophageal tumours by intralesional photodynamic therapy with methylene blue. *Lancet* **1995**, *345* (8948), 519-20.
54. Pal, P.; Zeng, H.; Durocher, G.; Girard, D.; Li, T.; Gupta, A. K.; Giasson, R.; Blanchard, L.; Gaboury, L.; Balassy, A.; Turmel, C.; Laperriere, A.; Villeneuve, L., Phototoxicity of some bromine-substituted rhodamine dyes: synthesis, photophysical properties and application as photosensitizers. *Photochem Photobiol* **1996**, *63* (2), 161-8.
55. Kessel, D.; Woodburn, K., Selective photodynamic inactivation of a multidrug transporter by a cationic photosensitising agent. *Br J Cancer* **1995**, *71* (2), 306-10.
56. Lewis, M. R.; Golland, P. P.; Sloviter, H. A., Selective action of certain dyestuffs on sarcomata and carcinomata. *Anat Rec* **1946**, *96* (2), 201-20.
57. Fiedorowicz, M.; Galindo, J. R.; Julliard, M.; Mannoni, P.; Chanon, M., Efficient photodynamic action of Victoria blue BO against the human leukemic cell lines K-562 and TF-1. *Photochem Photobiol* **1993**, *58* (3), 356-61.
58. Iwamoto, Y.; Itoyama, T.; Yasuda, K.; Morita, T.; Shimizu, T.; Masuzawa, T.; Yanagihara, Y., Photodynamic DNA strand breaking activities of acridine compounds. *Biol Pharm Bull* **1993**, *16* (12), 1244-7.
59. Loudet, A.; Burgess, K., BODIPY dyes and their derivatives: syntheses and spectroscopic properties. *Chem Rev* **2007**, *107* (11), 4891-932.

60. Celli, J. P.; Spring, B. Q.; Rizvi, I.; Evans, C. L.; Samkoe, K. S.; Verma, S.; Pogue, B. W.; Hasan, T., Imaging and photodynamic therapy: mechanisms, monitoring, and optimization. *Chem Rev* **2010**, *110* (5), 2795-838.
61. Shea, C. R.; Hefetz, Y.; Gillies, R.; Wimberly, J.; Dalickas, G.; Hasan, T., Mechanistic investigation of doxycycline photosensitization by picosecond-pulsed and continuous wave laser irradiation of cells in culture. *J Biol Chem* **1990**, *265* (11), 5977-82.
62. Plaetzer, K.; Krammer, B.; Berlanda, J.; Berr, F.; Kiesslich, T., Photophysics and photochemistry of photodynamic therapy: fundamental aspects. *Lasers Med Sci* **2009**, *24* (2), 259-68.
63. Ochsner, M., Photophysical and photobiological processes in the photodynamic therapy of tumours. *J Photochem Photobiol B* **1997**, *39* (1), 1-18.
64. Foote, C. S., Definition of type I and type II photosensitized oxidation. *Photochem Photobiol* **1991**, *54* (5), 659.
65. Halliwell, B., Oxygen radicals: a commonsense look at their nature and medical importance. *Med Biol* **1984**, *62* (2), 71-7.
66. Moan, J., On the Diffusion Length of Singlet Oxygen in Cells and Tissues. *J Photochem Photobiol B* **1990**, *6* (3), 343-347.
67. Bergamini, C. M.; Gambetti, S.; Dondi, A.; Cervellati, C., Oxygen, reactive oxygen species and tissue damage. *Curr Pharm Des* **2004**, *10* (14), 1611-26.
68. Wilson, B. C.; Patterson, M. S., The physics of photodynamic therapy. *Phys Med Biol* **1986**, *31* (4), 327-60.
69. Juarranz, A.; Jaen, P.; Sanz-Rodriguez, F.; Cuevas, J.; Gonzalez, S., Photodynamic therapy of cancer. Basic principles and applications. *Clin Transl Oncol* **2008**, *10* (3), 148-54.
70. Fingar, V. H.; Wieman, T. J.; Park, Y. J.; Henderson, B. W., Implications of a Preexisting Tumor Hypoxic Fraction on Photodynamic Therapy. *J Surg Res* **1992**, *53* (5), 524-528.

71. Buytaert, E.; Dewaele, M.; Agostinis, P., Molecular effectors of multiple cell death pathways initiated by photodynamic therapy. *Bba-Rev Cancer* **2007**, *1776* (1), 86-107.
72. Christensen, T.; Feren, K.; Moan, J.; Pettersen, E., Photodynamic effects of hematoporphyrin derivative on synchronized and asynchronous cells of different origin. *Br J Cancer* **1981**, *44* (5), 717-24.
73. Berns, M. W.; Dahlman, A.; Johnson, F. M.; Burns, R.; Sperling, D.; Guiltinan, M.; Siemens, A.; Walter, R.; Wright, W.; Hammer-Wilson, M.; Wile, A., In vitro cellular effects of hematoporphyrin derivative. *Cancer Res* **1982**, *42* (6), 2325-9.
74. Fingar, V. H.; Wieman, T. J., Mechanisms of Vessel Damage in Photodynamic Therapy. *Optical Methods for Tumor Treatment and Detection : Mechanisms and Techniques in Photodynamics Therapy* **1992**, *1645*, 98-103.
75. Fingar, V. H.; Wieman, T. J.; Wiehle, S. A.; Cerrito, P. B., The Role of Microvascular Damage in Photodynamic Therapy - the Effect of Treatment on Vessel Constriction, Permeability, and Leukocyte Adhesion. *Cancer Research* **1992**, *52* (18), 4914-4921.
76. Wieman, T. J.; Fingar, V. H., Photodynamic Therapy. *Surg Clin N Am* **1992**, *72* (3), 609-622.
77. Dewhirst, M. W.; Kimura, H.; Rehmus, S. W.; Braun, R. D.; Papahadjopoulos, D.; Hong, K.; Secomb, T. W., Microvascular studies on the origins of perfusion-limited hypoxia. *Br J Cancer Suppl* **1996**, *27*, S247-51.
78. Tromberg, B. J.; Kimel, S.; Orenstein, A.; Barker, S. J.; Hyatt, J.; Nelson, J. S.; Roberts, W. G.; Berns, M. W., Tumor oxygen tension during photodynamic therapy. *J Photochem Photobiol B* **1990**, *5* (1), 121-6.
79. Tromberg, B. J.; Orenstein, A.; Kimel, S.; Barker, S. J.; Hyatt, J.; Nelson, J. S.; Berns, M. W., In vivo tumor oxygen tension

measurements for the evaluation of the efficiency of photodynamic therapy. *Photochem Photobiol* **1990**, *52* (2), 375-85.

- 80.** Henderson, B. W.; Dougherty, T. J.; Malone, P. B., Studies on the mechanism of tumor destruction by photoradiation therapy. *Prog Clin Biol Res* **1984**, *170*, 601-12.
- 81.** Korbelik, M., Induction of tumor immunity by photodynamic therapy. *J Clin Laser Med Surg* **1996**, *14* (5), 329-34.
- 82.** Musser, D. A.; Fiel, R. J., Cutaneous photosensitizing and immunosuppressive effects of a series of tumor localizing porphyrins. *Photochem Photobiol* **1991**, *53* (1), 119-23.
- 83.** Lynch, D. H.; Haddad, S.; King, V. J.; Ott, M. J.; Straight, R. C.; Jolles, C. J., Systemic Immunosuppression Induced by Photodynamic Therapy (Pdt) Is Adoptively Transferred by Macrophages. *Photochemistry and Photobiology* **1989**, *49* (4), 453-458.
- 84.** Korbelik, M.; Naraparaju, V. R.; Yamamoto, N., Macrophage-directed immunotherapy as adjuvant to photodynamic therapy of cancer. *Brit J Cancer* **1997**, *75* (2), 202-207.
- 85.** Dou, S.; Yao, Y. D.; Yang, X. Z.; Sun, T. M.; Mao, C. Q.; Song, E. W.; Wang, J., Anti-Her2 single-chain antibody mediated DNMTs-siRNA delivery for targeted breast cancer therapy. *J Control Release* **2012**, *161* (3), 875-83.
- 86.** Liu, D.; Liu, F.; Liu, Z.; Wang, L.; Zhang, N., Tumor specific delivery and therapy by double-targeted nanostructured lipid carriers with anti-VEGFR-2 antibody. *Mol Pharm* **2011**, *8* (6), 2291-301.
- 87.** Berlin, J. M.; Pham, T. T.; Sano, D.; Mohamedali, K. A.; Marcano, D. C.; Myers, J. N.; Tour, J. M., Noncovalent functionalization of carbon nanovectors with an antibody enables targeted drug delivery. *ACS Nano* **2011**, *5* (8), 6643-50.
- 88.** Alley, S. C.; Okeley, N. M.; Senter, P. D., Antibody-drug conjugates: targeted drug delivery for cancer. *Curr Opin Chem Biol* **2010**, *14* (4), 529-37.

89. van Dongen, G. A. M. S.; Visser, G. W.; Vrouenraets, M. B., Photosensitizer-antibody conjugates for detection and therapy of cancer. *Adv Drug Deliver Rev* **2004**, *56* (1), 31-52.
90. Gravier, J.; Schneider, R.; Frochot, C.; Bastogne, T.; Schmitt, F.; Didelon, J.; Guillemin, F.; Barberi-Heyob, M., Improvement of meta-tetra(hydroxyphenyl)chlorin-like photosensitizer selectivity with folate-based targeted delivery. Synthesis and in vivo delivery studies. *J Med Chem* **2008**, *51* (13), 3867-3877.
91. Zhang, M.; Zhang, Z. H.; Blessington, D.; Li, H.; Busch, T. M.; Madrak, V.; Miles, J.; Chance, B.; Glickson, J. D.; Zheng, G., Pyropheophorbide 2-deoxyglucosamide: A new photosensitizer targeting glucose transporters. *Bioconjugate Chem* **2003**, *14* (4), 709-714.
92. Aina, O. H.; Sroka, T. C.; Chen, M. L.; Lam, K. S., Therapeutic cancer targeting peptides. *Biopolymers* **2002**, *66* (3), 184-199.
93. Conway, C. L.; Walker, I.; Bell, A.; Roberts, D. J. H.; Brown, S. B.; Vernon, D. I., In vivo and in vitro characterisation of a protoporphyrin IX-cyclic RGD peptide conjugate for use in photodynamic therapy. *Photoch Photobio Sci* **2008**, *7* (3), 290-298.
94. Famulok, M.; Hartig, J. S.; Mayer, G., Functional aptamers and aptazymes in biotechnology, diagnostics, and therapy. *Chem Rev* **2007**, *107* (9), 3715-3743.
95. Zilberstein, J.; Schreiber, S.; Bloemers, M. C. W. M.; Bendel, P.; Neeman, M.; Schechtman, E.; Kohen, F.; Scherz, A.; Salomon, Y., Antivascular treatment of solid melanoma tumors with bacteriochlorophyll-serine-based photodynamic therapy. *Photochemistry and Photobiology* **2001**, *73* (3), 257-266.
96. Marras, S. A. E.; Kramer, F. R.; Tyagi, S., Efficiencies of fluorescence resonance energy transfer and contact-mediated quenching in oligonucleotide probes. *Nucleic Acids Res* **2002**, *30* (21).

97. Lovell, J. F.; Chen, J.; Jarvi, M. T.; Cao, W. G.; Allen, A. D.; Liu, Y.; Tidwell, T. T.; Wilson, B. C.; Zheng, G., FRET quenching of photosensitizer singlet oxygen generation. *J Phys Chem B* **2009**, *113* (10), 3203-11.
98. Urano, Y.; Asanuma, D.; Hama, Y.; Koyama, Y.; Barrett, T.; Kamiya, M.; Nagano, T.; Watanabe, T.; Hasegawa, A.; Choyke, P. L.; Kobayashi, H., Selective molecular imaging of viable cancer cells with pH-activatable fluorescence probes. *Nat Med* **2009**, *15* (1), 104-9.
99. Ozlem, S.; Akkaya, E. U., Thinking outside the silicon box: molecular and logic as an additional layer of selectivity in singlet oxygen generation for photodynamic therapy. *J Am Chem Soc* **2009**, *131* (1), 48-9.
100. Chen, X.; Zhou, Y.; Peng, X.; Yoon, J., Fluorescent and colorimetric probes for detection of thiols. *Chem Soc Rev* **2010**, *39* (6), 2120-35.
101. Godwin, A. K.; Meister, A.; O'Dwyer, P. J.; Huang, C. S.; Hamilton, T. C.; Anderson, M. E., High resistance to cisplatin in human ovarian cancer cell lines is associated with marked increase of glutathione synthesis. *Proc Natl Acad Sci U S A* **1992**, *89* (7), 3070-4.
102. Tew, K. D.; Clapper, M. L.; Greenberg, R. E.; Weese, J. L.; Hoffman, S. J.; Smith, T. M., Glutathione S-transferases in human prostate. *Biochim Biophys Acta* **1987**, *926* (1), 8-15.
103. Valeur, B.; Leray, I., Design principles of fluorescent molecular sensors for cation recognition. *Coordin Chem Rev* **2000**, *205*, 3-40.
104. Wasielewski, M. R.; Fenton, J. M.; Govindjee, The Rate of Formation of P700<sup>+</sup>-A<sub>0</sub><sup>-</sup> in Photosystem-I Particles from Spinach as Measured by Picosecond Transient Absorption-Spectroscopy. *Photosynth Res* **1987**, *12* (2), 181-189.
105. Czarnik, A. W., Fluorescent Chemosensors of Ion and Molecule Recognition. *Abstr Pap Am Chem S* **1993**, *206*, 203-COLL.
106. Fabbrizzi, L.; Poggi, A., Sensors and Switches from Supramolecular Chemistry. *Chemical Society Reviews* **1995**, *24* (3), 197-202.

107. Czarnik, A. W., Supramolecular Chemistry, Fluorescence, and Sensing. *Acs Sym Ser* **1993**, 538, 1-9.
108. de Silva, A. P.; de Silva, S. A., Fluorescent signalling crown ethers; 'switching on' of fluorescence by alkali metal ion recognition and binding in situ. *Journal of the Chemical Society, Chemical Communications* **1986**, (23), 1709-1710.
109. Huston, M. E.; Haider, K. W.; Czarnik, A. W., Chelation-Enhanced Fluorescence in 9,10-Bis(Tmeda)Anthracene. *J Am Chem Soc* **1988**, 110 (13), 4460-4462.
110. Baki, C. N.; Akkaya, E. U., Boradiazaindacene-appended calix[4]arene: Fluorescence sensing of pH near neutrality. *J Org Chem* **2001**, 66 (4), 1512-1513.
111. Turfan, B.; Akkaya, E. U., Modulation of boradiazaindacene emission by cation-mediated oxidative PET. *Org Lett* **2002**, 4 (17), 2857-9.
112. Matsumoto, T.; Urano, Y.; Shoda, T.; Kojima, H.; Nagano, T., A thiol-reactive fluorescence probe based on donor-excited photoinduced electron transfer: Key role of ortho substitution. *Organic Letters* **2007**, 9 (17), 3375-3377.
113. Donckt, E. V., *Prog. React. Kinet.* 5, 273
114. Martin, M. M.; Plaza, P.; Meyer, Y. H.; Badaoui, F.; Bourson, J.; Lefevre, J. P.; Valeur, B., Steady-state and picosecond spectroscopy of Li<sup>+</sup> or Ca<sup>2+</sup> complexes with a crowned merocyanine. Reversible photorelease of cations. *J Phys Chem-Us* **1996**, 100 (17), 6879-6888.
115. Martin, M. M.; Plaza, P.; Hung, N. D.; Meyer, Y. H.; Bourson, J.; Valeur, B., Photoejection of Cations from Complexes with a Crown-Ether-Linked Merocyanine Evidenced by Ultrafast Spectroscopy. *Chem Phys Lett* **1993**, 202 (5), 425-430.
116. Valeur, B.; Bourson, J.; Pouget, J., Ion Recognition Detected by Changes in Photoinduced Charge or Energy-Transfer. *Acs Sym Ser* **1993**, 538, 25-44.

117. Callan, J. F.; de Silva, A. P.; Magri, D. C., Luminescent sensors and switches in the early 21st century. *Tetrahedron* **2005**, *61* (36), 8551-8588.
118. (a) Valeur, B.; Mugnier, J.; Pouget, J.; Bourson, J.; Santi, F., Calculation of the Distribution of Donor-Acceptor Distances in Flexible Bichromophoric Molecules - Application to Intramolecular Transfer of Excitation-Energy. *J Phys Chem-Us* **1989**, *93* (16), 6073-6079; (b) Bourson, J.; Valeur, B., Ion-Responsive Fluorescent Compounds .2. Cation-Steered Intramolecular Charge-Transfer in a Crowned Merocyanine. *J Phys Chem-Us* **1989**, *93* (9), 3871-3876.
119. Mitewa, M.; Mateeva, N.; Antonov, L.; Deligeorgiev, T., Spectrophotometric Investigation of the Complex-Formation of Aza-15-Crown-5 Containing Styryl Dyes with Ba<sup>2+</sup> and Ca<sup>2+</sup> Cations. *Dyes Pigments* **1995**, *27* (3), 219-225.
120. Martin, M. M.; Plaza, P.; Meyer, Y. H.; Bégin, L.; Bourson, J.; Valeur, B., A new concept of photogeneration of cations: Evidence for photoejection of Ca<sup>2+</sup> and Li<sup>+</sup> from complexes with a crown-ether-linked merocyanine by picosecond spectroscopy. *J Fluoresc* **1994**, *4* (4), 271-273.
121. Lin, W.; Yuan, L.; Cao, Z.; Feng, Y.; Long, L., A sensitive and selective fluorescent thiol probe in water based on the conjugate 1,4-addition of thiols to alpha,beta-unsaturated ketones. *Chem.-Eur. J.* **2009**, *15* (20), 5096-103.
122. Förster, T., *Ann. Phys.* **1948**, *2*, 55-75
123. Forster, T., 10th Spiers Memorial Lecture. Transfer mechanisms of electronic excitation. *Discussions of the Faraday Society* **1959**, *27*, 7-17.
124. Turro, N. J., *Modern Molecular Photochemistry*. Sausalito, **1991**.
125. Lakowicz, J. R., *Principles of Fluorescence Spectroscopy*. 3 ed.; Springer: New York, **2006**; p 954.

126. Piggott, A. M.; Karuso, P., Fluorometric assay for the determination of glutathione reductase activity. *Analytical Chemistry* **2007**, *79* (22), 8769-8773.
127. Huang, S.-T.; Ting, K.-N.; Wang, K.-L., Development of a long-wavelength fluorescent probe based on quinone–methide-type reaction to detect physiologically significant thiols. *Analytica Chimica Acta* **2008**, *620* (1–2), 120-126.
128. Chow, C.-F.; Chiu, B. K. W.; Lam, M. H. W.; Wong, W.-Y., A Trinuclear Heterobimetallic Ru(II)/Pt(II) Complex as a Chemodosimeter Selective for Sulfhydryl-Containing Amino Acids and Peptides. *J Am Chem Soc* **2003**, *125* (26), 7802-7803.
129. Maeda, H.; Matsuno, H.; Ushida, M.; Katayama, K.; Saeki, K.; Itoh, N., 2,4-Dinitrobenzenesulfonyl Fluoresceins as Fluorescent Alternatives to Ellman's Reagent in Thiol-Quantification Enzyme Assays. *Angewandte Chemie International Edition* **2005**, *44* (19), 2922-2925.
130. Tang, B.; Xing, Y.; Li, P.; Zhang, N.; Yu, F.; Yang, G., A Rhodamine-Based Fluorescent Probe Containing a Se–N Bond for Detecting Thiols and Its Application in Living Cells. *J Am Chem Soc* **2007**, *129* (38), 11666-11667.
131. Allen, C. M.; Sharman, W. M.; Van Lier, J. E., Current status of phthalocyanines in the photodynamic therapy of cancer. *J Porphyr Phthalocya* **2001**, *5* (2), 161-169.

# Appendix A

## NMR Spectrum

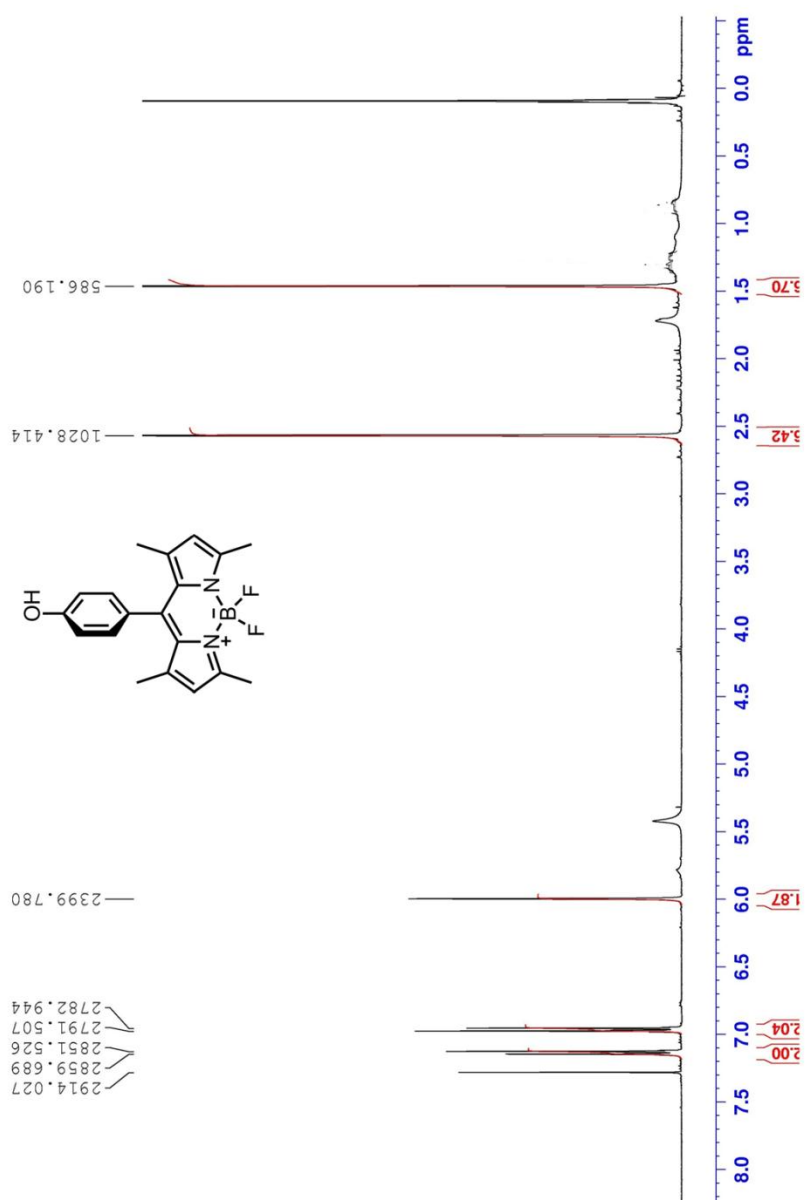
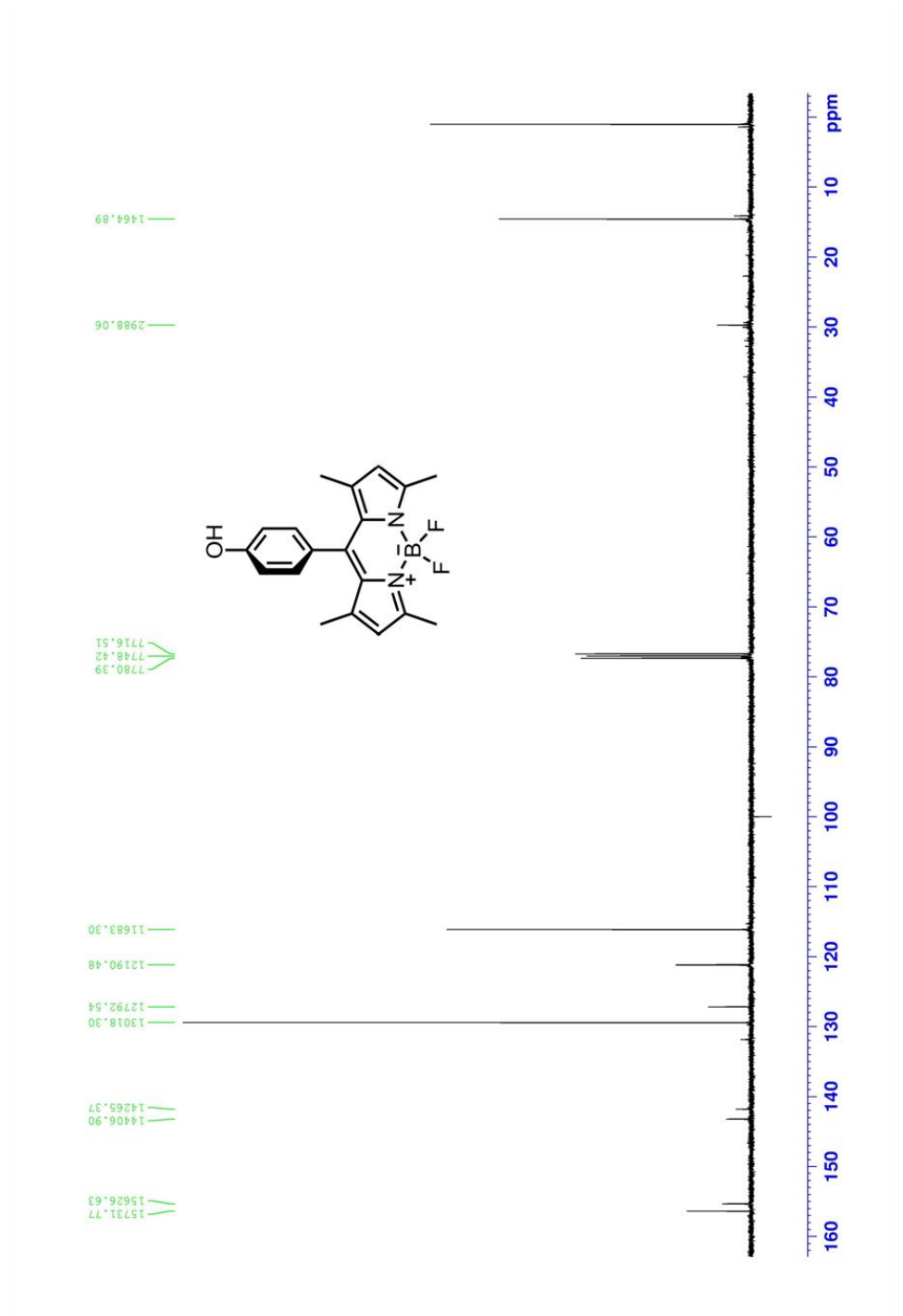


Figure 43.  $^1\text{H}$  NMR spectra of compound 30



**Figure 44.**  $^{13}\text{C}$  NMR spectra of compound 30

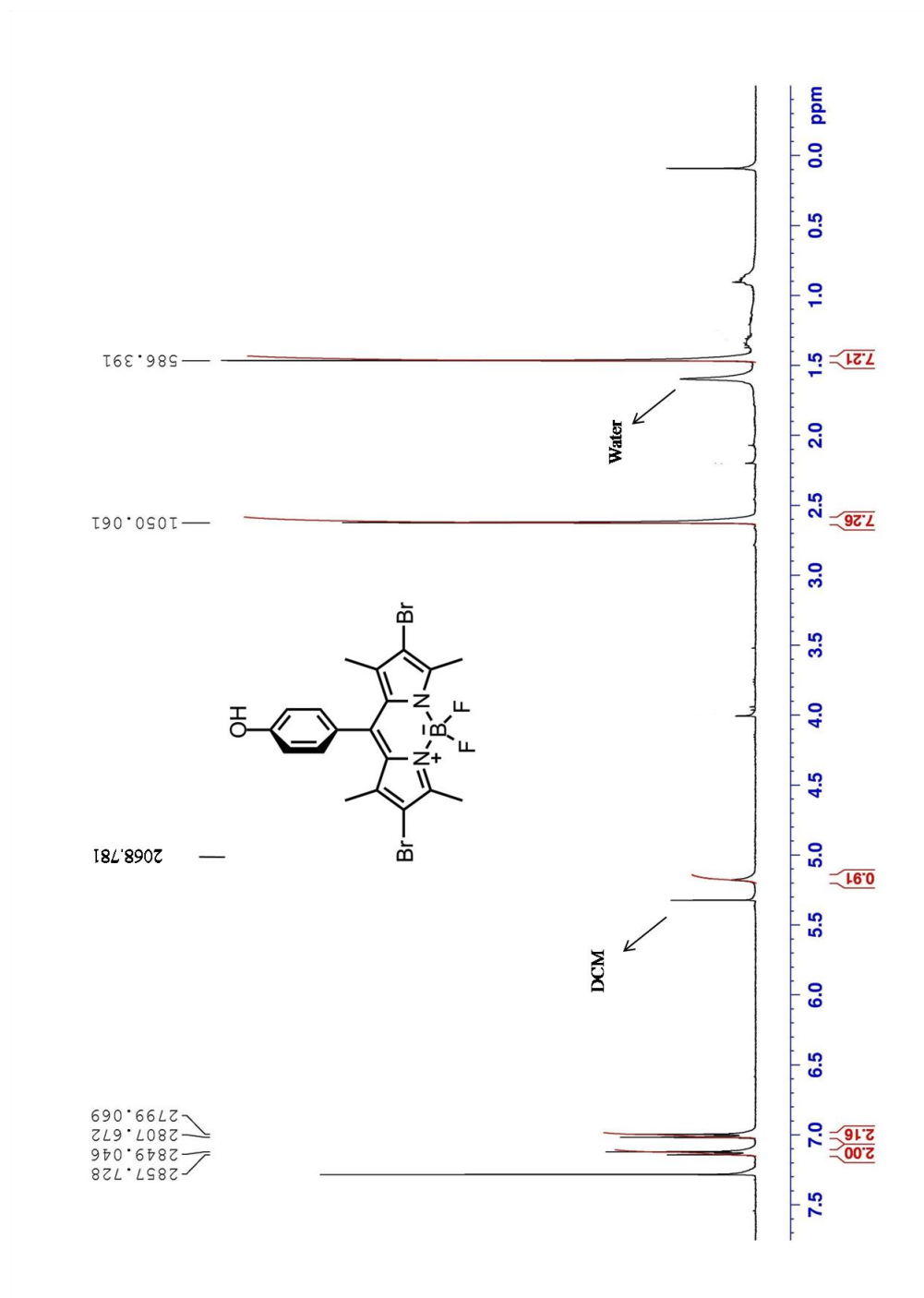
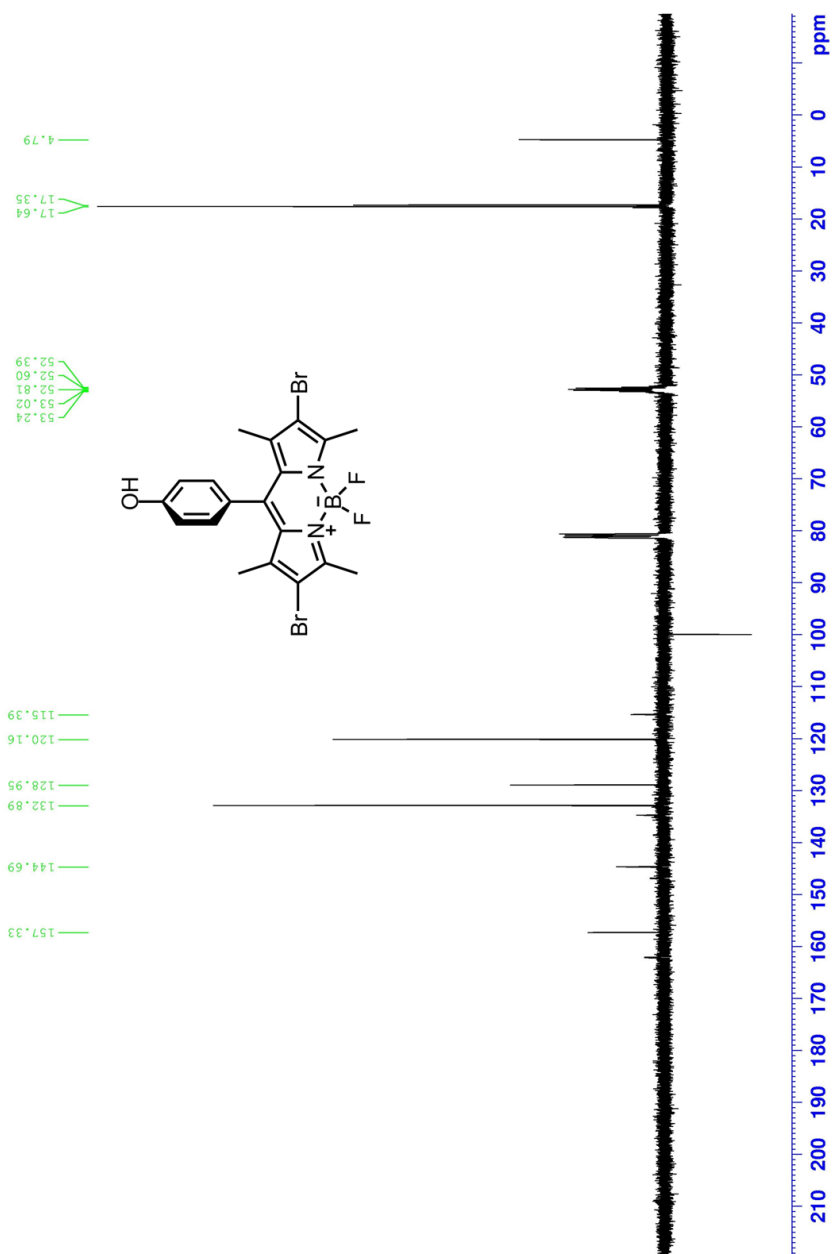


Figure 45. <sup>1</sup>H NMR spectra of compound 31



**Figure 46.**  $^{13}\text{C}$  NMR spectra of compound 31

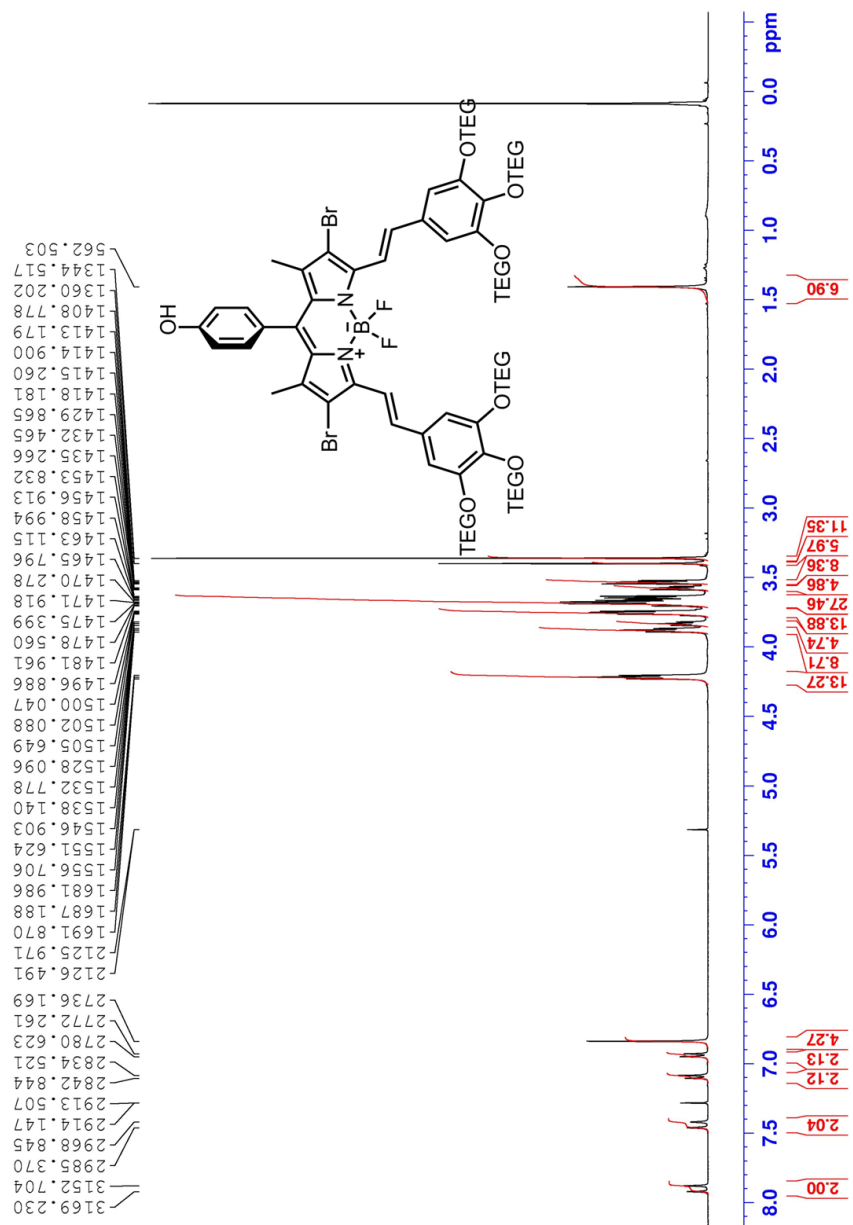


Figure 47. <sup>1</sup>H NMR spectra of compound 32

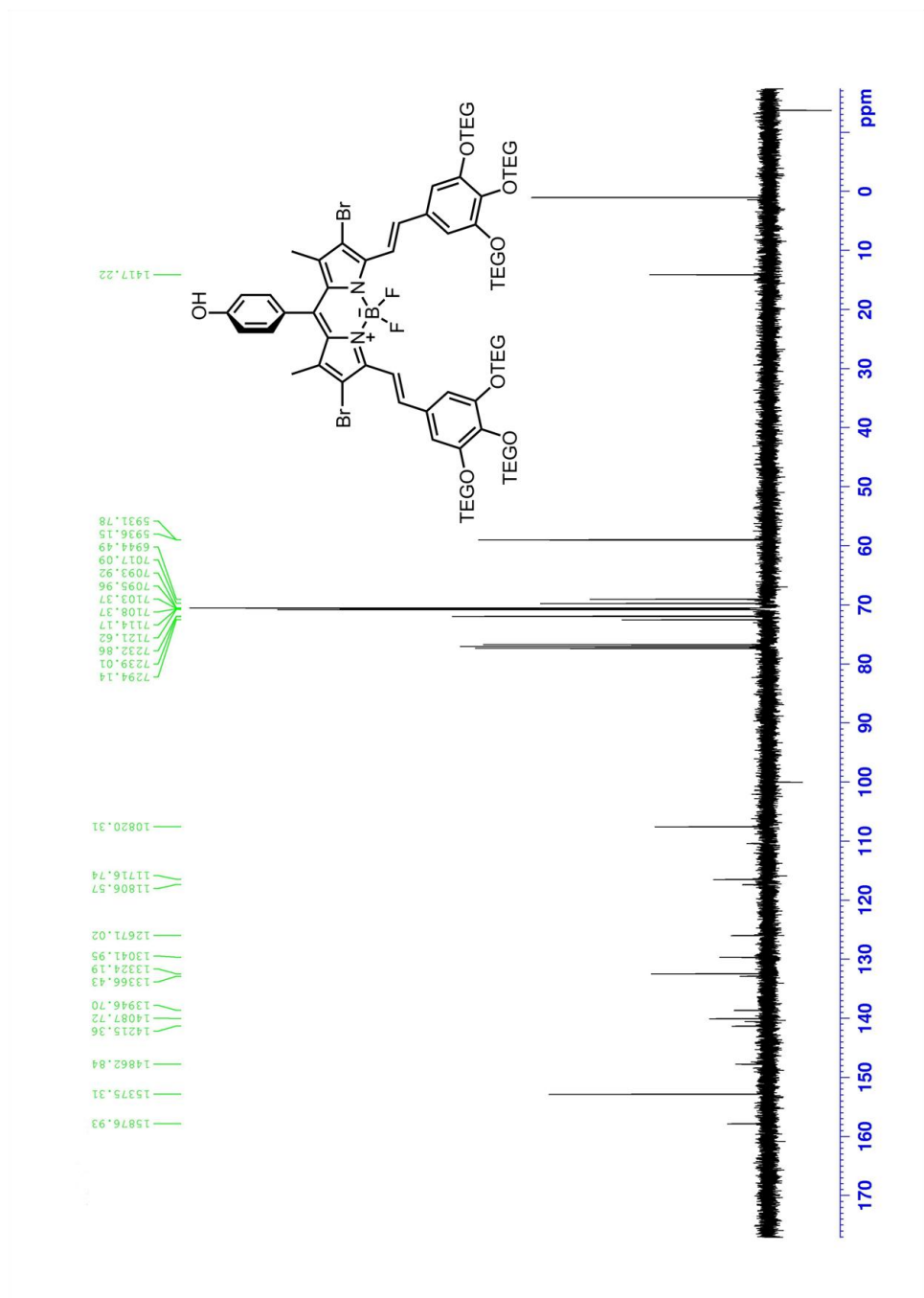


Figure 48.  $^{13}\text{C}$  NMR spectra of compound 32

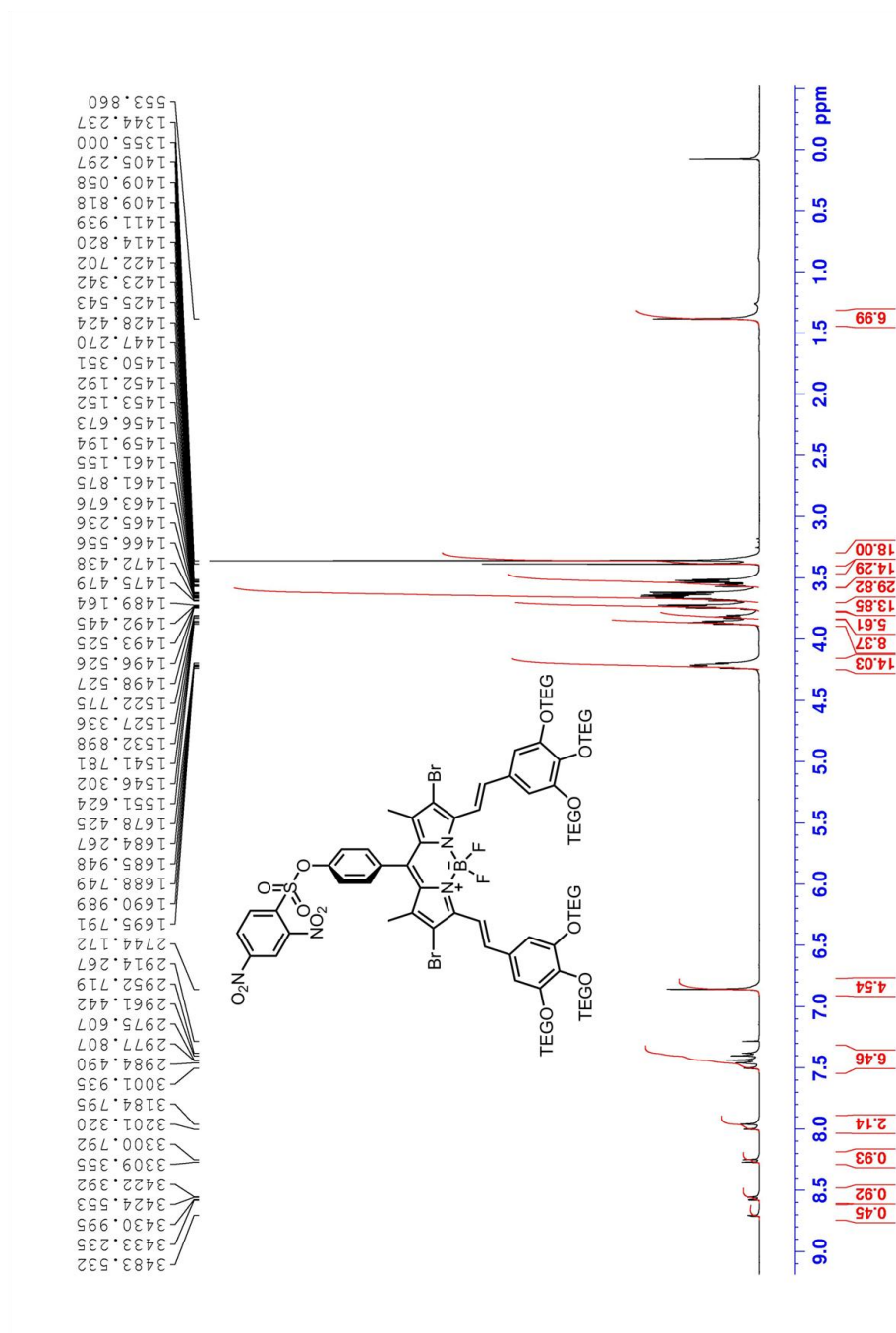


Figure 49.  $^1\text{H}$  NMR spectra of compound 33

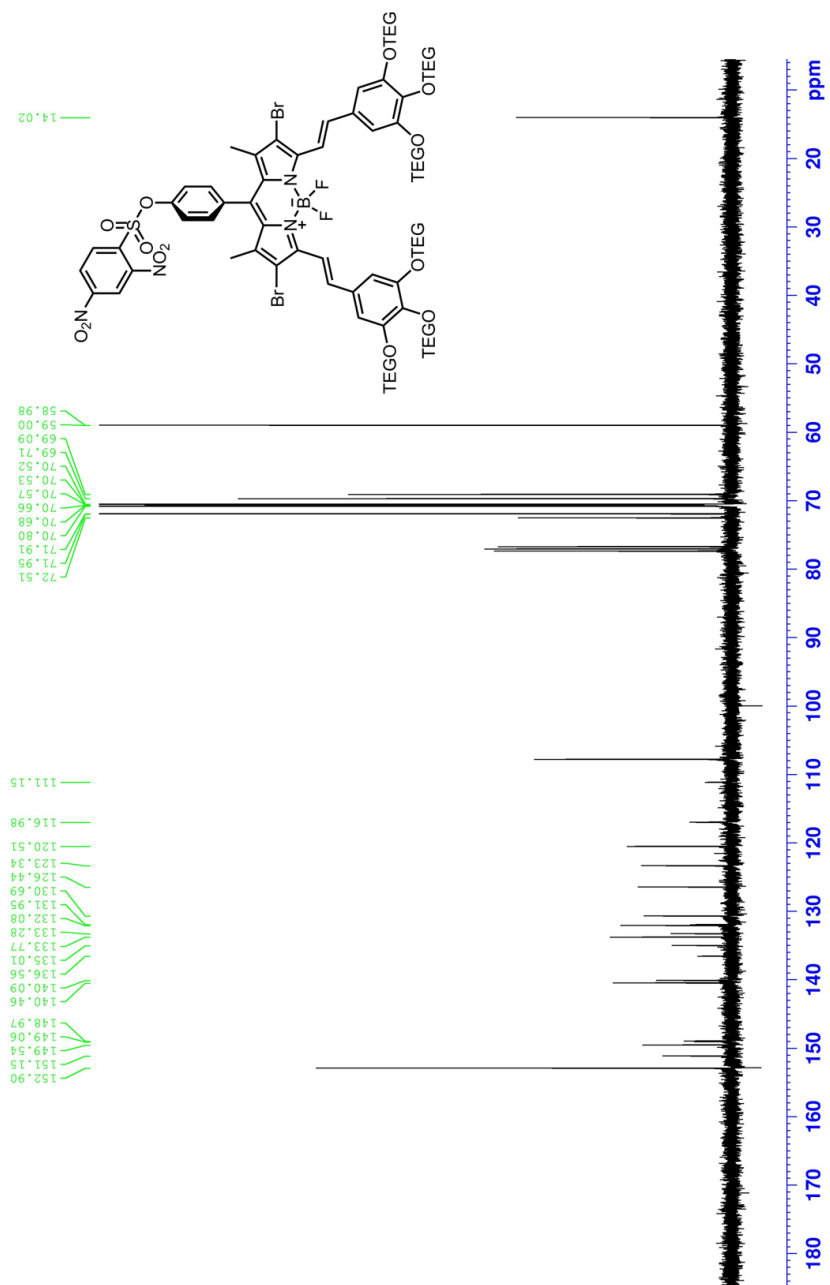
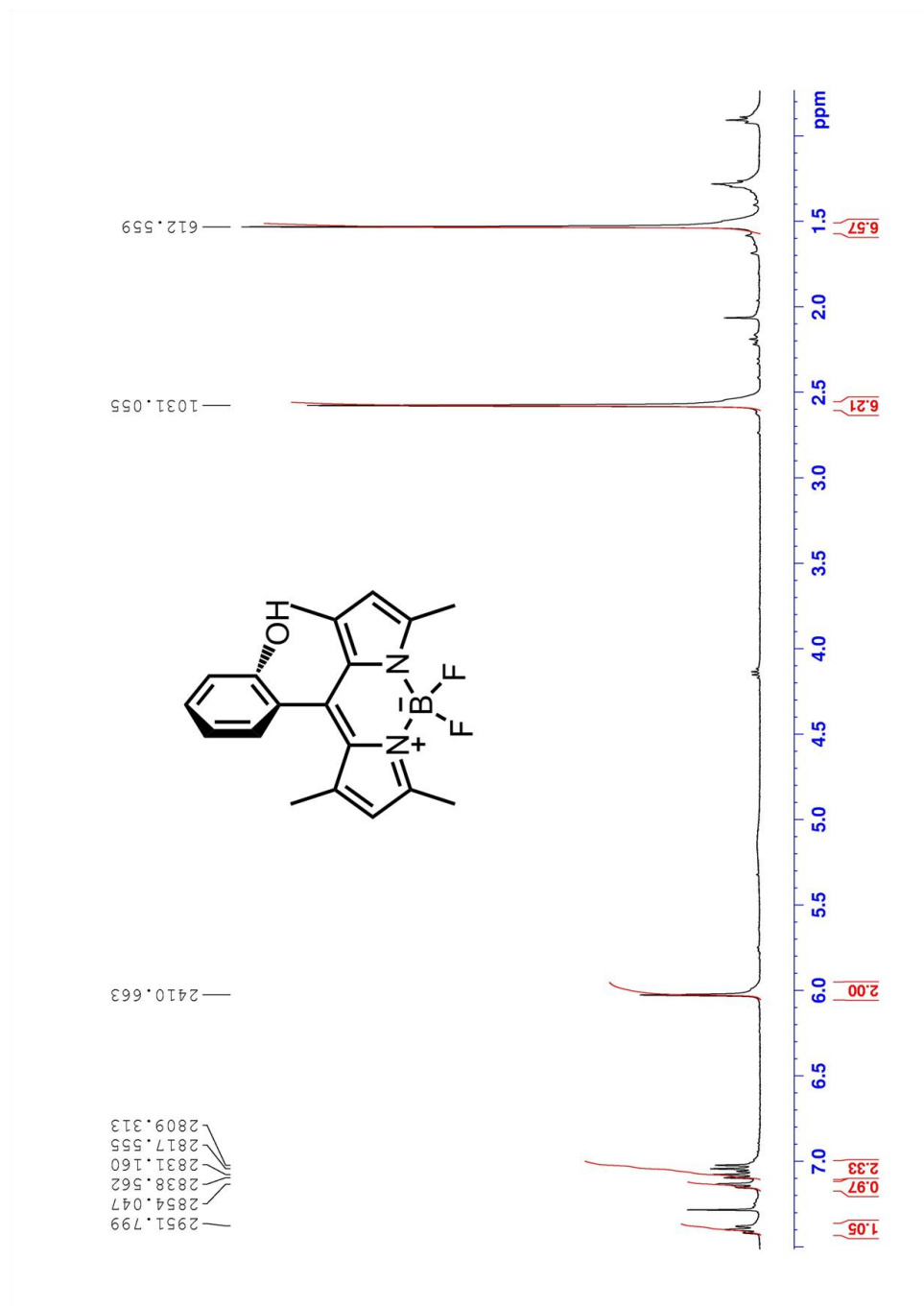
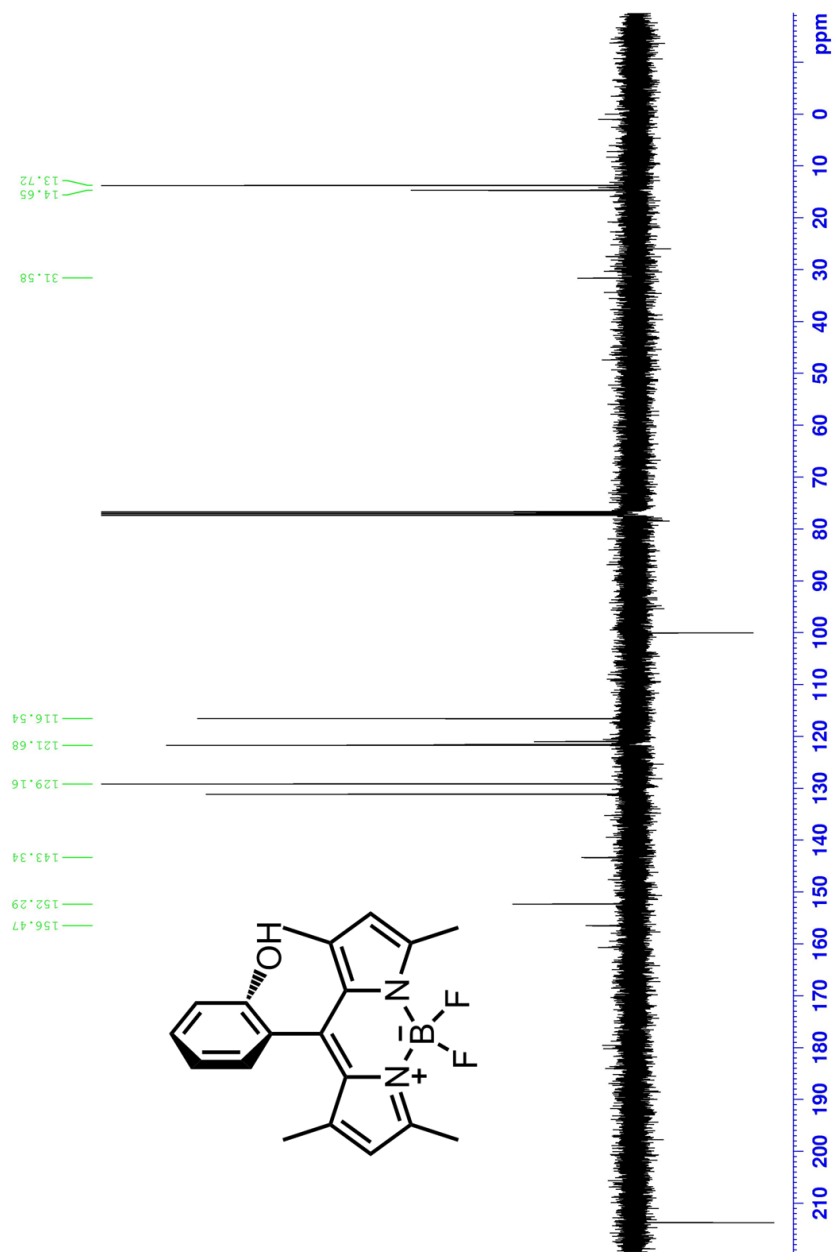


Figure 50. <sup>13</sup>C NMR spectra of compound 33



**Figure 51.** <sup>1</sup>H NMR spectra of compound 34



**Figure 52.** <sup>13</sup>C NMR spectra of compound 34

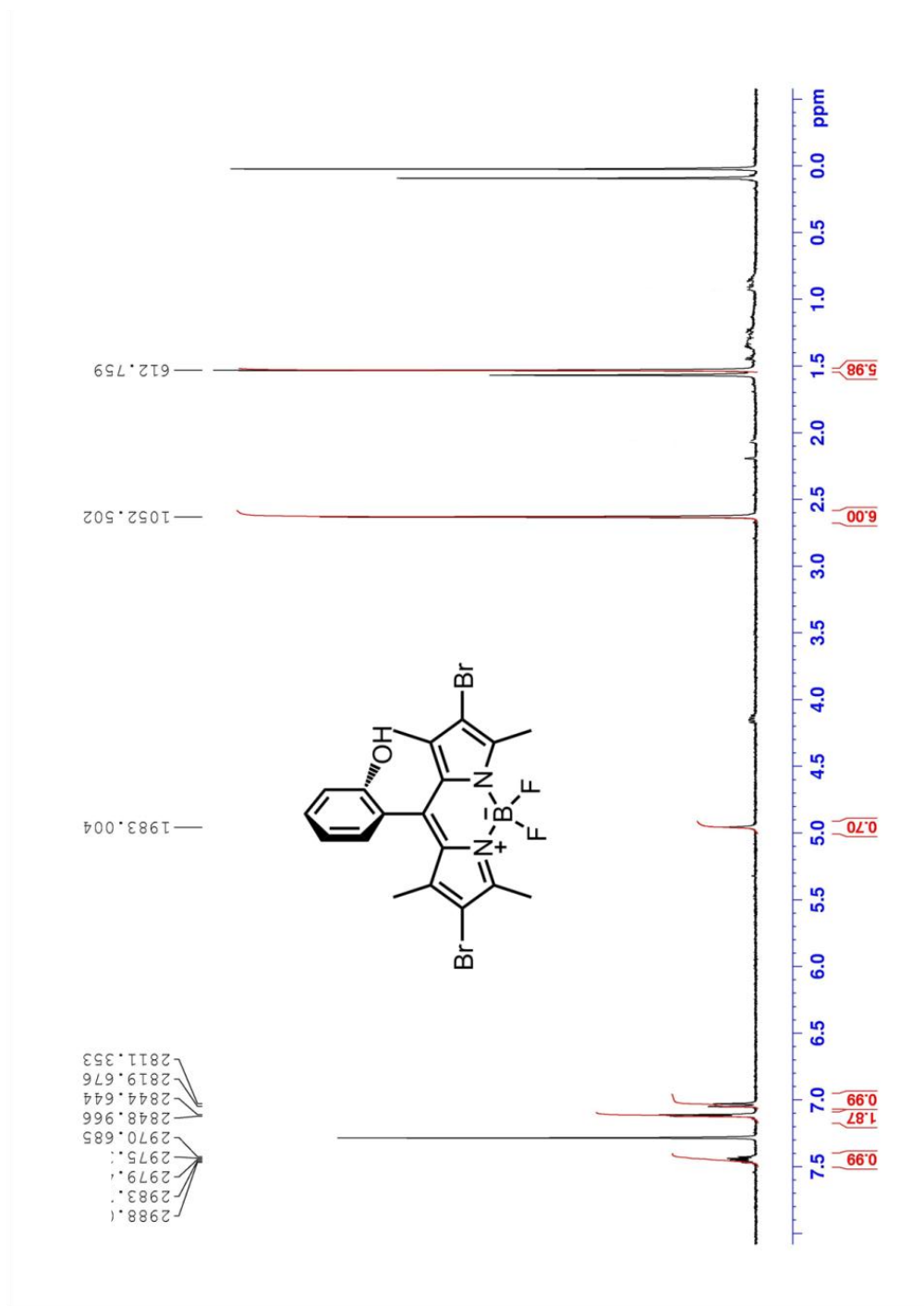
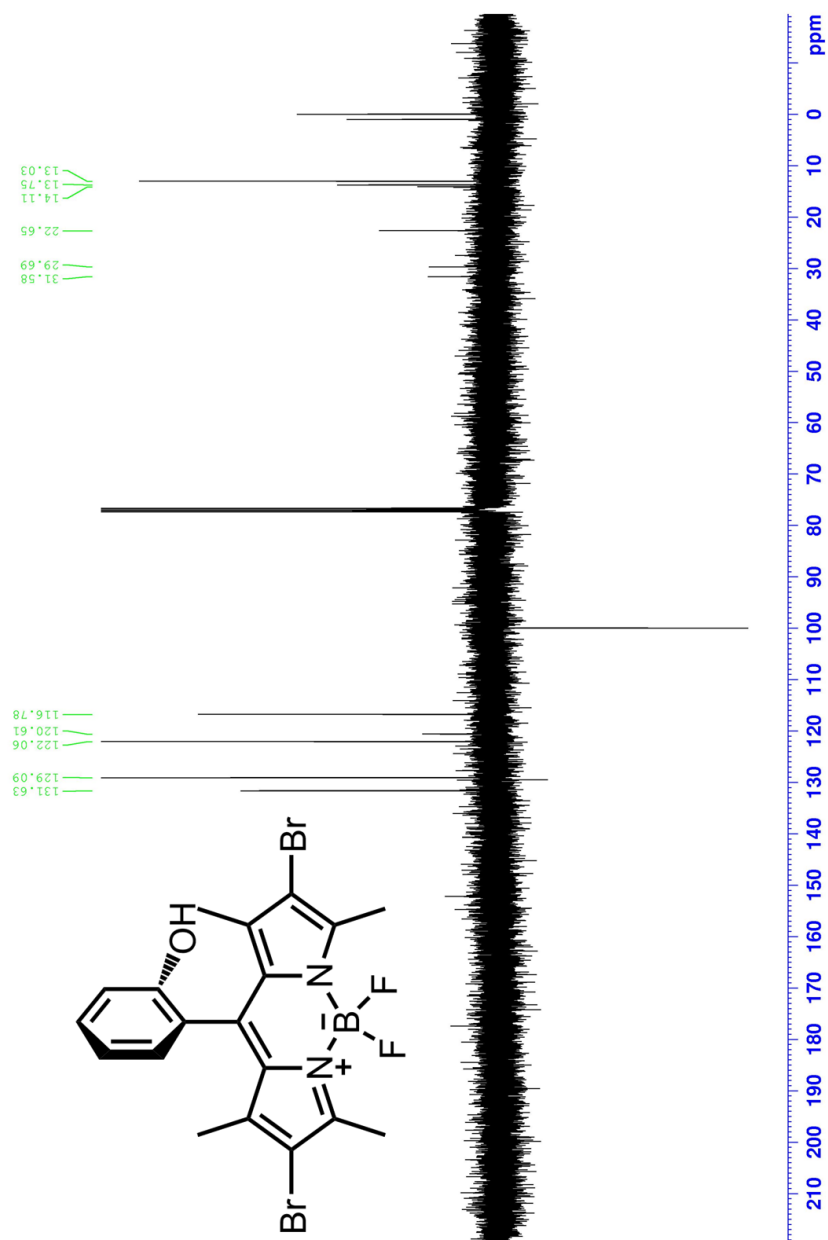


Figure 53.  $^1\text{H NMR}$  spectra of compound 35



**Figure 54.**  $^{13}\text{C}$  NMR spectra of compound 35

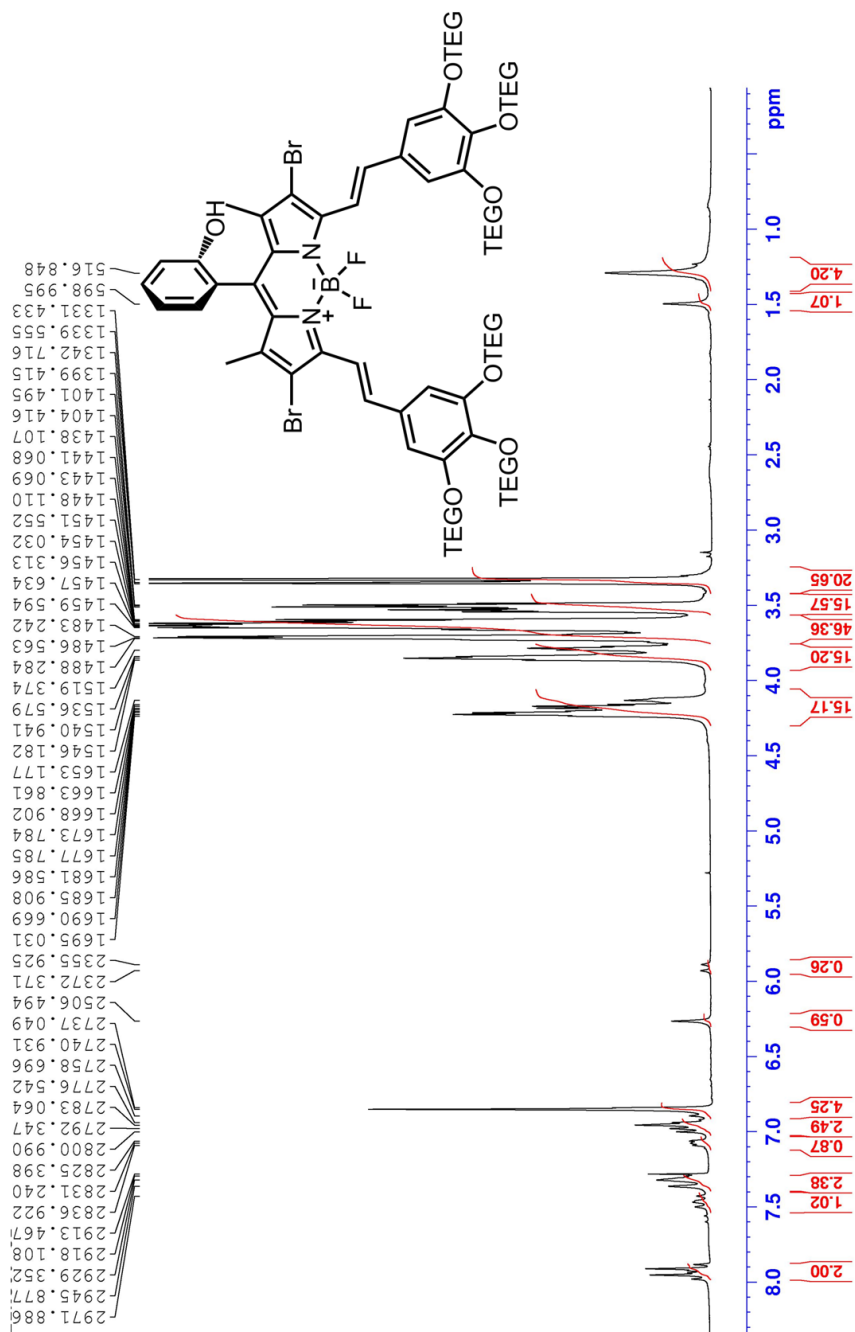
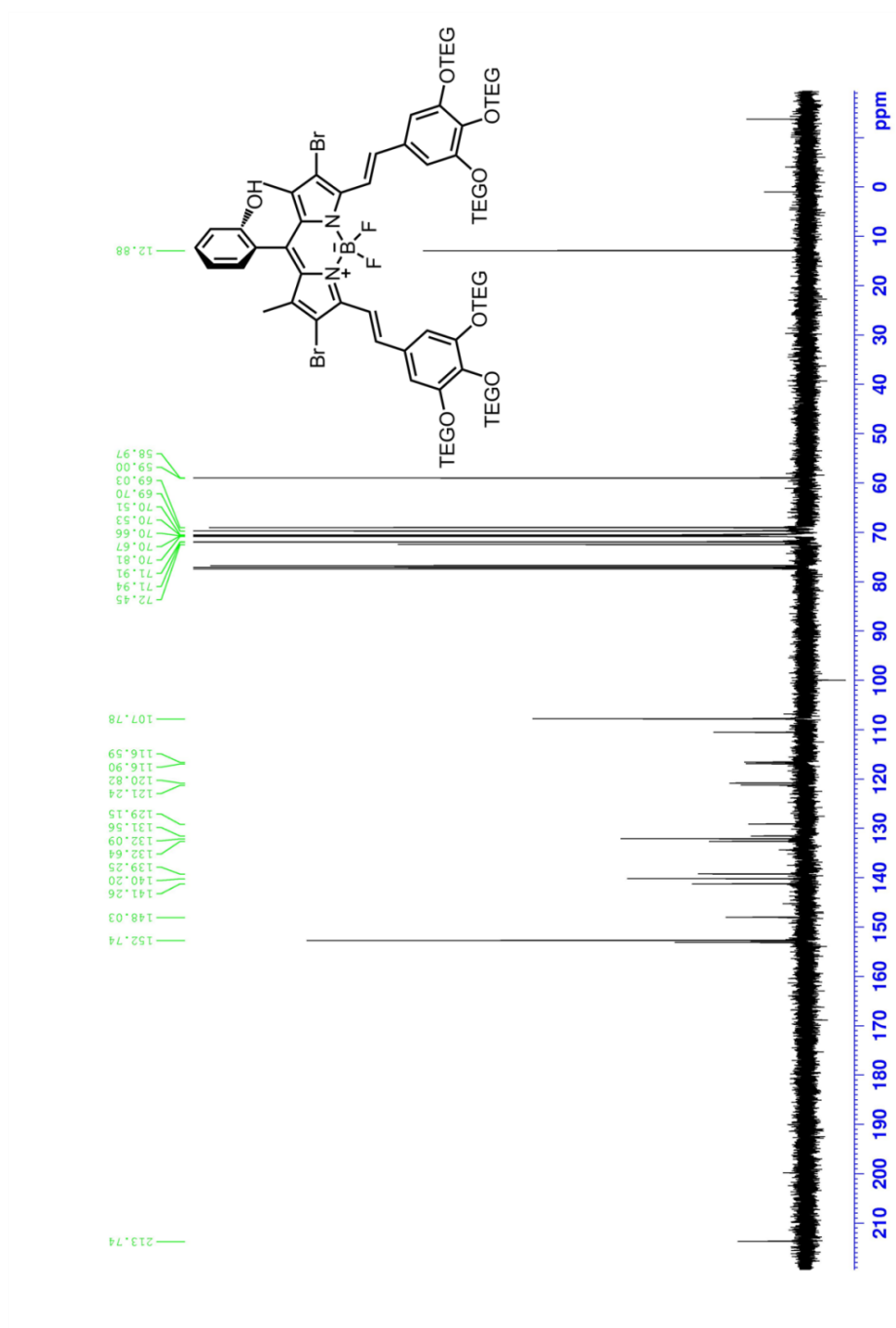
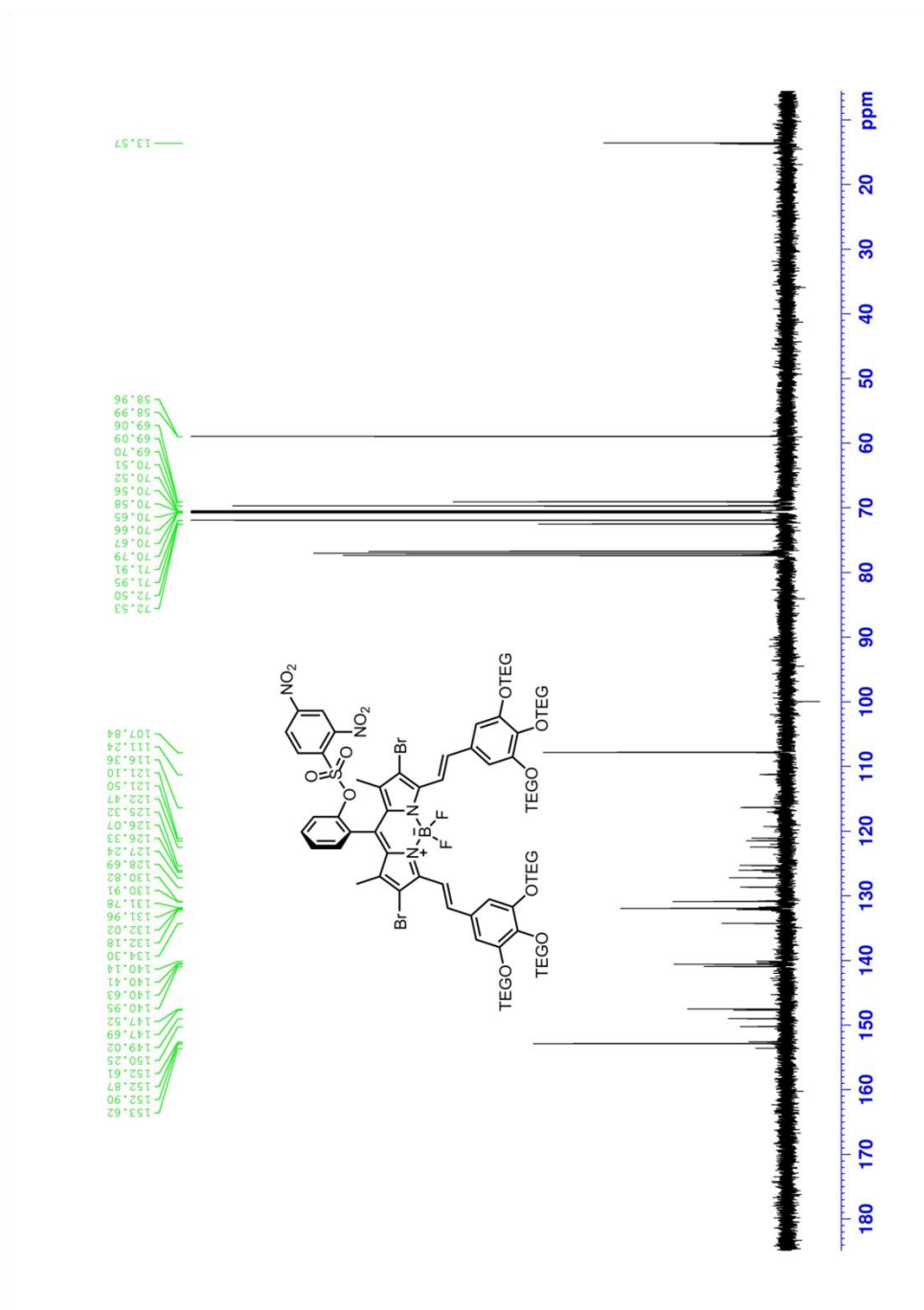


Figure 55.  $^1\text{H}$  NMR spectra of compound 36



**Figure 56.** <sup>13</sup>C NMR spectra of compound 36





**Figure 58.**  $^{13}\text{C}$  NMR spectra of compound 37

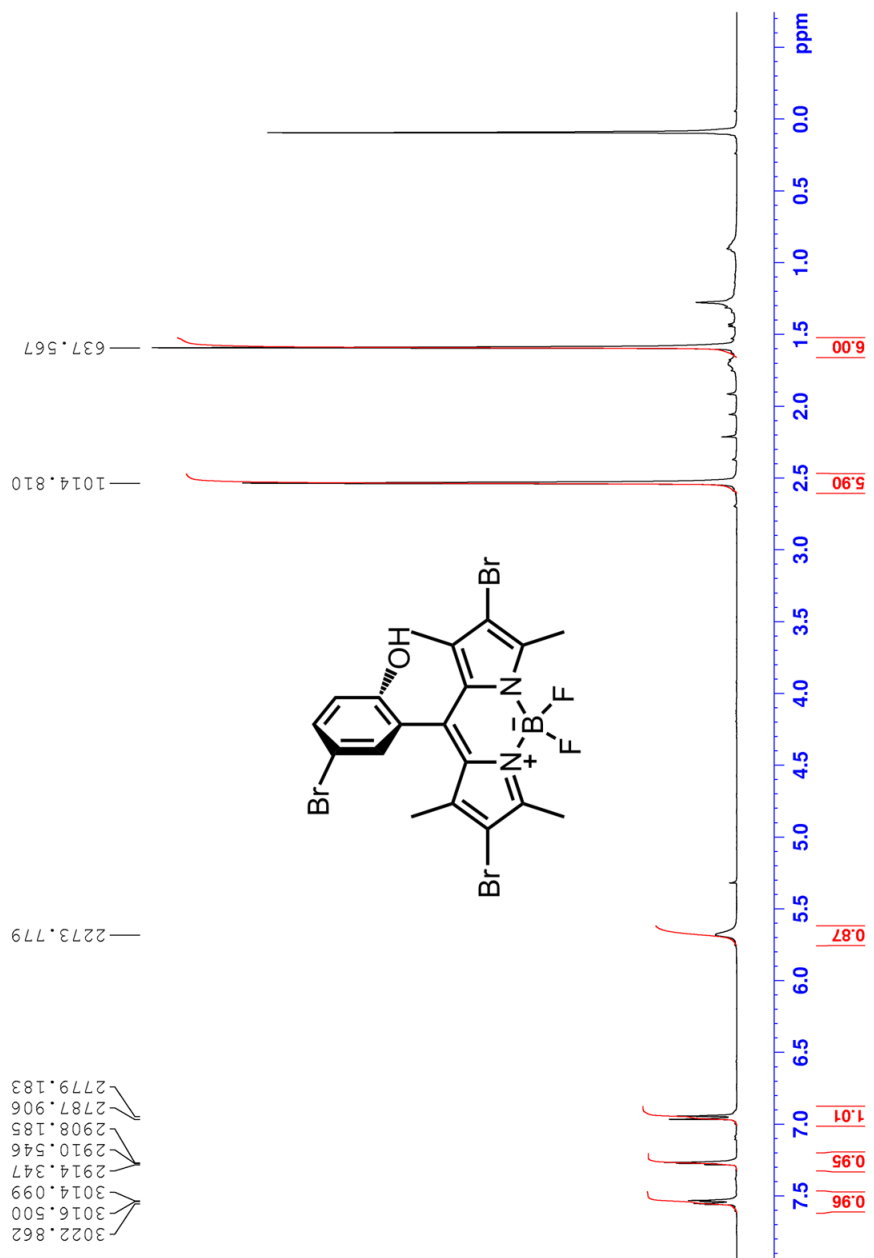
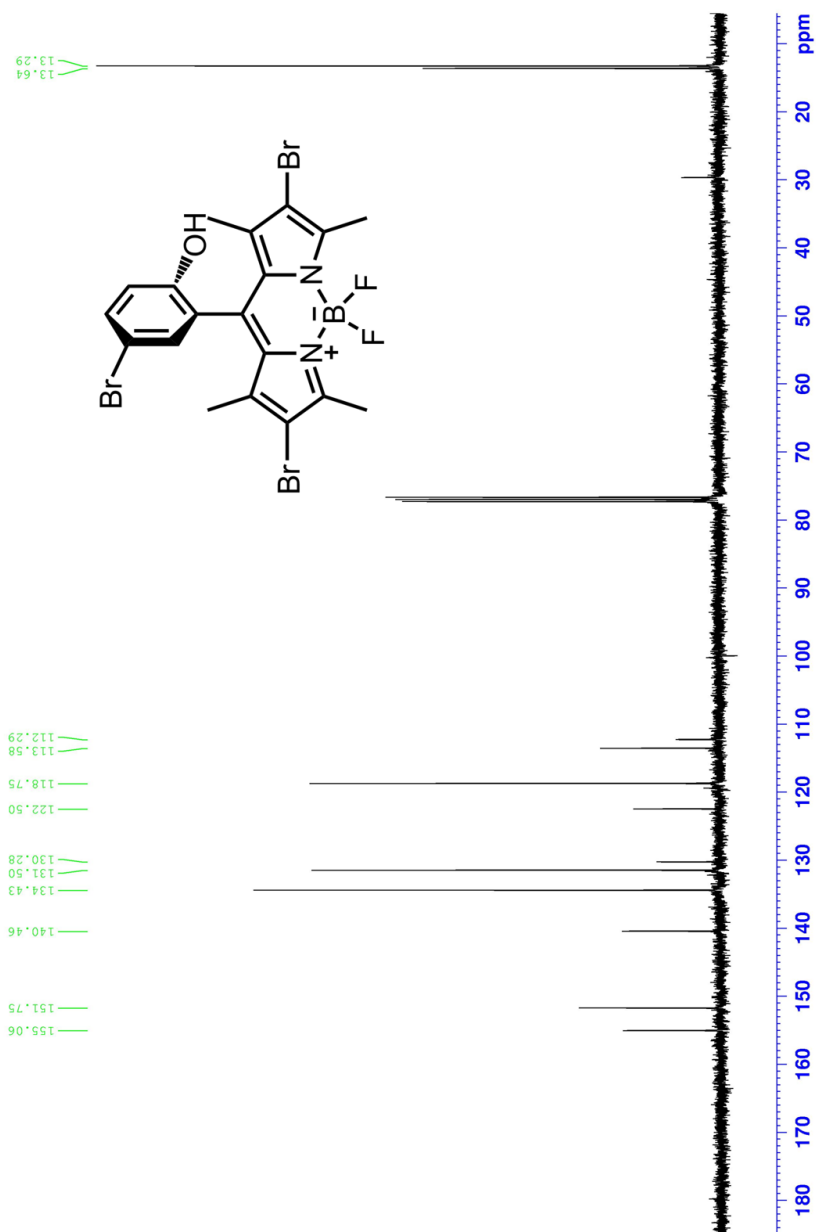


Figure 59. <sup>1</sup>H NMR spectra of compound 38



**Figure 60.**  $^{13}\text{C}$  NMR spectra of compound 38

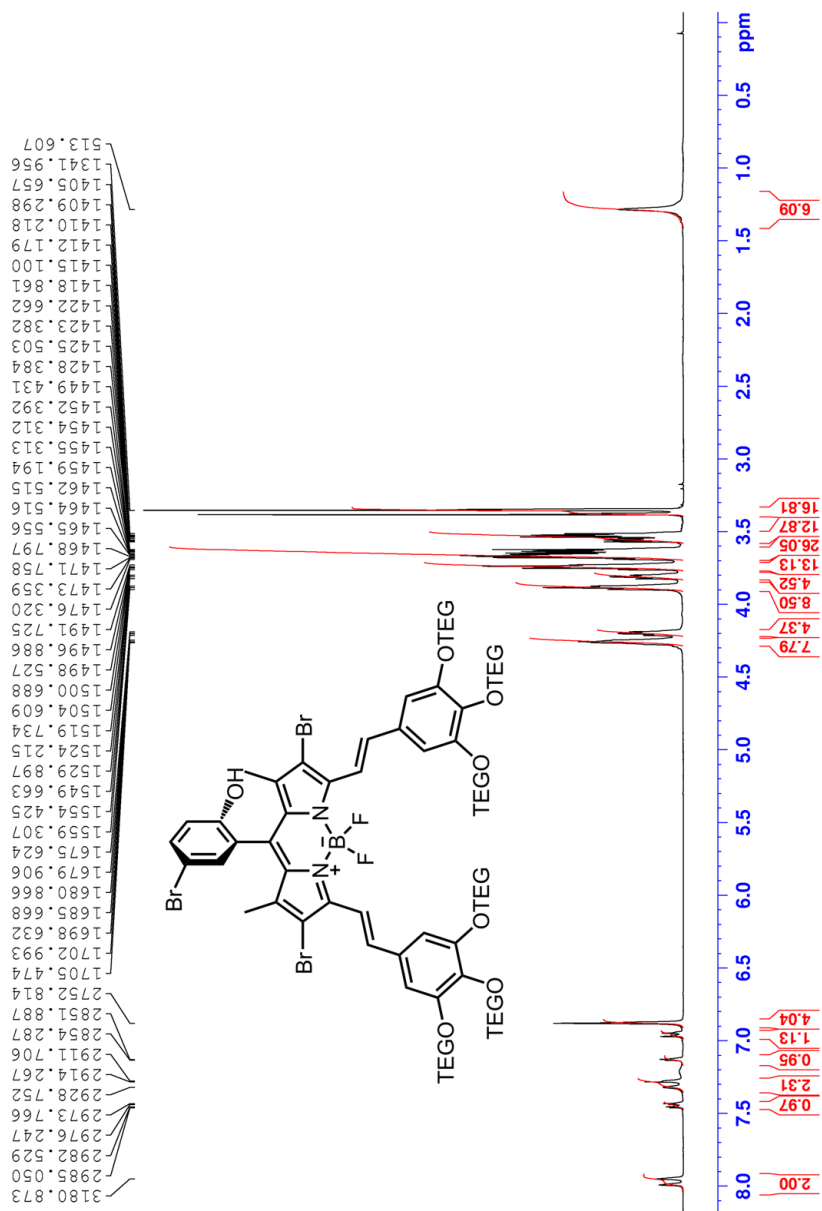
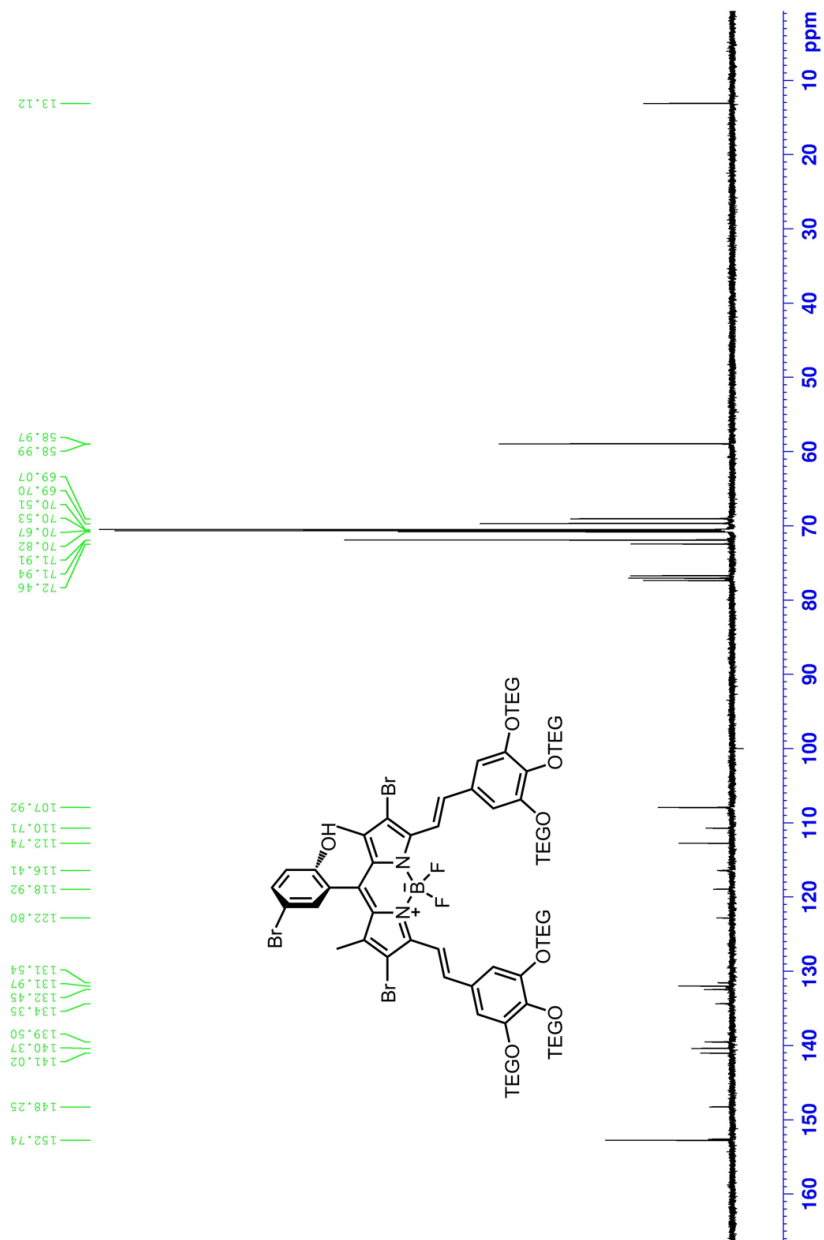


Figure 61.  $^1\text{H NMR}$  spectra of compound 39



**Figure 62.**  $^{13}\text{C}$  NMR spectra of compound 39

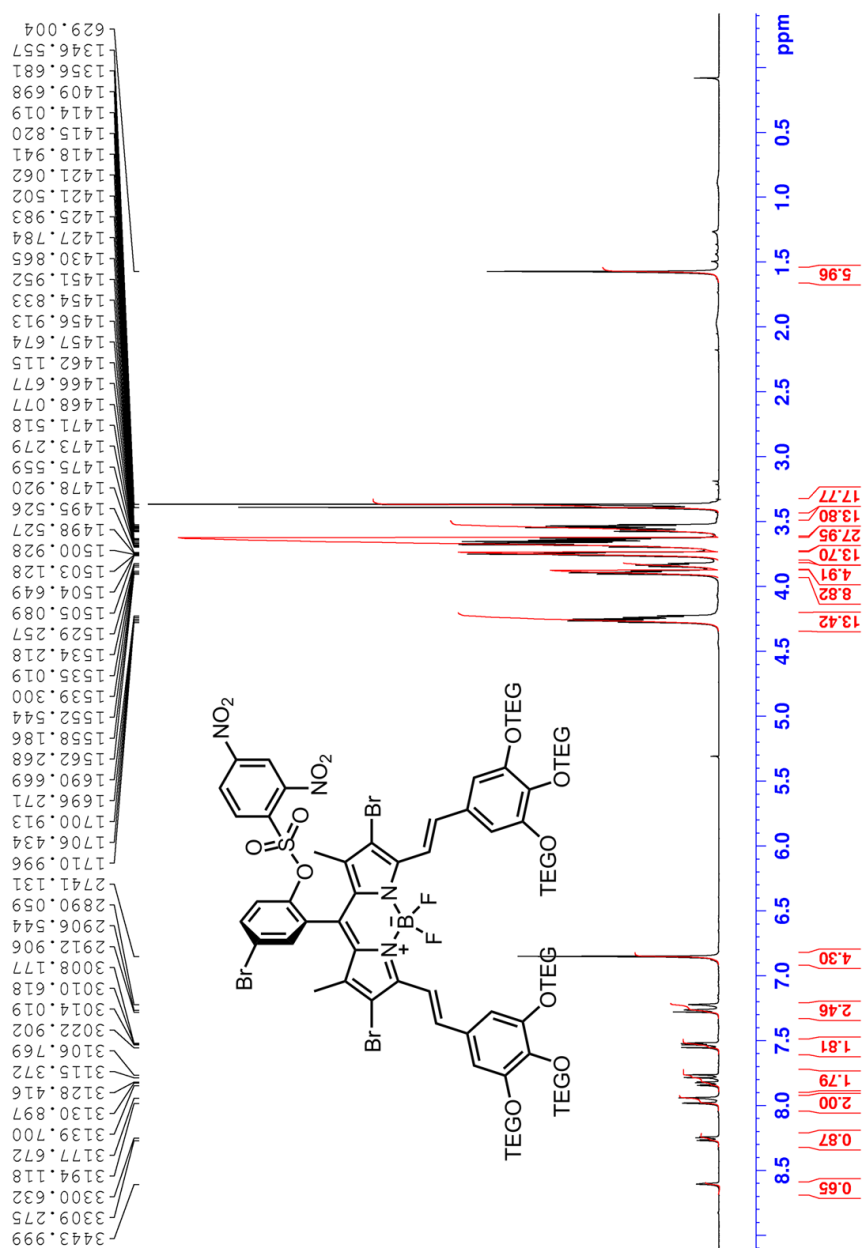


Figure 63. <sup>1</sup>H NMR spectra of compound 40

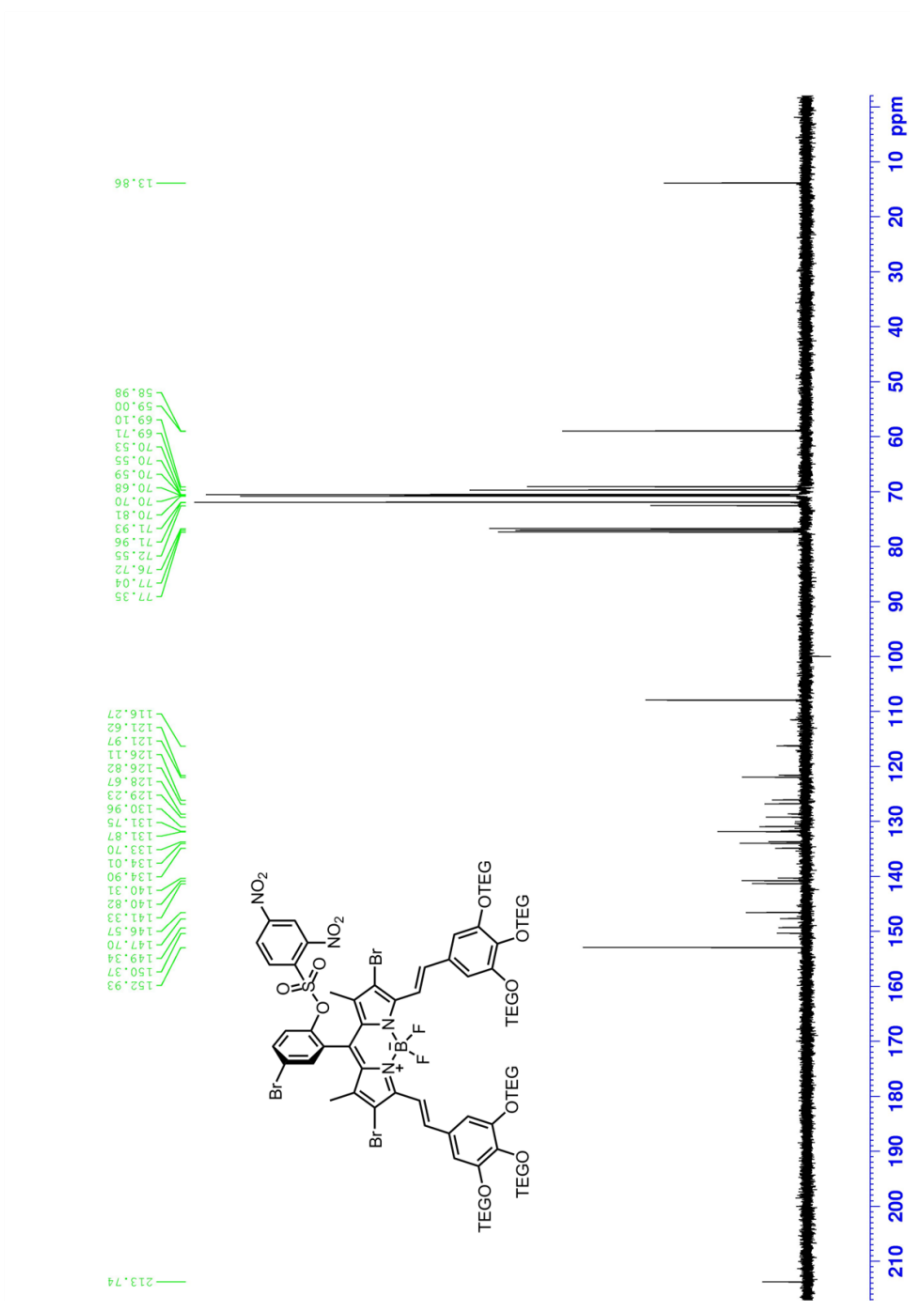
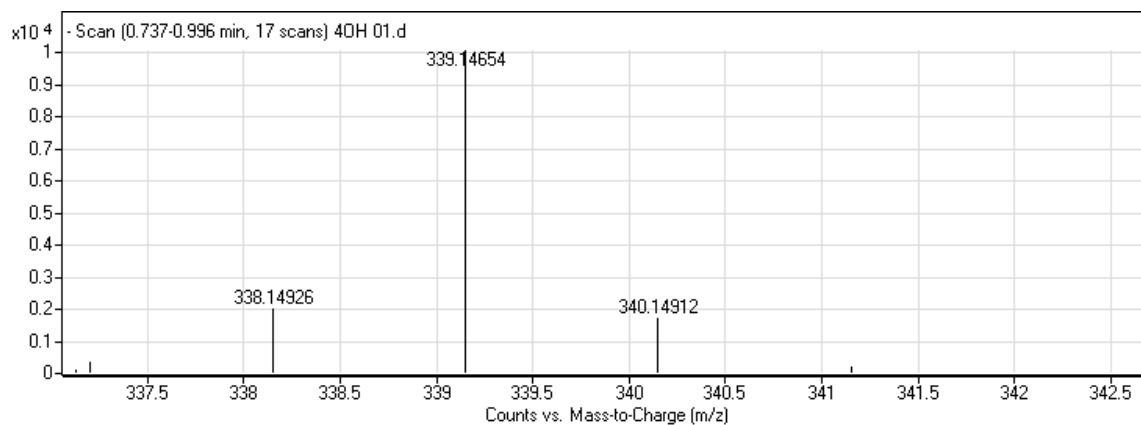


Figure 64.  $^{13}\text{C}$  NMR spectra of compound 40

## APPENDIX B

### MASS SPECTRA



**Figure 65.** ESI-HRMS of compound 30

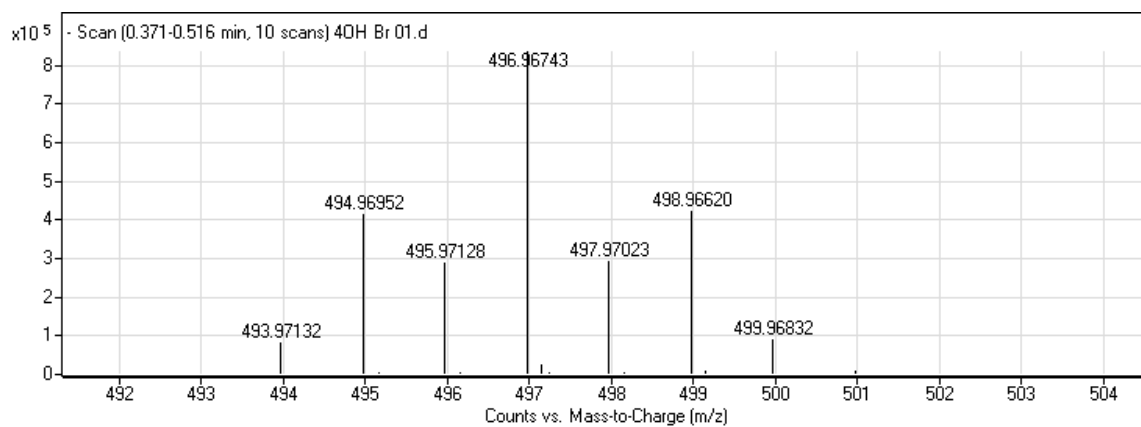


**Figure 66.** ESI-HRMS of compound 31

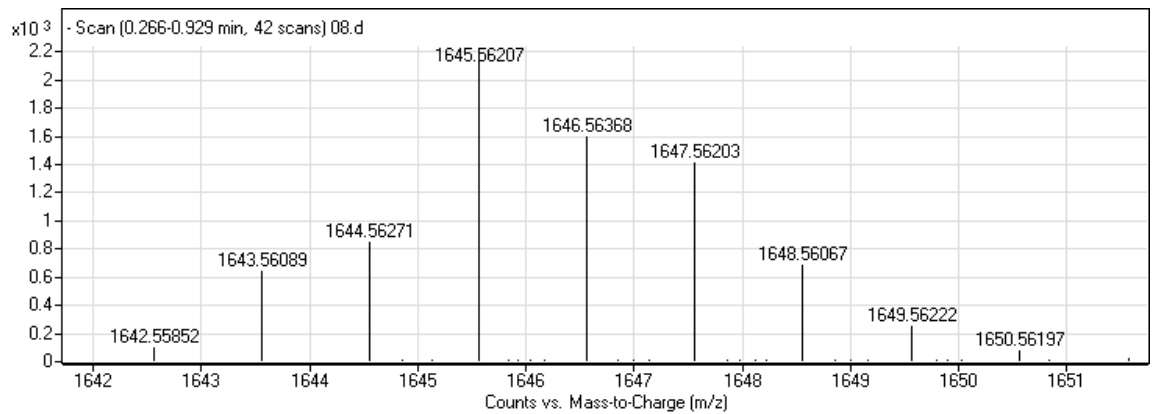


**Figure 67.** ESI-HRMS of compound 32

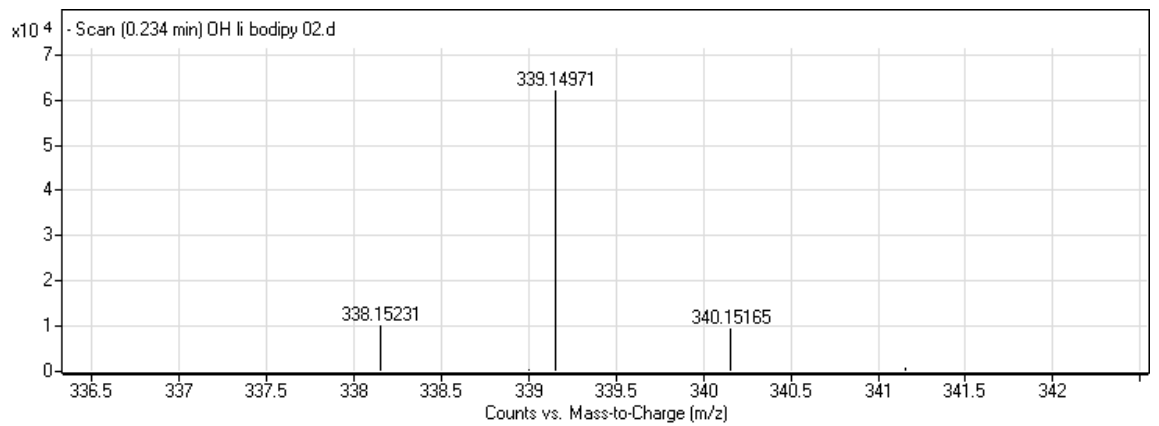


**Figure 68.** ESI-HRMS of compound 34

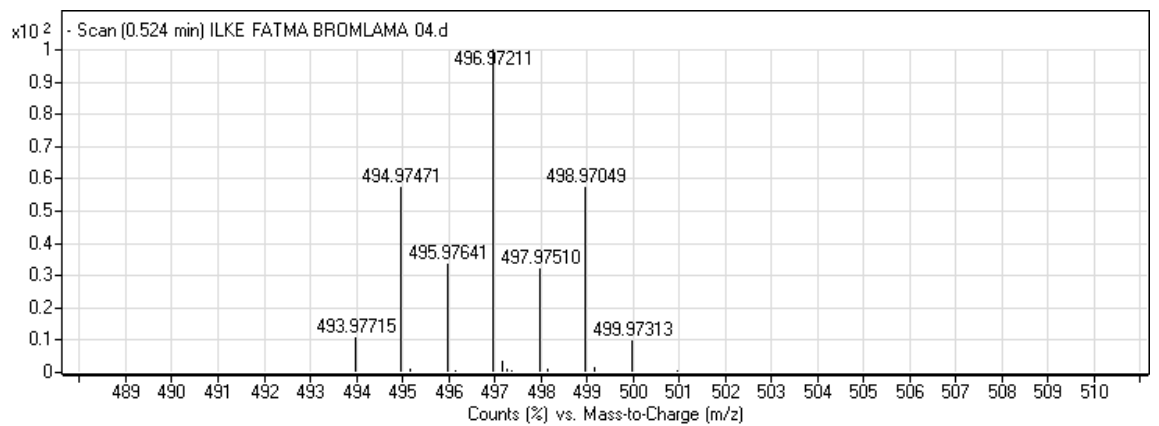


**Figure 69.** ESI-HRMS of compound 35

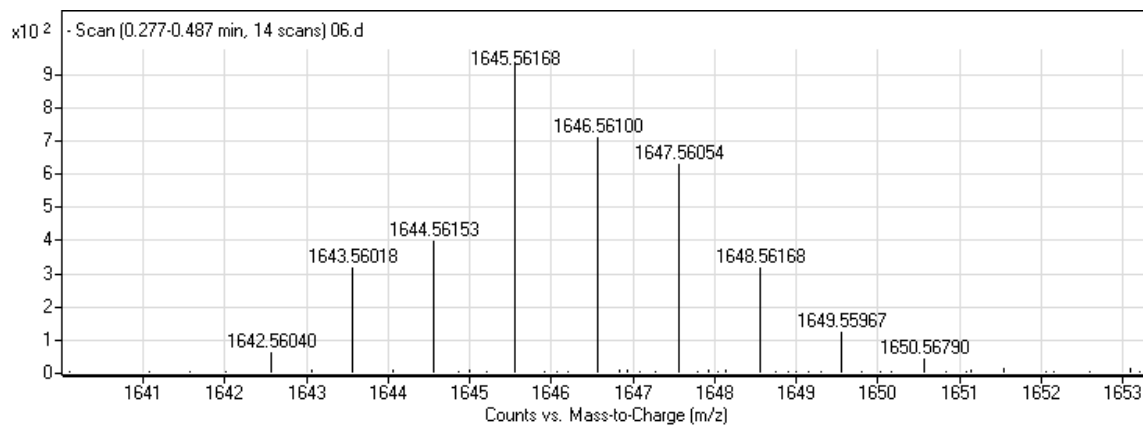


**Figure 70.** ESI-HRMS of compound 36

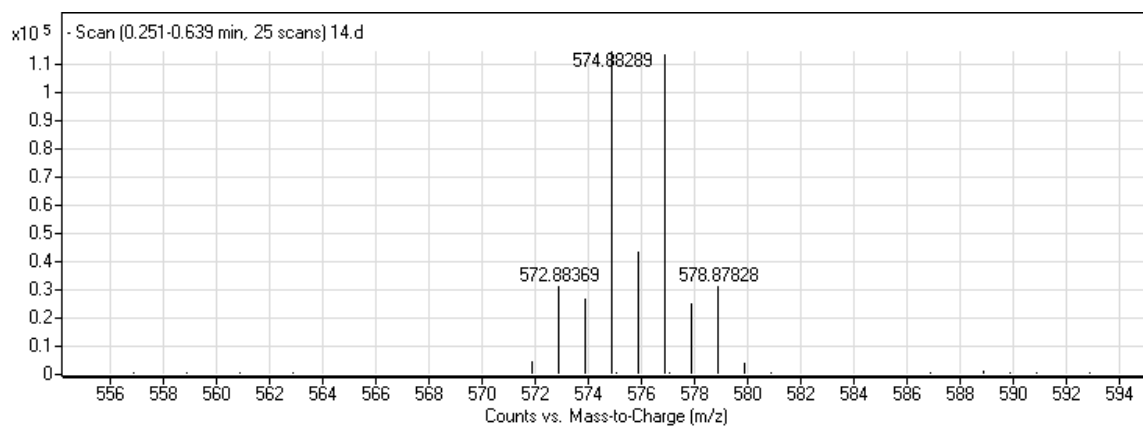


**Figure 71.** ESI-HRMS of compound 38

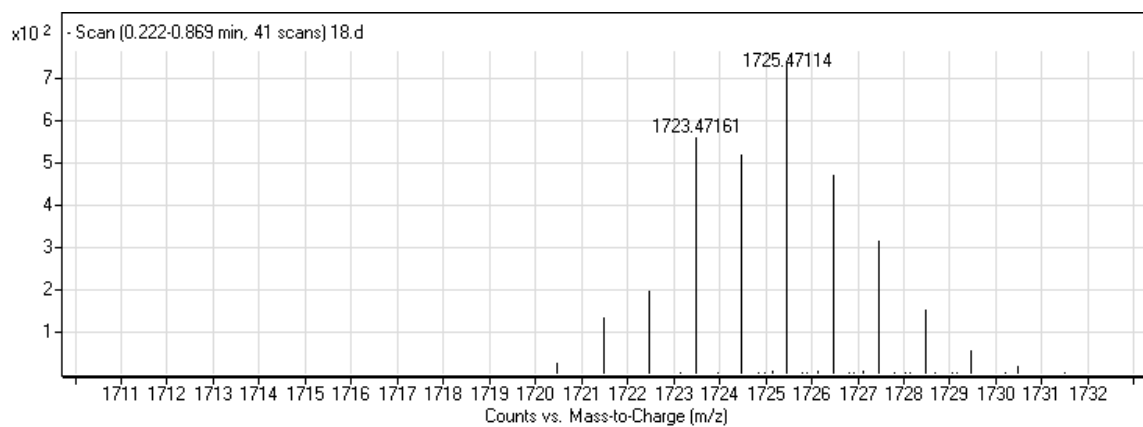


**Figure 72.** ESI-HRMS of compound 39